Master's Thesis

M2 Probabilités et Modèles Aléatoires (PMA)

The Long-Range Ising Model in 1D at Inverse-Square Decay

FK Renormalisation, Random Currents and a Discrete Gaussian Perspective

Author

Yuguang Xiao

Sorbonne Université

Examination Committee

Arnaud Le Ny (*Internship Supervisor*)

LAMA, Université Paris-Est Créteil

Nicolas Fournier (*Examiner*)

LPSM, Sorbonne Université

Pierre Monmarché (*Examiner*)

LAMA, Université Gustave Eiffel

Academic Year 2025–2026

Master 2 PMA

Abstract

Garban's Open Problem 4 asks whether, at $\alpha = 2$, delocalisation of the inverse-square Discrete Gaussian Chain is discontinuous. This report approaches the question through the inverse-square Ising model, whose critical magnetisation jump is known. The central technical chapter reconstructs the renormalisation proof of Duminil-Copin, Garban and Tassion. The two Bernoulli recurrences are reconstructed at the conceptual and lemma level, with routine checks consolidated in an appendix. For the FK theorem, we reconstruct the proof conditional on the admissible-specification statement of [DCGT24, Section 3.3]. The good-block recurrence establishes positive percolation density. The failed-crossing recurrence gives a quantitative density gap, which the Edwards–Sokal coupling transfers to the Thouless jump of the Ising magnetisation.

Random currents provide a second comparison. On any finite ferromagnetic weighted graph, the Taylor expansion, source parity and switching lemma do not depend on a maximum interaction range. The geometry and thermodynamic estimates do. Under the additional assumption that free-state long-range order vanishes, the ADCS argument uses switching, uniqueness of the infinite current cluster and spatial averaging to exclude doubled-current percolation. That assumption fails at the critical point of the inverse-square Ising model, so the criterion does not settle this case.

The report also derives a positive moment-weighted current expansion for the Discrete Gaussian Chain. Its vertex factors depend on the full current degree, and the canonical Ising path switch does not preserve the weight. This obstruction leaves Garban's problem open.

Keywords: long-range Ising model; inverse-square interaction; FK random-cluster representation; block renormalisation; *random currents*; switching lemma; Discrete Gaussian Chain.

Acknowledgements

I thank **Arnaud Le Ny** for offering me this M2 internship, for his guidance and for the mathematical discussions behind this report. The internship also prepared me for an ambitious doctoral project, and I appreciate the confidence he placed in me.

LAMA and *Université Paris-Est Créteil (UPEC)* gave me a place to work and discuss mathematics.

I also thank **Pierre Monmarché** for agreeing to join our team and to bring another point of view to future discussions of the doctoral project.

Jingbei Song, who will soon begin a PhD at the *Hong Kong University of Science and Technology* under **Maximilian Nitzschner**, encouraged me throughout my search for a doctoral project. I thank him for that support.

During that search, **Pierre Tarrago**, **David García-Zelada**, **Thierry Lévy**, **Quentin Berger**, **Guillaume Barraquand**, **Sandro Franceschi** and **Irina Kourkova** suggested possible supervisors and research topics. I also thank the academics who could not offer me a position but nevertheless took the time to read and reply to my messages.

I thank my friends **Yuxuan Pei**; **Tianyang Wang** (*Sorbonne Université*) and **Wenbin Yan** (*Université Paris Dauphine–PSL*), both doctoral students in mathematics; my *M2 PMA* classmates **Jianzhang Li**, **Yeye Hu** and **Jie Sheng**; and **Chenyu Bai**, who holds a PhD in mathematics from *Sorbonne Université*. Jianzhang will soon begin a PhD at *UCLouvain* under **Christophe Charlier**. They supported me both mathematically and personally during this period.

My girlfriend, **Chenzi Sun**, is in the second year of her PhD in rheology at *ESPCI Paris*. I thank her for her patience and support.

My interest in mathematical physics began with my father, who taught physics at middle school. I thank both of my parents, and especially my father, for the financial support that made my studies possible.

Finally, I would like to recall the title of a chapter from Victor Hugo's *Les Misérables*, which has accompanied me throughout this period:

Nuit derrière laquelle il y a le jour

Victor Hugo, *Les Misérables*, Part V, Book IX, Chapter V

Contents

1 Introduction

The starting point of this internship was Garban's Open Problem 4 for the inverse-square Discrete Gaussian Chain (DGC): at $\alpha = 2$, is delocalisation discontinuous? The inverse-square Ising chain provides a comparison at the same marginal decay exponent. Its spontaneous magnetisation is known to jump at criticality, although it is a different model with a different order parameter. The comparison below concerns the proofs, not an identification of the two systems.

1.1 Garban's open problem 4

Let $\Lambda_N = \{-N, \ldots, N\}$, and extend $\varphi \in \mathbb{Z}^{\Lambda_N}$ by $\varphi_i = 0$ outside Λ_N. For a nonnegative translation-invariant kernel $J_\alpha(r) \asymp r^{-\alpha}$, the DGC energy and Gibbs measure are

$$H^{\mathrm{DGC}}_{N,\alpha}(\varphi) = \frac{1}{2} \sum_{\substack{i,j \in \mathbb{Z} \\ i \neq j \\ \{i,j\} \cap \Lambda_N \neq \varnothing}} J_\alpha(|i-j|)(\varphi_i - \varphi_j)^2, \qquad \mu^{\mathrm{DGC}}_{N,\beta_{\mathrm{D}},\alpha}(\varphi) = \frac{e^{-\beta_{\mathrm{D}} H^{\mathrm{DGC}}_{N,\alpha}(\varphi)}}{Z_{N,\beta_{\mathrm{D}},\alpha}}.$$

The integer-valued field φ is an effective interface height, and β_{D} is the DGC inverse temperature. The principal observable in this report is

$$\mathrm{Var}^{\mathrm{DGC}}_{N,\beta_{\mathrm{D}},2}(\varphi_0),$$

not an Ising magnetisation.

Figure 1 depicts the finite height field and its zero exterior boundary condition.

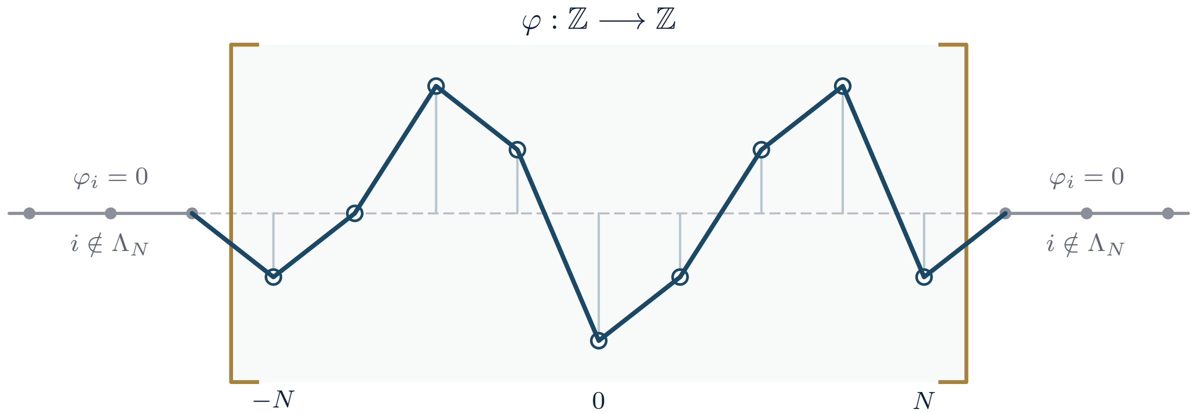

Figure 1: A signed DGC height profile with zero exterior boundary condition. The stems locate the integer heights φ_i, and the polygonal line only guides the eye.

At the inverse-square exponent $\alpha = 2$, results are known at sufficiently small and sufficiently large inverse temperature, but not at the endpoint. For the classical inverse-square DGC studied by Fröhlich and Zegarlinski, write $\beta_{\mathrm{D}} \ll 1$ and $\beta_{\mathrm{D}} \gg 1$ for these two regimes. Then

$$\begin{cases} \mathrm{Var}^{\mathrm{DGC}}_{N,\beta_{\mathrm{D}},2}(\varphi_0) \asymp \log N, & \beta_{\mathrm{D}} \ll 1, \\ \sup_N \mathrm{Var}^{\mathrm{DGC}}_{N,\beta_{\mathrm{D}},2}(\varphi_0) < \infty, & \beta_{\mathrm{D}} \gg 1. \end{cases}$$

Here $\beta_{\mathrm{D}} \ll 1$ and $\beta_{\mathrm{D}} \gg 1$ mean only that the inverse temperature is sufficiently small or sufficiently large for the corresponding theorem. This notation does not suggest that the critical inverse temperature is 1; its precise value is not known. The first line is delocalisation, whereas the second is localisation. Garban proved the general small-β_{D} logarithmic bounds for nonnegative kernels comparable to r^{-2} [Gar23]. Earlier, for periodic boundary conditions at $\beta_{\mathrm{D}} = 1$, Kjaer and Hilhorst obtained an exact variance identity for the special kernel $J(r) = (r^2 - \frac{1}{4})^{-1}$, which implies logarithmic divergence [KH82]. Fröhlich and Zegarlinski proved the large-β_{D} localisation statement for the kernel class treated in their work [FZ91]. For kernels in Garban's extension class, the small-β_{D} result is stronger: after rescaling, the integer-valued chain has the same Gaussian limit and effective temperature as the corresponding real-valued chain. This is the *invisibility of the integers*.

Garban's Open Problem 4 asks whether, at $\alpha = 2$, DGC delocalisation is discontinuous. In Garban's formulation, the integers are predicted to be invisible for $T > T_c$, whereas $T = T_c$ should display intermediate behaviour [Gar23, Open Problem 4]. The available finite-volume results establish small- and large-β_{D} regimes but do not by themselves define a unique inverse temperature $\beta_{D,c}$.

Subsection 4.7 introduces the auxiliary coefficients $\rho_-(\beta_{\mathrm{D}})$ and $\rho_+(\beta_{\mathrm{D}})$, and the report-specific parameters $\beta^{\log}_{\mathrm{D,deloc}}$ and $\beta_{\mathrm{D,loc}}$. These parameters record delocalisation and localisation, respectively, but are not part of Garban's formulation. Conductance monotonicity makes their defining sets an initial interval and a terminal interval, with $\beta^{\log}_{\mathrm{D,deloc}} \le \beta_{\mathrm{D,loc}}$. We neither assume that the endpoints coincide nor identify either parameter with a unique thermodynamic transition.

1.2 The inverse-square Ising chain as a reference model

The reference model is the ferromagnetic Ising chain on $\mathbb{Z}$, with spins $\sigma_i \in \{-1, +1\}$ and translation-invariant coupling

$$J_{i,j} = J(|i-j|), \qquad J(r) \asymp r^{-\alpha}.$$

For a finite $\Lambda \Subset \mathbb{Z}$, the free-boundary Hamiltonian is

$$H^{\mathrm{Ising},0}_{\Lambda}(\sigma) = -\sum_{\substack{i,j\in\Lambda \\ i<j}} J_{i,j}\sigma_i\sigma_j.$$

The plus and minus boundary conditions are obtained by fixing every exterior spin to $+1$ and -1, respectively:

$$H_\Lambda^{\mathrm{Ising},+}(\sigma) = H_\Lambda^{\mathrm{Ising},0}(\sigma) - \sum_{i\in\Lambda}\sum_{j\notin\Lambda} J_{i,j}\sigma_i,$$
$$H_\Lambda^{\mathrm{Ising},-}(\sigma) = H_\Lambda^{\mathrm{Ising},0}(\sigma) + \sum_{i\in\Lambda}\sum_{j\notin\Lambda} J_{i,j}\sigma_i.$$

These boundary fields are absolutely convergent because the interaction is summable. Thus $H_\Lambda^{\mathrm{Ising},\xi}$, for $\xi \in \{+,-,0\}$, has an explicit plus, minus or free boundary condition; 0 means that exterior interactions are omitted, not that the exterior spins are fixed to zero. The Gibbs law and expectation are

$$\mu^\xi_{\Lambda,\beta_\mathrm{I}}(\sigma) = \frac{e^{-\beta_\mathrm{I} H_\Lambda^{\mathrm{Ising},\xi}(\sigma)}}{Z^\xi_{\Lambda,\beta_\mathrm{I}}}, \qquad \langle f\rangle^\xi_{\Lambda,\beta_\mathrm{I}} := \mu^\xi_{\Lambda,\beta_\mathrm{I}}(f). \tag{1}$$

For the summable interactions considered here, the selected thermodynamic limits along $\Lambda_n = [-n,n]\cap\mathbb{Z}$ are

$$\mu^+_{\beta_\mathrm{I}} = \lim_{n\to\infty}\mu^+_{\Lambda_n,\beta_\mathrm{I}}, \qquad \mu^-_{\beta_\mathrm{I}} = \lim_{n\to\infty}\mu^-_{\Lambda_n,\beta_\mathrm{I}}, \qquad \mu^0_{\beta_\mathrm{I}} = \lim_{n\to\infty}\mu^0_{\Lambda_n,\beta_\mathrm{I}}. \tag{2}$$

They are DLR states; the notation selects three limits without asserting uniqueness. We write $\langle f\rangle^\xi_{\beta_\mathrm{I}} = \mu^\xi_{\beta_\mathrm{I}}(f)$.

The plus-state spontaneous magnetisation is

$$m^+(\beta_\mathrm{I}) := \mu^+_{\beta_\mathrm{I}}(\sigma_0) = \langle\sigma_0\rangle^+_{\beta_\mathrm{I}}, \tag{3}$$

and the critical inverse temperature is

$$\beta_{\mathrm{I},c} = \inf\{\beta_\mathrm{I} > 0 : m^+(\beta_\mathrm{I}) > 0\}. \tag{4}$$

The ordered-side limit is $\lim_{\beta_\mathrm{I}\downarrow\beta_{\mathrm{I},c}} m^+(\beta_\mathrm{I})$. Monotonicity and upper semicontinuity give $m^+(\beta_{\mathrm{I},c}) = \lim_{\beta_\mathrm{I}\downarrow\beta_{\mathrm{I},c}} m^+(\beta_\mathrm{I})$; thus a positive value at $\beta_{\mathrm{I},c}$ is a jump from the disordered side $\beta_\mathrm{I}\uparrow\beta_{\mathrm{I},c}$.

The exponent $\alpha = 2$ is marginal between the regime with bounded droplet cost and the regime with power-law droplet cost. For the exact kernel $J(r) = c/r^2$, Fröhlich and Spencer proved low-temperature phase coexistence, and Aizenman, Chayes, Chayes and Newman proved

$$m^+(\beta_{\mathrm{I},c}) > 0$$

[FS82; ACCN88]. This is the Thouless jump predicted in [Tho69]. Section 2 derives the droplet scaling and separates low-temperature order from the critical endpoint statement.

This comparison with the DGC is structural. Both systems are one-dimensional and long range, and inverse-square decay is marginal in each case. Their Gibbs measures and configuration spaces differ, however, and no Edwards–Sokal-type coupling relates them. In particular, Ising magnetisation is not DGC height variance. What can be compared is the mechanism behind the known Ising discontinuity.

1.3 Three parts of the internship

1. Duminil-Copin, Garban and Tassion (DCGT) study independent inverse-square Bernoulli percolation and then its FK random-cluster extension [DCGT24]. Their parameter β_{tail} is the inverse-square edge intensity and λ controls nearest-neighbour edges; it is not the physical Ising inverse temperature β_{I}. The first recurrence makes dense good blocks merge and establishes positive percolation density. The second proves that failed crossings persist unless a positive density satisfies a quantitative gap. The wired FK extension and the Edwards–Sokal coupling then translate the gap along the physical Ising parameter ray into the magnetisation jump. Section 3 reconstructs the two Bernoulli recurrences at the conceptual and lemma level, consolidates routine checks in an appendix, and isolates the modifications needed for dependent FK edges, conditional on DCGT's admissible-specification statement.

2. Aizenman, Duminil-Copin and Sidoravicius (ADCS) use *random currents* to prove a continuity criterion for ferromagnetic Ising systems [ADCS15]. On a finite long-range volume, the interaction graph is finite but generally dense. The edgewise Taylor expansion, source parity and switching involution use only the weighted graph; they do not use a maximum edge length. The exact switching identity used here is proved in Lemma 4.1. Its two-point specialisation is

   $$\left(\langle\sigma_x\sigma_y\rangle^0_{\Lambda,\beta_{\mathrm{I}}}\right)^2 = \mathbf{P}^{\varnothing}_{\Lambda,\beta_{\mathrm{I}}} \otimes \mathbf{P}^{\varnothing}_{\Lambda,\beta_{\mathrm{I}}}\left(x \leftrightarrow y \text{ in } \operatorname{supp}(\mathbf{n}_1+\mathbf{n}_2)\right).$$

   Long range changes connectivity geometry and infinite-volume estimates, not this finite-volume parity identity.

   The ADCS application combines switching with uniqueness of the infinite doubled-current cluster, spatial averaging and Cauchy–Schwarz. Under the additional hypothesis that free-state long-range order vanishes, it excludes doubled-current percolation and yields continuity of m^+. The inverse-square critical point does not satisfy that hypothesis, so ADCS does not compete with the DCGT jump conclusion.

3. The finite-volume Ising algebra is independent of the interaction range, which suggests testing the same expansion on the DGC. We derive a positive moment-weighted current-type expansion. Field insertions can impose parity-source constraints, but the vertex factors depend on the full current degree. The canonical Ising path switch is therefore not weight preserving. This rules out that particular proof mechanism, but not every possible DGC switching identity.

Bernoulli-open connectivity, FK-open connectivity and current-support connectivity refer to three different random objects throughout the report. The inverse-temperature parameters are likewise kept distinct globally: β_{tail} is the DCGT inverse-square tail intensity, β_{I} is the physical Ising inverse temperature, and β_{D} is the DGC inverse temperature. Appendix A collects these conventions.

1.4 Scope and organisation

The DCGT renormalisation argument is reconstructed selectively. The main text contains both Bernoulli proof chains and the inverse-square estimates, while routine interval and constant checks are collected in Appendix B. For the FK extension, we reconstruct the changes caused by dependent edges and the FK–Ising parameter translation, while importing the admissible-specification step from [DCGT24, Section 3.3]. Direct finite-box estimates support the reconstruction but are not a new phase-transition theorem. The ADCS framework is then used to separate the finite-volume current identities, which remain exact for long-range interactions, from the infinite-volume geometry. The last part derives a moment-weighted current expansion for the DGC and identifies a degree-dependent obstruction to the canonical Ising switch. These results do not settle Garban's Open Problem 4.

Section 2 introduces the inverse-square Ising chain through its droplet energy and phase diagram. Section 3 reconstructs the good-block and failed-crossing recursions, then passes from Bernoulli percolation to FK and Ising. Section 4 separates the finite-volume Ising current algebra from the geometric and infinite-volume estimates in the ADCS criterion. It then tests, in Subsection 4.7, which parts of the current expansion survive for the DGC. Section 5 records the conclusions and the remaining questions.

2 The inverse-square Ising chain as a special reference model

This chapter uses the Ising configuration spaces, Gibbs states and expectation notation fixed in Section 1.2, together with the critical inverse temperature and spontaneous magnetisation defined in (4) and (3). Throughout this section, β_{I} is the physical Ising inverse temperature and $J_r = J(r)$.

2.1 Domain walls and droplet energy

In the nearest-neighbour chain, reversing an interval creates two domain walls and therefore costs only $O(1)$ energy. For a long-range interaction, the reversed interval remains coupled to its entire exterior, and the resulting cost depends on its length.

Let

$$I_\ell = \{1, \ldots, \ell\}, \qquad \sigma_i^{(\ell)} = \begin{cases} -1, & i \in I_\ell, \\ +1, & i \notin I_\ell. \end{cases}$$

Relative to the all-plus configuration, each pair crossing the boundary of I_ℓ changes its contribution from $-J_{|i-j|}$ to $+J_{|i-j|}$. The exact droplet-energy difference is consequently

$$\Delta E(\ell) = 2 \sum_{i \in I_\ell} \sum_{j \notin I_\ell} J_{|i-j|}.$$

Proposition 2.1 (Droplet-energy scaling). *If $J_r \asymp r^{-\alpha}$ with $\alpha > 1$, then*

$$\Delta E(\ell) \asymp \begin{cases} \ell^{2-\alpha}, & 1 < \alpha < 2, \\ \log \ell, & \alpha = 2, \\ 1, & \alpha > 2. \end{cases}$$

Proof. The two sides of the interval contribute equally, so

$$\frac{1}{4} \Delta E(\ell) = \sum_{i=1}^{\ell} \sum_{r \geq i} J_r = \sum_{r \geq 1} \min\{r, \ell\} J_r.$$

For a power-law kernel, the last expression satisfies

$$\sum_{r \geq 1} \min\{r, \ell\} J_r \asymp \sum_{r \leq \ell} r^{1-\alpha} + \ell \sum_{r > \ell} r^{-\alpha}.$$

When $1 < \alpha < 2$, both terms have order $\ell^{2-\alpha}$. At $\alpha = 2$, the first is of order $\log \ell$ and the second is bounded. For $\alpha > 2$, their sum stays bounded above and below uniformly in ℓ. $\square$

Thus large droplets have bounded cost for $\alpha > 2$, power-law cost for $1 < \alpha < 2$, and logarithmic cost at $\alpha = 2$. This is the energy–entropy balance behind the Landau–Lifshitz and Thouless heuristics

[LL80; Tho69]. The calculation identifies the borderline exponent, but it treats only one reversed interval and does not by itself prove the rigorous phase diagram for arbitrary configurations.

The comparison with entropy explains why the logarithm is special. A bounded domain-wall cost can be overwhelmed by the number of possible wall positions, whereas a power-law droplet cost has a clear energetic advantage at low temperature. At inverse-square decay, energy and positional entropy both enter on logarithmic scales. There is no spare power of ℓ with which to discard configurations containing several droplets, nested intervals or interacting contours. A rigorous proof must therefore organise fluctuations across scales rather than extrapolate from the single interval above.

2.2 The rigorous phase picture

The phase diagram involves three distinct questions: absence of phase coexistence, existence of an ordered phase at sufficiently low temperature and behaviour of the order parameter at the critical endpoint.

Absence of phase coexistence. Ruelle's one-dimensional uniqueness theorem gives

$$\sum_{r\geq 1} rJ_r < \infty \quad \Longrightarrow \quad \text{the Gibbs state is unique for every finite } \beta_{\mathrm{I}}.$$

Hence a kernel satisfying $J_r \asymp r^{-\alpha}$ has no finite-temperature phase transition when $\alpha > 2$ [Rue68].

Existence of an ordered phase. For $1 < \alpha < 2$, Dyson proved that $m^+(\beta_{\mathrm{I}}) > 0$ for all sufficiently large β_{I} [Dys69]. This establishes low-temperature phase coexistence but does not determine $m^+(\beta_{\mathrm{I},c})$ throughout the whole regime $1 < \alpha < 2$.

At the marginal exponent, the statement below is restricted to the exact kernel

$$J_r = \frac{c}{r^2}, \qquad c > 0.$$

Fröhlich and Spencer proved that this model has an ordered phase at sufficiently low temperature [FS82].

Behaviour at the critical endpoint. Thouless predicted that the exact inverse-square chain has a positive jump of the spontaneous magnetisation [Tho69]. Aizenman, Chayes, Chayes and Newman proved the endpoint statement

$$m^+(\beta_{\mathrm{I},c}) > 0$$

for this model [ACCN88]. The Fröhlich–Spencer theorem establishes the existence of an ordered phase, whereas the ACCN theorem determines the endpoint behaviour at $\beta_{\mathrm{I},c}$; these are distinct statements. The resulting jump is called the Thouless effect, but it should not be identified without qualification with an ordinary first-order transition.

The three regimes are summarised as follows; the $\alpha = 2$ row refers to the exact inverse-square kernel introduced above.

regime	droplet energy	rigorous phase behaviour
$\alpha > 2$	$O(1)$	unique Gibbs state at every finite β_{I}
$1 < \alpha < 2$	$\ell^{2-\alpha}$	phase coexistence at sufficiently low temperature
$\alpha = 2$	$\log \ell$	low-temperature coexistence and $m^{+}(\beta_{\mathrm{I},c}) > 0$

2.3 Relation to the DGC problem

The inverse-square Ising chain and Garban's model are both one-dimensional long-range systems at marginal inverse-square decay. The known Ising endpoint behaviour makes it possible to separate steps that depend on the spin representation from multiscale estimates with a potentially wider scope.

There is also a more direct interface motivation for the DGC, distinct from the comparison with the one-dimensional Ising chain. In a two-dimensional Ising box in the phase-coexistence regime, Dobrushin boundary conditions fix opposite boundary arcs in the plus and minus phases and thereby force a crossing contour Γ between them. After selecting this contour and coarse-graining its finite droplets and overhangs, one can record its vertical position above each horizontal coordinate i by an integer height h_i. The microscopic phase boundary is then represented by a one-dimensional random height profile.

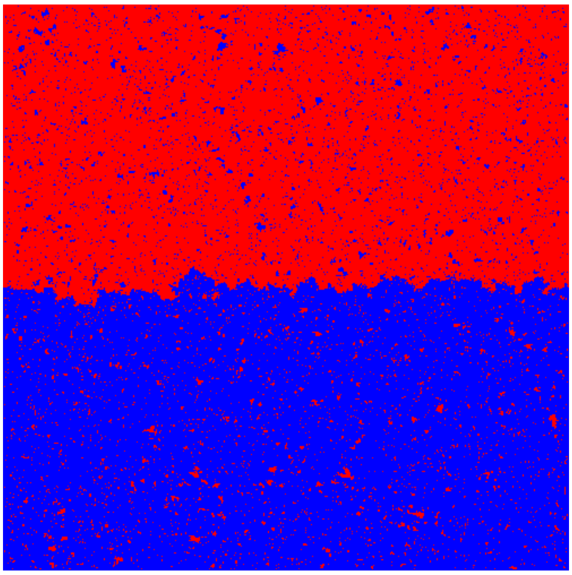

Figure 2: A two-dimensional Ising configuration with Dobrushin boundary conditions. The red and blue regions represent the two spin phases. Their separating contour is a random interface; after selecting a crossing contour and coarse-graining bubbles and overhangs, its position can be encoded by a one-dimensional integer-valued height profile. Image courtesy of Vincent Beffara.

Sheffield's random-surface framework treats precisely such integer- or real-valued lattice height functions with energies depending on height differences [She05]. Velenik explains the role of these fields as effective interface models and notes that, for one-dimensional interfaces, the large-scale behaviour can in suitable regimes be matched rigorously with that of two-dimensional Ising interfaces [Vel06]. More specifically, for power-law interactions, the DGC was introduced as an effective model for the interface between two ordered phases of a two-dimensional long-range Ising system [FZ91; Gar23]. The modelling passage is therefore

$$\text{2D Dobrushin interface} \;\longrightarrow\; \text{1D integer height profile} \;\longrightarrow\; \text{DGC.}$$

The arrows describe height encoding and coarse-graining. They do not denote a finite-volume bijection or an exact identity of probability laws. Ising configurations take values in $\{-1,+1\}^{\mathbb{Z}^2}$, while DGC configurations are unbounded integer-valued heights on $\mathbb{Z}$, and their Gibbs measures are different. In the one-dimensional reference model used in this report, the Ising order parameter $m^+(\beta_\mathrm{I})$ detects phase coexistence through a one-point spin expectation; the DGC observable is the finite-volume growth of $\mathrm{Var}^{\mathrm{DGC}}_{N,\beta_\mathrm{D},2}(\varphi_0)$. In particular, the known Ising jump neither proves nor predicts by itself a jump of the DGC variance coefficient.

The proof of the Ising jump shows how a positive order parameter is prevented from decreasing continuously to zero. Through the Edwards–Sokal coupling, the relevant Ising observable is an FK connectivity probability. No comparable cluster-density representation is known for the DGC. The question for the rest of the report is therefore which geometric or algebraic steps can be recovered without that representation.

The next chapter turns to the DCGT argument. Its central estimate states that positive inverse-square connectivity cannot have arbitrarily small density.

3 The DCGT renormalisation argument

This chapter selectively reconstructs the two DCGT renormalisation inequalities and their passage to the inverse-square Ising magnetisation jump. The good-block recurrence constructs a percolating phase by merging dense clusters across scales; the failed-crossing recurrence proves that a positive percolation density cannot decay continuously to zero.

The main text reconstructs both Bernoulli recurrences at the conceptual and lemma level. It keeps the two-defect/one-defect merger mechanism, the bridge exploration, the inverse-square estimates and the multiscale iterations. Repeated first/last-index constructions, interval counts and fixed-constant checks are consolidated in Appendix B; the full results remain attributed to DCGT [DCGT24]. For the FK extension, only the steps changed by dependence are reconstructed, conditional on the admissible-specification statement of DCGT Section 3.3: worst-boundary estimates, spatial Markov conditioning, the mesoscopic merger argument and FKG. The deterministic geometry is reused from the Bernoulli proof. The $q = 2$ Edwards–Sokal identity then transfers the FK density gap to the physical Ising magnetisation.

Throughout this chapter we follow the notation of the DCGT paper: β_{tail} is the coefficient of the inverse-square percolation tail. When passing back to the Ising model, its physical inverse temperature is denoted β_{I}.

3.1 The Bernoulli model and its main result

Duminil-Copin, Garban and Tassion begin with the complete graph on $\mathbb{Z}$: every unordered pair $\{i, j\}$ is an edge, and the edge states are independent. As in the paper, set

$$J_{i,j} = J(i-j) = \frac{1}{|i-j|^2} \qquad (i \neq j),$$

and, for $\beta_{\mathrm{tail}}, \lambda > 0$, define

$$p_{i,j}(\beta_{\mathrm{tail}}, \lambda) := \begin{cases} 1 - \exp(-\beta_{\mathrm{tail}} J_{i,j}), & |i-j| \geq 2, \\ 1 - \exp(-\lambda), & |i-j| = 1. \end{cases} \tag{5}$$

We denote this product probability measure by $\mathbb{P}_{\beta_{\mathrm{tail}},\lambda}$. The parameter β_{tail} controls the inverse-square tail, while λ controls the nearest-neighbour edges. A *cluster* is a connected component of the graph made of the open edges, and

$$\theta(\beta_{\mathrm{tail}}, \lambda) := \mathbb{P}_{\beta_{\mathrm{tail}},\lambda}[0 \leftrightarrow \infty]. \tag{6}$$

The quantity $\theta(\beta_{\mathrm{tail}}, \lambda)$ is the percolation density. Large λ favours the local connections, while β_{tail} governs the inverse-square edges used across scales.

Theorem 3.1 (DCGT Theorem 1, restated in our notation: Bernoulli case)**.** *For inverse-square long-range Bernoulli percolation on* $\mathbb{Z}$*:*

(i) *if* $\beta_{\text{tail}} > 1$*, then* $\theta(\beta_{\text{tail}}, \lambda) > 0$ *for sufficiently large finite* λ*;*

(ii) *for every* $\beta_{\text{tail}}, \lambda > 0$*,*

$$\theta(\beta_{\text{tail}}, \lambda) > 0 \quad \Longrightarrow \quad \beta_{\text{tail}}\, \theta(\beta_{\text{tail}}, \lambda)^2 \geq 1. \tag{7}$$

Part (i) establishes $\theta(\beta_{\text{tail}}, \lambda) > 0$. Part (ii) gives the density gap $\theta \geq \beta_{\text{tail}}^{-1/2}$ whenever $\theta > 0$, pointwise in the $(\beta_{\text{tail}}, \lambda)$-plane. For fixed $\lambda > 0$, if the monotone function $\beta_{\text{tail}} \mapsto \theta(\beta_{\text{tail}}, \lambda)$ has a nontrivial onset, define

$$\beta_{\text{tail,perc}}(\lambda) := \inf\{\beta_{\text{tail}} > 0 : \theta(\beta_{\text{tail}}, \lambda) > 0\}.$$

If $\beta_{\text{tail,perc}}(\lambda) < \infty$, then

$$\liminf_{\beta_{\text{tail}} \downarrow \beta_{\text{tail,perc}}(\lambda)} \theta(\beta_{\text{tail}}, \lambda) \geq \beta_{\text{tail,perc}}(\lambda)^{-1/2} > 0.$$

Along this fixed-λ path, the Bernoulli percolation density cannot approach zero through positive values. This is a Thouless-type density jump for percolation. The corresponding Ising statement uses the physical path specified in (115).

Both parts use one multiscale scheme. In part (i), overlapping good blocks merge, and the recurrence (8) preserves a positive cluster density. In part (ii), the failed-crossing recurrence keeps obstructions at arbitrarily large scales when $\beta_{\text{tail}}\theta^2 < 1$. The uniform annulus bound (53) then contradicts Kolmogorov's 0-1 law if percolation occurs [DCGT24]. Newman and Schulman had proved existence for sufficiently strong tails, a regime later extended by Imbrie and Newman. Aizenman and Newman established the discontinuity [NS86; IN88; AN86]; the DCGT scheme also applies to FK measures.

3.2 Building the infinite cluster: dense blocks merge

For the existence proof, let $K \geq 1$ and $i \in \mathbb{Z}$, and define the overlapping block (all intervals are understood as subsets of $\mathbb{Z}$)

$$B_K^i = [K(i-1), K(i+1)), \qquad B_K = B_K^0.$$

For $S \subset \mathbb{Z}$, a *cluster in* S means a connected component of the graph with vertex set S and open edges having both endpoints in S. The block B_K^i has $2K$ vertices, and consecutive blocks overlap on an interval of length K. It is θ-good if it contains a cluster with at least $2\theta K$ vertices; otherwise it is θ-bad. Following the paper, write

$$p_{\beta_{\text{tail}},\lambda}(K, \theta) := \mathbb{P}_{\beta_{\text{tail}},\lambda}[B_K \text{ is } \theta\text{-bad}].$$

When $\theta > 3/4$, a cluster with more than $3K/2$ vertices is unique inside a block of size $2K$. The large clusters of two consecutive good blocks must meet in their overlap, so a run of good blocks lies in one connected set.

Remark (The role of θ_∞). Fixing θ_∞ keeps the geometric and summability estimates uniform throughout the renormalisation. Since $\beta_{\text{tail}} > 1$, choose it close enough to 1 that

$$\theta_\infty > \frac{3}{4}, \qquad \beta_{\text{tail}}\theta_\infty^2 > 1.$$

The inequality $\theta_\infty > 3/4$ preserves uniqueness and overlap of the dense clusters. The inequality $\beta_{\text{tail}}\theta_\infty^2 > 1$ controls the one-defect series

$$\sum_{d \geq C_0} \left(\frac{c_\star}{d}\right)^{\beta_{\text{tail}}\theta^2}.$$

For every $\theta \geq \theta_\infty$, the same convergent series with exponent $\beta_{\text{tail}}\theta_\infty^2 > 1$ is an upper bound. A single choice of C_0 therefore works at every scale.

Each renormalisation step loses a small amount of density:

$$\theta_{n+1} = \theta_n - \frac{C_0}{C_{n+1}}.$$

The scale ratios C_{n+1} make these losses summable. Choosing θ_1 above θ_∞ by more than their sum gives $\theta_n \geq \theta_\infty$ for every n. Without this fixed lower bound, the exponent $\beta_{\text{tail}}\theta_n^2$ could approach 1, preventing a scale-independent choice of C_0.

The resulting renormalisation inequality is as follows.

Lemma 3.2 (DCGT Lemma 2, restated in our notation: good-block inequality). *Let $\beta_{\text{tail}} > 1$, and choose $\theta_\infty \in (3/4, 1)$ such that $\beta_{\text{tail}}\theta_\infty^2 > 1$. There exists C_0 such that, for $\theta \geq \theta_\infty$ and integers $C \geq C_0$, $K \geq 2$,*

$$p_{\beta_{\text{tail}},\lambda}\left(CK, \theta - \frac{C_0}{C}\right) \leq \frac{1}{100} p_{\beta_{\text{tail}},\lambda}(K,\theta) + 2C^2 p_{\beta_{\text{tail}},\lambda}(K,\theta)^2. \tag{8}$$

The proof separates two ways in which the parent block can fail to contain a dense cluster. It may contain two separated bad child blocks, an event whose probability is quadratic because the two internal edge families are disjoint, or all bad children are confined to one three-block defect zone. In the latter case, the good blocks on the two sides merge into two large connected sets. The parent can remain bad only if every edge between these sets is closed. The estimate of this disconnection event is where the inverse-square kernel produces the power $d^{-\beta_{\text{tail}}\theta^2}$. Summing this power over the possible defect locations gives the linear term in (8).

Proof. Write $p(K,\theta) = p_{\beta_{\text{tail}},\lambda}(K,\theta)$ and put $\alpha_0 = \beta_{\text{tail}}\theta_\infty^2 > 1$. We make the permanent choices for this recursion at the outset. Fix $c_\star = 48$, choose $C_0 \geq c_\star$ so that

$$2 \sum_{d \geq C_0} \left(\frac{c_\star}{d}\right)^{\alpha_0} \leq \frac{1}{100}. \tag{9}$$

We also take $C_0 \geq 6$. Set

$$\theta' = \theta - \frac{C_0}{C}, \qquad I_C = \{-C+1, \dots, C-1\}.$$

The indices in I_C are exactly those of the overlapping K-blocks used to inspect the parent B_{CK}. The only local symbols needed below are i, the defect index, and $d_i = C - |i|$, its distance in block units from the nearer end of the parent.

We begin with the deterministic geometry. For each $j \in I_C$, choose a largest cluster C_j in B_K^j, using a deterministic tie-breaking rule. If B_K^j is θ-good, then $|C_j| \geq 2\theta K$. Such a cluster is unique: two different clusters of this size would contain more than $2K$ vertices altogether. More importantly, if B_K^j and B_K^{j+1} are both good, then $C_j \cap C_{j+1} \neq \varnothing$. Indeed, their union lies in $B_K^j \cup B_K^{j+1}$, which has only $3K$ vertices, whereas two disjoint clusters would contain at least $4\theta K > 3K$ vertices.

It follows by chaining the intersections that the chosen clusters in any run of N consecutive good blocks belong to one connected component. There is also a robust size estimate. Every vertex lies in at most two of the overlapping blocks, and hence

$$\left| \bigcup_{j=a}^{b} C_j \right| \geq \frac{1}{2} \sum_{j=a}^{b} |C_j| \geq \theta K(b-a+1). \tag{10}$$

Equivalently, one may retain every other block, which makes the counted clusters disjoint. This elementary observation is the geometric backbone of the recursion: good children on the same side of a defect coalesce without using any additional edge.

Let

$$A = \{B_{CK} \text{ is } \theta'\text{-bad}\}.$$

If every child block indexed by I_C is good, their large clusters form one connected component. Retaining the C alternating indices gives at least $2\theta CK \geq 2\theta' CK$ distinct vertices in that component. Thus A forces at least one bad child.

Let D be the event that two vertex-disjoint child blocks are both θ-bad. On $A \cap D^c$, choose one bad block B_K^i. Every block whose index is outside $\{i-1, i, i+1\}$ is vertex-disjoint from B_K^i, and must therefore be good. Denote this one-defect event by E_i, and set $F_i = E_i \cap A$. We have obtained the deterministic inclusion

$$A \subset D \cup \bigcup_{i \in I_C} F_i. \tag{11}$$

Everything up to this point is deterministic.

We first estimate the two-defect event. The badness of B_K^j is determined by the edge variables with both endpoints in that block. For two vertex-disjoint blocks these edge families are disjoint. Since the present model is Bernoulli percolation, the two badness events are therefore independent, and each has probability $p(K,\theta)$ by translation invariance. A union bound over the order C^2 possible pairs gives

$$\mathbb{P}_{\beta_{\mathrm{tail}},\lambda}(D) \le \binom{2C-1}{2} p(K,\theta)^2 \le 2C^2 p(K,\theta)^2. \tag{12}$$

Independence is used here only after vertex-disjointness has identified two disjoint sets of Bernoulli coordinates. This is the origin of the quadratic term; the exact combinatorial prefactor is immaterial to the iteration.

It remains to analyse one defect. Fix i and work on F_i. The defect cannot lie within fewer than C_0 child blocks of an end of the parent. For if, say, $i > C - C_0$, all the good blocks to its left form, by (10), a connected set of size at least $\theta K(2C - C_0 - 1) \ge 2\theta' CK$; this would make the parent good. The left-right symmetric case is identical. Hence

$$|i| \le C - C_0, \qquad d_i := C - |i| \ge C_0. \tag{13}$$

The fixed numerical inequality in this boundary check is recorded with the other constant verifications in Appendix B.

The good blocks outside the defect zone form two runs. Define

$$C_i^- := \bigcup_{j=-C+1}^{i-2} C_j, \qquad C_i^+ := \bigcup_{j=i+2}^{C-1} C_j.$$

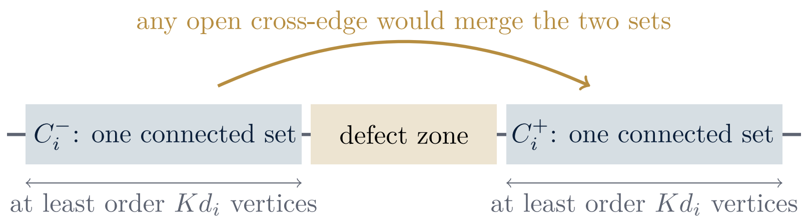

Figure 3: One-defect geometry in the good-block recursion. Runs of overlapping good blocks form the connected sets C_i^- and C_i^+. If the parent block is bad, every edge joining these sets must be closed. The drawing is schematic and not to scale.

The first set lies to the left of the defect and the second to its right, so they are disjoint. Each is connected by the overlap argument above. Both runs contain at least $d_i - 2$ blocks; consequently

$$|C_i^-|, |C_i^+| \ge \theta K(d_i - 2) \ge \frac{K}{2} d_i. \tag{14}$$

Thus one defect produces two macroscopic connected sets whose sizes grow linearly with the available distance d_i on both sides, as summarised in Figure 3.

Badness of the parent now has a concrete consequence: no open edge can join C_i^- to C_i^+. If such an edge existed, it would merge the two connected sets. Their disjoint union contains at least

$$\theta K\big[(i + C - 2) + (C - i - 2)\big] = \theta K(2C - 4) \geq 2\theta' CK$$

vertices, by the permanent choice of C_0. The merged component would therefore make B_{CK} θ'-good, contradicting F_i. This is why the probability problem reduces to a disconnection event between the two sets.

We next locate enough vertices of these sets near the defect. Order them as

$$Ki > x_1 > x_2 > \cdots \quad \text{in } C_i^-, \qquad Ki < y_1 < y_2 < \cdots \quad \text{in } C_i^+,$$

and put $M_i = \lfloor K d_i/2 \rfloor$. Select every other good block on the right. The selected blocks are disjoint and each contributes at least $2\theta K$ vertices. Therefore the first $\lceil b/(2\theta K) \rceil$ selected blocks already contain b vertices of C_i^+, which gives

$$y_b \leq Ki + 3K + \frac{b}{\theta}.$$

The symmetric selection on the left gives

$$x_a \geq Ki - 3K - \frac{a}{\theta}.$$

The choices $d_i \geq C_0 \geq 48$ and $a, b \leq M_i$ ensure that all selected blocks remain in the two good runs; the short floor and endpoint check is Lemma B.1. Subtraction yields the useful ordered-point estimate

$$\theta(y_b - x_a) \leq 6K + a + b, \qquad 1 \leq a, b \leq M_i. \tag{15}$$

The probability that these two dense sets fail to merge is estimated next. Let $\mathcal{H}_i$ be the sigma-field generated by all edges internal to one of the child blocks. The event E_i, the deterministically chosen clusters, and hence C_i^- and C_i^+, are $\mathcal{H}_i$-measurable. Every edge between the two sets crosses the three-block defect zone and has length greater than $2K$, whereas an edge internal to a child block has length at most $2K - 1$. These cross-edges have therefore not been exposed. Conditionally on $\mathcal{H}_i$, they remain mutually independent with their original Bernoulli probabilities. This is the second, and final, use of Bernoulli independence in the good-block proof.

Let A_i be the event that every edge joining C_i^- to C_i^+ is closed. On E_i, parent badness implies A_i, and the product law gives

$$\mathbb{P}_{\beta_{\mathrm{tail}},\lambda}(A_i \mid \mathcal{H}_i) = \exp\left[-\beta_{\mathrm{tail}} \sum_{x\in C_i^-} \sum_{y\in C_i^+} \frac{1}{(y-x)^2}\right]. \tag{16}$$

The origin of the critical exponent is already visible in this sum. Each side supplies order $\theta K d_i$ available vertices. Ordering the vertices turns these two density factors into the prefactor θ^2 in the energy lower bound. Summing the inverse-square interaction over pairs at increasing separations produces a logarithm in d_i, while the tail intensity contributes β_{tail}. Exponentiating the resulting energy therefore produces $d_i^{-\beta_{\mathrm{tail}}\theta^2}$. The next computation makes this heuristic exact.

Restrict the double sum in (16) to the first M_i vertices on each side. By (15),

$$\sum_{x\in C_i^-} \sum_{y\in C_i^+} \frac{1}{(y-x)^2} \ge \theta^2 \sum_{a,b\le M_i} \frac{1}{(6K+a+b)^2}. \tag{17}$$

For $(x,y) \in [a-1,a]\times[b-1,b]$, one has $8K+x+y \ge 6K+a+b$. Summing the corresponding unit-square integrals gives

$$\begin{aligned}\sum_{a,b\le M_i} \frac{1}{(6K+a+b)^2} &\ge \int_0^{M_i}\int_0^{M_i} \frac{dx\,dy}{(8K+x+y)^2} \\ &= \log\left(\frac{(8K+M_i)^2}{8K(8K+2M_i)}\right). \end{aligned} \tag{18}$$

Since $M_i = \lfloor K d_i/2\rfloor \ge K d_i/3$ for $d_i \ge C_0$, the right-hand side is at least

$$\log\left(\frac{(d_i+24)^2}{48(d_i+12)}\right) \ge \log\left(\frac{d_i}{48}\right).$$

The last comparison is equivalent to $(d_i+24)^2 \ge d_i(d_i+12)$. With $c_\star = 48$, we have proved the rigorous energy bound

$$\sum_{x\in C_i^-} \sum_{y\in C_i^+} \frac{1}{(y-x)^2} \ge \theta^2 \log\left(\frac{d_i}{c_\star}\right). \tag{19}$$

Lemma B.2 records the same comparison as a reusable statement together with the floor convention. Combining the last display with (16) and the deterministic no-joining-edge implication gives

$$\mathbb{P}_{\beta_{\mathrm{tail}},\lambda}\left(B_{CK} \text{ is } \theta'\text{-bad} \,\middle|\, E_i\right) \le \left(\frac{c_\star}{d_i}\right)^{\beta_{\mathrm{tail}}\theta^2}. \tag{20}$$

Here is the conditioning step explicitly. Since E_i is $\mathcal{H}_i$-measurable and $F_i \subset E_i \cap A_i$,

$$\begin{aligned}\mathbb{P}(F_i) &\le \mathbb{E}[\mathbf{1}_{E_i}\mathbf{1}_{A_i}] \\ &= \mathbb{E}[\mathbf{1}_{E_i}\mathbb{P}(A_i \mid \mathcal{H}_i)] \\ &\le \mathbb{P}(E_i)\left(\frac{c_\star}{d_i}\right)^{\beta_{\text{tail}}\theta^2}.\end{aligned} \tag{21}$$

Thus (20) is obtained by division when $\mathbb{P}(E_i) > 0$; if $\mathbb{P}(E_i) = 0$, the unconditional form (21) is already sufficient. This makes clear that conditioning on the event E_i is only shorthand: the product calculation itself is performed after conditioning on the full internal-edge sigma-field, where the random dense sets have become fixed.

To finish, sum over the possible defect locations. Since E_i requires B_K^i to be bad, $\mathbb{P}(E_i) \le p(K,\theta)$. Only indices with $d_i \ge C_0$ contribute, and each value of $d_i = C - |i|$ occurs at most twice. Since $\theta \ge \theta_\infty$ and $c_\star/d_i \le 1$, so

$$\left(\frac{c_\star}{d_i}\right)^{\beta_{\text{tail}}\theta^2} \le \left(\frac{c_\star}{d_i}\right)^{\alpha_0}.$$

Consequently, (9) gives

$$\sum_{i\in I_C} \mathbb{P}_{\beta_{\text{tail}},\lambda}(F_i) \le 2p(K,\theta)\sum_{d\ge C_0}\left(\frac{c_\star}{d}\right)^{\alpha_0} \le \frac{1}{100}p(K,\theta). \tag{22}$$

Combining the deterministic decomposition (11), the two-defect estimate (12), and the one-defect estimate (22) proves (8). □

At scale K, the induction variable is the bad-block probability $p(K,\theta)$. Equation (8) says that failure at scale CK comes from either two independent small-scale failures, giving the quadratic term, or one defect whose possible locations have a summable disconnection cost, giving the small linear term. The proof of existence below chooses the scale ratios so that both mechanisms contract while the density threshold remains above θ_∞.

For the iteration, choose scales K_n and density thresholds θ_n. The thresholds decrease, because each merger step may lose a small fraction of vertices, but their total loss is summable and they stay above θ_∞. The invariant will be $C_n^2 p(K_n,\theta_n) \le \delta$: after rescaling, the quadratic error in (8) is small enough to preserve this bound. A large nearest-neighbour intensity makes the invariant true at the initial scale. The resulting positive probability of a macroscopic cluster at every scale is then converted, by translation invariance, into a positive probability that the origin belongs to an infinite cluster.

Reconstruction of the proof of DCGT Theorem 1(i). Fix $\beta_{\text{tail}} > 1$, and choose $\theta_\infty \in (3/4,1)$ with $\beta_{\text{tail}}\theta_\infty^2 > 1$. Let $C_0 = C_0(\beta_{\text{tail}},\theta_\infty)$ be supplied by Lemma 3.2. Choose $\theta_1 < 1$ and $C_1 \ge C_0$ so that the sequences

$$C_{n+1} = (n+1)^3 C_1, \qquad \theta_{n+1} = \theta_n - \frac{C_0}{C_{n+1}} \qquad (n \geq 1) \tag{23}$$

satisfy $\theta_n \geq \theta_\infty$ for every n. This is possible because

$$\sum_{n\geq 1} \frac{C_0}{C_{n+1}} = \frac{C_0}{C_1} \sum_{m \geq 2} \frac{1}{m^3},$$

which can be made smaller than $1 - \theta_\infty$.

Use the scales from the paper:

$$K_1 = C_1, \qquad K_{n+1} = C_{n+1} K_n. \tag{24}$$

These definitions give $K_n = (n!)^3 C_1^n$. If every nearest-neighbour edge in B_{C_1} is open, then B_{C_1} is θ_1-good. Taking $\lambda < \infty$ sufficiently large,

$$u_1 := p_{\beta_{\mathrm{tail}},\lambda}(K_1, \theta_1) \leq \mathbb{P}_{\beta_{\mathrm{tail}},\lambda}[\text{some nearest-neighbour edge in } B_{C_1} \text{ is closed}] \leq 2C_1 \mathrm{e}^{-\lambda}$$

can be made arbitrarily small.

For

$$u_n := p_{\beta_{\mathrm{tail}},\lambda}(K_n, \theta_n),$$

Lemma 3.2 and (23) give

$$u_{n+1} \leq \frac{1}{100} u_n + 2C_{n+1}^2 u_n^2. \tag{25}$$

This is the scale transition in its unnormalised form. The first term is already contractive, but the coefficient of the quadratic term grows with the next scale ratio. We compensate by measuring the bad probability in units of C_n^{-2}. Since $C_{n+1}/C_n = ((n+1)/n)^3 \leq 8$, multiplication by C_{n+1}^2 gives a recurrence with coefficients independent of n. Since $C_{n+1}/C_n \leq 8$, the variables $v_n := C_n^2 u_n$ satisfy

$$v_{n+1} \leq \frac{64}{100} v_n + 8192 v_n^2.$$

The invariant is the interval $[0, \delta]$. The linear part maps it strictly inside itself, and choosing δ small makes the quadratic correction fit into the remaining margin. It is therefore enough to make the initial bad probability small; no further increase of λ is needed at later scales. The choice $\delta = 1/50000$, for example, obeys $\frac{64}{100}\delta + 8192\delta^2 < \delta$. Choose λ above so that $v_1 \leq \delta$. Induction yields

$$C_n^2 u_n = v_n \leq \delta \qquad (n \geq 1).$$

In particular,

$$\mathbb{P}_{\beta_{\text{tail}},\lambda}[B_{K_n} \text{ is } \theta_n\text{-good}] \geq 1 - \delta C_n^{-2} \geq \frac{1}{2}.$$

The two parts of the induction have now done different jobs. The bound $v_n \leq \delta$ makes a macroscopic cluster likely at scale K_n, while $\theta_n \geq \theta_\infty$ ensures that "macroscopic" always means at least the same positive density. The latter is indispensable: without it, the large component supplied by the recurrence could occupy a vanishing fraction of the block even though the bad probability remained small.

On this event, $\theta_n \geq \theta_\infty > 3/4$ implies that the largest cluster $C(B_{K_n})$ has at least $3K_n/2$ vertices. Translation invariance gives

$$\begin{aligned}\frac{3}{4}K_n &\leq \mathbb{E}_{\beta_{\text{tail}},\lambda}\left[|C(B_{K_n})|\mathbf{1}_{\{B_{K_n} \text{ is 3/4-good}\}}\right] \\ &\leq 2K_n\,\mathbb{P}_{\beta_{\text{tail}},\lambda}\left[0 \text{ lies in a cluster of size at least } \frac{3}{2}K_n\right].\end{aligned}$$

The second inequality follows from a mass-transport count. On the good event, every vertex of the chosen cluster belongs in the full configuration to a cluster of size at least $3K_n/2$. Hence

$$|C(B_{K_n})|\mathbf{1}_{\{B_{K_n} \text{ is 3/4-good}\}} \leq \sum_{x \in B_{K_n}} \mathbf{1}_{\{|C(x)| \geq 3K_n/2\}},$$

where $C(x)$ is the full open cluster of x. Taking expectations and using translation invariance makes every summand equal to the probability for the origin, producing the factor $|B_{K_n}| = 2K_n$ above. The probability on the right is at least $3/8$ for every n. These events decrease to $\{0 \leftrightarrow \infty\}$ as $K_n \to \infty$. Continuity from above gives

$$\theta(\beta_{\text{tail}}, \lambda) \geq \frac{3}{8} > 0,$$

which proves part (i). □

Remark 3.3 (DCGT Remark 1: the regime $1 < s < 2$). Consider the slower decay

$$J_{i,j} = \frac{1}{|i-j|^s}, \qquad 1 < s < 2.$$

The single-defect estimate is stronger. Here s is the decay exponent denoted by α elsewhere in this report; we retain s to follow DCGT Remark 1. The polynomial disconnection estimate (20) is replaced by

$$\mathbb{P}_{\beta_{\text{tail}},\lambda}\left[B_{CK} \text{ is } \theta'\text{-bad} \mid E_i\right] \leq \exp\!\Big[-c(\beta_{\text{tail}}, \theta)\big((C-|i|)K\big)^{2-s}\Big].$$

Put $M \asymp (C-|i|)K$. The interaction between the two dense sets contains the double sum

$$\sum_{a,b \leq M} \frac{1}{(6K+a+b)^s} \gtrsim_s M^{2-s},$$

for fixed $s \in (1,2)$; the implicit constant may depend on s. The single-defect term is then stretched-exponentially small in the scale. For every $\beta_{\text{tail}} > 0$, one can choose a sufficiently large finite $\lambda = \lambda(\beta_{\text{tail}}) > 0$ and obtain percolation. Along the resulting renormalisation sequence,

$$p_{\beta_{\text{tail}},\lambda}(K_n, \theta_n)$$

decays stretched-exponentially in K_n. At $s = 2$, the double sum grows only logarithmically, so the bad-block probability decays polynomially. The summability proof at this exponent requires $\beta_{\text{tail}}\theta_\infty^2 > 1$ [DCGT24].

The good-block recurrence propagates a positive-density connected component from scale K to scale CK. Its quadratic error records two separated defects, while its summable linear error records one defect and the cost of disconnecting the two dense runs around it. The exponent $\beta_{\text{tail}}\theta^2 > 1$ is used for existence because it makes the defect locations summable. The next subsection studies the complementary regime: if $\beta_{\text{tail}}\theta^2 < 1$, failed crossings instead persist and rule out a positive density smaller than the threshold.

3.3 Forcing a jump: failed crossings persist

Part (ii) requires a lower bound on failed crossings across successive scales. A block B_{3K}^i is called K-crossed if there exist

$$x < 3Ki - 3K, \qquad y \geq 3Ki + 3K,$$

that are connected by an open path using only edges of length at most K. Set

$$\overline{p}_{\beta_{\text{tail}},\lambda}(K) = 1 - \mathbb{P}_{\beta_{\text{tail}},\lambda}(B_{3K} \text{ is } K\text{-crossed}).$$

For fixed $\beta_{\text{tail}}, \lambda$, we abbreviate this as $\overline{p}(K)$.

Geometrically, B_{3K}^i has width $6K$, while the witnessing path is forbidden from using any single edge longer than K. A crossing must therefore traverse the block through genuinely mesoscopic structure rather than jump over it in one step. The quantity $\overline{p}(K)$ is the probability that this short-edge traversal fails. The scale induction will compare that failure with the corresponding event for a block of width $6CK$, where edges up to length CK are allowed.

Lemma 3.4 (Strengthened form of DCGT Lemma 3 after enlarging the scale thresholds)**.** *Assume that $\theta(\beta_{\mathrm{tail}}, \lambda) < \theta$ and $\beta_{\mathrm{tail}}\theta^2 < 1$. There exist integers*

$$C_1 = C_1(\beta_{\mathrm{tail}}, \lambda, \theta), \qquad K_1 = K_1(\beta_{\mathrm{tail}}, \lambda, \theta),$$

such that, for all integers $C \geq C_1$ and $K \geq K_1$,

$$\overline{p}_{\beta_{\mathrm{tail}},\lambda}(CK) \geq C^{1-\beta_{\mathrm{tail}}\theta^2} \min\{\overline{p}_{\beta_{\mathrm{tail}},\lambda}(K), C^{-1}\}. \tag{26}$$

This is an adapted, strengthened formulation rather than a verbatim copy of DCGT Lemma 3. The displayed DCGT bound contains the fixed prefactor $1/(9\mathrm{e})$. In the proof below, the strict slack $\eta < \theta^2$ first gives a stronger power of C; after increasing C_1 and K_1, that power absorbs the fixed prefactor and yields the stated form [DCGT24].

This lower bound prevents failed crossings from disappearing too quickly.

Suppose that a large CK-crossing exists and inspect order C well-separated candidate blocks of size K. For each candidate, the global crossing either contains a crossing made entirely of short edges, or it must use a long edge. A first-entry/last-exit decomposition shows that the latter edge either lies near the candidate or spans it and leaves a long arm at each endpoint; in both cases the block is declared bridged. Thus every unbridged candidate must be crossed by short edges. After revealing the long-edge geometry, the crossing events of the unbridged candidates factorise. The bridge probability is bounded by an open-edge probability times a two-arm probability. Inverse-square kernel sums then show that sufficiently many candidates remain unbridged, producing the factor $C^{1-\beta_{\mathrm{tail}}\theta^2}$.

Proof. Fix $\beta_{\mathrm{tail}}, \lambda, \theta$, and abbreviate $\overline{p}_{\beta_{\mathrm{tail}},\lambda}$ to $\overline{p}$. We first make the permanent parameter choices. For

$$q_R := \mathbb{P}_{\beta_{\mathrm{tail}},\lambda}(0 \leftrightarrow \mathbb{Z} \setminus B_R),$$

continuity from above gives $q_R \downarrow \theta(\beta_{\mathrm{tail}}, \lambda) < \theta$. Choose R and numbers ρ, η such that

$$q_R^2 < \rho < \eta < \theta^2. \tag{27}$$

The first strict inequality leaves room for the interaction between the two endpoint neighbourhoods; the second will later turn a bridge estimate into a product over long edges; the last is the slack that ultimately permits the exponent $\beta_{\mathrm{tail}}\theta^2$.

For $K > 2R$, set

$$\varepsilon_{R,K} := |B_R|^2 \sup_{r \geq K-2R} \left(1 - e^{-\beta_{\mathrm{tail}}/r^2}\right) \leq \frac{\beta_{\mathrm{tail}}|B_R|^2}{(K-2R)^2}. \tag{28}$$

Choose K_1 sufficiently large that $K_1 > 2R$ and $q_R^2 + \varepsilon_{R,K} \leq \rho$ for all $K \geq K_1$. We shall enlarge K_1, and then choose C_1, only finitely many times below. These are the permanent scale choices for the argument.

Fix $K \geq K_1$ and $C \geq 2$. We first set up the truncated geometry. Work in the configuration $\omega^{(\leq CK)}$ obtained by deleting every edge longer than CK. This does not change whether B_{3CK} is CK-crossed, since such a crossing is defined using only edges of length at most CK. Call an edge *short* if its length is at most K, and *long* if its length belongs to $(K, CK]$.

A long open edge $e = \{x, y\}$ is a *bridge* if, after deleting e from $\omega^{(\leq CK)}$, each endpoint remains connected to the exterior of its translate of B_R. The definition therefore requires a long edge together with two surviving R-arms.

Use the well-separated candidate indices

$$\mathcal{I}_C^{\mathrm{cand}} := \{i \in 3\mathbb{Z} : B_{3K}^i \subset B_{CK}\}.$$

For $i \in \mathcal{I}_C^{\mathrm{cand}}$, write

$$c_i = 3Ki, \qquad \ell_i = c_i - 3K, \qquad r_i = c_i + 3K,$$

so that $B_{3K}^i = [\ell_i, r_i)$, and introduce the buffered intervals

$$I_i = [c_i - 4K, c_i + 4K), \qquad J_i = [c_i - 5K, c_i + 5K).$$

The smaller buffer I_i contains every short-edge witness of a crossing; the larger buffer J_i protects those witnesses during the exploration.

Call B_{3K}^i *bridged* if either

(a) a bridge has one endpoint left of ℓ_i and the other on or right of r_i; or

(b) an open long edge has at least one endpoint in J_i.

Otherwise it is *unbridged.* Condition (a) records a genuine long jump across the candidate; condition (b) removes candidates whose local short-edge configuration could be touched by the long-edge exploration. Let $\mathbf{U}$ be the random set of unbridged candidate blocks. Distinct candidate centres are separated by at least $9K$, so the intervals I_i attached to them are disjoint.

Remark (Local notation for the failed-crossing proof). Only six pieces of local notation remain active through the proof. The radius R is fixed first and specifies the two arms required of a bridge. The variable K is the current crossing scale, while C is the scale ratio and CK is both the next crossing scale and the long-edge truncation. For a candidate block, I_i contains every local short-crossing witness, and J_i is the larger protective interval used during exploration. The symbol $\mathbf{U}$ denotes the random set of candidates protected from every bridge and nearby long edge. The proof first conditions on the information determining $\mathbf{U}$, then uses the still-unrevealed short edges inside the disjoint intervals I_i.

The next implication is deterministic: a large crossing forces each candidate to be crossed or bridged. Suppose that B_{3CK} is CK-crossed, and erase loops from a witnessing path to obtain a self-avoiding open path

$$\gamma = (v_0, v_1, \ldots, v_m), \qquad v_0 < -3CK, \quad v_m \geq 3CK,$$

whose edges all have length at most CK. Fix a candidate index i. Choose

$$t := \min\{j : v_j \geq r_i\}, \qquad s := \max\{j < t : v_j < \ell_i\}. \tag{29}$$

The index t is the first time the global path reaches the right side of the candidate; s is its last visit to the left side before that time. They exist because the global endpoints lie well beyond the candidate. Their defining minimality and maximality imply

$$v_s < \ell_i, \qquad v_t \geq r_i, \qquad v_j \in [\ell_i, r_i) \quad (s < j < t). \tag{30}$$

Thus the subpath $(v_s, \ldots, v_t)$ genuinely traverses the candidate, even if the global path entered and left it several times earlier.

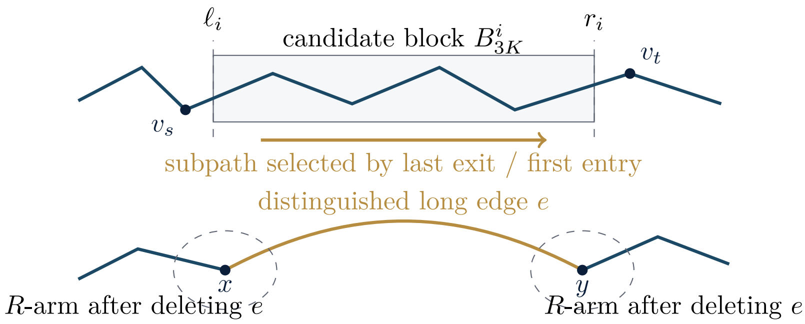

Figure 4: Schematic crossing geometry. Top: the indices s, t isolate a genuine traversal of the candidate block. Bottom: if a long spanning edge is used, deleting it leaves two endpoint arms; this is the bridge alternative. The drawing is not to scale.

Figure 4 displays the two geometric alternatives used in the next paragraph.

If every edge of this subpath is short, it witnesses that B^i_{3K} is K-crossed. Hence failure of K-crossing forces a long edge e on the subpath. If an endpoint of e lies in J_i, condition (b) makes the candidate bridged. Suppose that neither endpoint lies in J_i. Every intermediate vertex in (30) lies in $[\ell_i, r_i) \subset J_i$, so no intermediate vertex can be an endpoint of e. Therefore $t = s + 1$, $e = \{v_s, v_t\}$, and this single edge jumps across the whole candidate.

It remains to verify that this spanning edge is a bridge, rather than merely a long open edge. Deleting e leaves the two open path pieces $(v_0, \ldots, v_s)$ and $(v_t, \ldots, v_m)$. Because the candidate is contained in B_{CK} and $|e| = v_t - v_s \leq CK$, the endpoint distances can be read directly from the block boundaries. Since $v_t \geq r_i$,

$$v_s \geq r_i - CK.$$

Moreover $\ell_i \geq -CK$ and $r_i = \ell_i + 6K$, so $v_s \geq -2CK + 6K$. As $v_0 < -3CK$,

$$v_s - v_0 > CK + 6K > K > R. \tag{31}$$

The right side is symmetric but worth recording. From $v_s < \ell_i$ and $v_t - v_s \leq CK$, $v_t < \ell_i + CK$; since $r_i \leq CK$ and $\ell_i = r_i - 6K$, this gives $v_t < 2CK - 6K$. Hence

$$v_m - v_t > CK + 6K > K > R. \tag{32}$$

Both remaining path pieces therefore leave the R-neighbourhood of their endpoint. They are the required two arms, so e satisfies condition (a). Notice that self-avoidance of γ ensures that deleting e does not damage either arm.

We have proved the pointwise implication

$$\{B_{3CK} \text{ is } CK\text{-crossed}\} \subset \{\text{every } B \in \mathbf{U} \text{ is } K\text{-crossed}\}. \tag{33}$$

The (s,t) construction verifies the inclusion directly. A global crossing cannot pass an unbridged candidate without leaving a short crossing inside it.

We next reveal the bridge geometry and recover a product of short-crossing probabilities. Reveal first every long edge. For each revealed open long edge $e = \{x, y\}$, also reveal every short edge lying within distance R of x or y. Let $\mathcal{F}$ be the resulting sigma-field. Stopping an arm at its first exit from the appropriate translate of B_R shows that the bridge status of every long edge is $\mathcal{F}$-measurable. Indeed, every long edge on the stopped arm was exposed in the first stage, while every short edge before the first exit has an endpoint within distance R of the arm's starting vertex and was exposed in the second stage. The exploration therefore knows whether both arms survive after deleting the distinguished edge. It also knows whether an open long edge is incident to J_i. Hence the bridge status of every candidate, and thus the random set $\mathbf{U}$, is known after this exploration.

For a fixed candidate, the K-crossing event is determined by the short edges with both endpoints in I_i. Indeed, applying the same first-entry and last-exit construction to any short crossing shows that the first and last vertices of the reduced witness lie within distance K of the candidate. More explicitly, for a short crossing path let s, t be defined by (29). Since $v_{s+1} \geq \ell_i$ and $|v_{s+1} - v_s| \leq K$,

$$v_s \geq \ell_i - K = c_i - 4K.$$

Similarly, $v_{t-1} < r_i$ and $|v_t - v_{t-1}| \leq K$ imply

$$v_t < r_i + K = c_i + 4K.$$

All intermediate vertices already lie in $[\ell_i, r_i)$, so the entire reduced witness is contained in I_i. Conversely, an open short path in I_i joining the two sides is plainly a K-crossing. Hence, with

$$\mathcal{E}_i^{\mathrm{loc}} := \{\{x,y\} : x, y \in I_i,\ |x-y| \le K\},$$

the event $X_i = \{B_{3K}^i \text{ is } K\text{-crossed}\}$ satisfies

$$X_i \in \sigma(\omega_e : e \in \mathcal{E}_i^{\mathrm{loc}}). \tag{34}$$

This is the localisation part of Lemma B.3.

If the candidate belongs to $\mathbf{U}$, condition (b) says that no open long edge has an endpoint in J_i. The distance from I_i to J_i^c is K, whereas $R < K$. The second revealing stage therefore does not expose any short edge internal to I_i. Moreover, the intervals I_i of distinct candidates are disjoint. Conditional on $\mathcal{F}$, the corresponding local short-edge families remain disjoint families of unrevealed Bernoulli variables. Their crossing events are thus independent and each retains probability $1 - \overline{p}(K)$. Independence is used only at this point in the crossing recurrence.

To spell out the adaptive-conditioning point, once the long-edge configuration is fixed, the second-stage set of revealed short edges is determined solely by the endpoints of the open long edges. It does not depend on the values of any short edge left unrevealed. Product structure therefore survives on the remaining coordinates. For every deterministic set $S \subset \mathcal{I}_C^{\mathrm{cand}}$, on the event that $\mathbf{U} = \{B_{3K}^i : i \in S\}$,

$$\mathbb{P}\left(\bigcap_{i\in S} X_i \,\middle|\, \mathcal{F}\right) = \prod_{i\in S} \mathbb{P}(X_i) = (1 - \overline{p}(K))^{|S|}. \tag{35}$$

The separation of the candidates is essential here: their centres differ by at least $9K$, while each I_i has length $8K$, so the determining families in (34) are disjoint.

Taking conditional probabilities in (33) gives DCGT (12):

$$\overline{p}(CK) \ge 1 - \mathbb{E}\Big[(1 - \overline{p}(K))^{|\mathbf{U}|}\Big]. \tag{36}$$

Set $t = \min\{\overline{p}(K), C^{-1}\}$. There are at most C candidates, so $0 \le t|\mathbf{U}| \le 1$. The inequalities $(1-t)^m \le e^{-tm}$ and $1 - e^{-s} \ge e^{-1}s$ for $0 \le s \le 1$ yield

$$\overline{p}(CK) \ge e^{-1}\mathbb{E}[|\mathbf{U}|] \min\{\overline{p}(K), C^{-1}\}. \tag{37}$$

The geometric problem has now been reduced to proving that the expected number of unbridged candidates is large.

It remains to estimate the bridge probability through its two-arm structure. Fix a long edge

$e = \{x, y\}$, and write

$$p_e = 1 - e^{-\beta_{\mathrm{tail}}/|x-y|^2}.$$

In the truncated configuration with e deleted, let A_x and A_y be the events that x and y, respectively, have an R-arm. The status of e is independent of all other Bernoulli variables, so

$$\mathbb{P}(e \text{ is a bridge}) = p_e\, \mathbb{P}(A_x \cap A_y). \tag{38}$$

Because $|x-y| > K > 2R$, the endpoint neighbourhoods $\Lambda_x := x + B_R$ and $\Lambda_y := y + B_R$ are disjoint. Let $\mathcal{J}_{x,y}$ be the family of truncated edges, other than e, with one endpoint in each neighbourhood, and let

$$G_{x,y} := \{\text{some edge in } \mathcal{J}_{x,y} \text{ is open}\}.$$

We separate the only source of overlap between the two arm explorations:

$$\mathbb{P}(A_x \cap A_y) \le \mathbb{P}(A_x \cap A_y \cap G_{x,y}^c) + \mathbb{P}(G_{x,y}). \tag{39}$$

On $G_{x,y}^c$, stop each arm at its first exit from its endpoint neighbourhood. The stopped x-arm uses edges internal to or leaving Λ_x, while the stopped y-arm uses the analogous family for Λ_y. Their only common coordinates are edges in $\mathcal{J}_{x,y}$, all of which are fixed closed on $G_{x,y}^c$. The remaining determining families are disjoint, so Bernoulli independence gives

$$\mathbb{P}(A_x \cap A_y \mid G_{x,y}^c) = \mathbb{P}(A_x \mid G_{x,y}^c)\mathbb{P}(A_y \mid G_{x,y}^c).$$

Forcing the joining edges closed can only decrease either increasing arm event. By translation invariance and by comparison with the untruncated one-arm event, each conditional factor is at most q_R. Hence

$$\mathbb{P}(A_x \cap A_y \cap G_{x,y}^c) \le q_R^2. \tag{40}$$

There are at most $|B_R|^2$ possible joining edges, and each has length at least $K - 2R$. By the union bound and (28),

$$\mathbb{P}(G_{x,y}) \le \varepsilon_{R,K}.$$

Combining the two alternatives with (38) gives the bridge estimate DCGT (14):

$$\mathbb{P}_{\beta_{\mathrm{tail}},\lambda}(e \text{ is a bridge}) \le p_e(q_R^2 + \varepsilon_{R,K}) \le \rho\left(1 - e^{-\beta_{\mathrm{tail}}/|e|^2}\right). \tag{41}$$

The estimate accounts separately for opening the distinguished edge and for the two arms that remain after its deletion. The separated endpoint neighbourhoods give near-factorisation, while the inverse-square tail makes the joining-edge error of order K^{-2}.

The deterministic argument says that long edges are the only way a global crossing can bypass a failed candidate. Equation (41) charges both the long edge and the two arms. The inequality $\rho < \theta^2$ leaves enough exponent to show that many candidates have no such bypass.

We can now count unbridged candidates. For a fixed candidate, let $\mathcal{E}_i^{\mathrm{span}}$ be the long edges with one endpoint left of ℓ_i and the other on or right of r_i, and let $\mathcal{E}_i^{\mathrm{near}}$ be the long edges with an endpoint in J_i. The block is unbridged exactly when every edge in the first family is not a bridge and every edge in the second family is closed. Both are decreasing events. Harris–FKG therefore yields

$$\mathbb{P}(B_{3K}^i \text{ is unbridged}) \geq \prod_{e \in \mathcal{E}_i^{\mathrm{span}}} \mathbb{P}(e \text{ is not a bridge}) \prod_{e \in \mathcal{E}_i^{\mathrm{near}}} \mathbb{P}(e \text{ is closed}). \tag{42}$$

For u sufficiently small, the slack $\rho < \eta$ implies

$$1 - \rho(1 - e^{-u}) \geq e^{-\eta u}.$$

After enlarging K_1, this applies to $u = \beta_{\mathrm{tail}}/|e|^2$ for every long edge. The bridge estimate then gives

$$\mathbb{P}(e \text{ is not a bridge}) \geq e^{-\beta_{\mathrm{tail}}\eta/|e|^2}.$$

The two products in (42) are controlled by the inverse-square kernel sums

$$\sum_{e \in \mathcal{E}_i^{\mathrm{span}}} \frac{1}{|e|^2} \leq \log C + c_2, \qquad \sum_{e \in \mathcal{E}_i^{\mathrm{near}}} \frac{1}{|e|^2} \leq 20. \tag{43}$$

Here is the counting behind the different scale behaviours. For a fixed length r, a spanning edge $\{z, z+r\}$ must satisfy $z < \ell_i$ and $z+r \geq r_i$. There are no such edges for $r < 6K$, and for $6K \leq r \leq CK$ there are at most r choices of z. Therefore

$$\sum_{e \in \mathcal{E}_i^{\mathrm{span}}} \frac{1}{|e|^2} \leq \sum_{r=6K}^{CK} \frac{r}{r^2} = \sum_{r=6K}^{CK} \frac{1}{r} \leq \log C + c_2. \tag{44}$$

This logarithm is the second decisive use of inverse-square decay in the failed-crossing proof. It converts the product of nonbridge probabilities into a power of C.

The nearby family behaves differently. There are $10K$ vertices in J_i, and for each such vertex at most two vertices at distance r. Even allowing double counting,

$$\sum_{e \in \mathcal{E}_i^{\mathrm{near}}} \frac{1}{|e|^2} \leq 10K \cdot 2 \sum_{r > K} \frac{1}{r^2} \leq 20. \tag{45}$$

Thus excluding nearby long edges costs only a scale-independent constant. The endpoint conventions in these two finite edge families are consolidated in Lemma B.4.

Equations (42) and (43) can now be read product by product. For the spanning edges,

$$\prod_{e\in\mathcal{E}_i^{\mathrm{span}}} \mathbb{P}(e \text{ is not a bridge}) \geq \exp\left[-\beta_{\mathrm{tail}}\eta \sum_{e\in\mathcal{E}_i^{\mathrm{span}}} |e|^{-2}\right] \geq e^{-\beta_{\mathrm{tail}}\eta c_2} C^{-\beta_{\mathrm{tail}}\eta}.$$

For the nearby edges, the exact Bernoulli closed probability gives

$$\prod_{e\in\mathcal{E}_i^{\mathrm{near}}} \mathbb{P}(e \text{ is closed}) = \exp\left[-\beta_{\mathrm{tail}} \sum_{e\in\mathcal{E}_i^{\mathrm{near}}} |e|^{-2}\right] \geq e^{-20\beta_{\mathrm{tail}}}.$$

Consequently there is a constant $c_4 > 0$, independent of i, C, K, such that

$$\mathbb{P}(B_{3K}^i \text{ is unbridged}) \geq c_4 C^{-\beta_{\mathrm{tail}}\eta}. \tag{46}$$

Now $\eta < \theta^2$. By choosing C_1 large enough, the power $C^{\beta_{\mathrm{tail}}(\theta^2-\eta)}$ absorbs c_4 and the fixed counting constant, giving uniformly for $C \geq C_1$

$$\mathbb{P}(B_{3K}^i \text{ is unbridged}) \geq 6e\, C^{-\beta_{\mathrm{tail}}\theta^2}. \tag{47}$$

The candidate-index set contains at least $C/6$ blocks once C_1 is large. Linearity of expectation, which does not require independence between candidates, now yields DCGT (13):

$$\mathbb{E}_{\beta_{\mathrm{tail}},\lambda}[|\mathbf{U}|] \geq e\, C^{1-\beta_{\mathrm{tail}}\theta^2}. \tag{48}$$

The exponent in this expectation has a direct scale interpretation. There are order C places at which a large crossing must negotiate a candidate block. For one fixed place, preventing a bridge across all scales up to CK costs order $C^{-\beta_{\mathrm{tail}}\theta^2}$: the logarithmic inverse-square energy contributes β_{tail}, while the two endpoint-arm density bounds contribute θ^2. Multiplying the number of locations by the one-location cost leaves

$$C \times C^{-\beta_{\mathrm{tail}}\theta^2} = C^{1-\beta_{\mathrm{tail}}\theta^2}.$$

Thus the value 1 is not introduced by an arbitrary choice of constants. It is the balance point between the linear growth in candidate locations and the power-law suppression of bridge-free locations. Below that balance the expected number of usable obstructions grows with the scale ratio; above it, this failed-crossing mechanism no longer supplies a growing factor.

Substituting (48) into (37). This gives

$$\overline{p}(CK) \geq C^{1-\beta_{\mathrm{tail}}\theta^2} \min\{\overline{p}(K), C^{-1}\},$$

which is (26). □

The induction variable is now the failed-crossing probability $\overline{p}(K)$. A failure at scale K survives at scale CK because order C candidate locations are available, while the inverse-square bridge cost removes only a factor $C^{\beta_{\text{tail}}\theta^2}$. When $\beta_{\text{tail}}\theta^2 < 1$, the remaining positive power of C prevents the obstruction probability from decaying through the scales. The theorem below turns that persistent local obstruction into a contradiction with percolation.

To obtain the density gap, assume that the percolation density m is positive but $\beta_{\text{tail}}m^2 < 1$, and choose $\theta > m$ with $\beta_{\text{tail}}\theta^2 < 1$. The failed-crossing recurrence then maintains a uniformly positive failure probability along geometric scales. Two failed side crossings, together with the closure of all longer edges crossing the annulus, prevent the central block from reaching the exterior; this annulus obstruction also has a scale-independent positive probability. On the other hand, positive percolation and the 0-1 law imply that expanding central blocks meet an infinite cluster with probability tending to one. The annulus crossing probability would therefore have to tend to one, which contradicts the uniform obstruction bound.

Reconstruction of the proof of DCGT Theorem 1 (ii). Let

$$m = \theta(\beta_{\text{tail}}, \lambda).$$

Assume for contradiction that $m > 0$ but $\beta_{\text{tail}}m^2 < 1$. Choose

$$m < \theta < \beta_{\text{tail}}^{-1/2}.$$

Let $C_1 = C_1(\beta_{\text{tail}}, \lambda, \theta)$ and $K_1 = K_1(\beta_{\text{tail}}, \lambda, \theta)$ be the thresholds supplied by Lemma 3.4, and fix an integer $K_0 \geq K_1$. Consider the cut-edge set

$$\mathcal{C}_{K_0} := \{\{x, y\} : x \leq -1,\ y \geq 0,\ |x - y| \leq K_0\}.$$

This set is finite. Every K_0-crossing path of B_{3K_0} starts at a negative vertex and ends at a nonnegative vertex. At its first visit to $[0, \infty)$, the path therefore uses an edge in $\mathcal{C}_{K_0}$. Consequently, closing every edge in $\mathcal{C}_{K_0}$ prevents a K_0-crossing. This is a finite closure event and has strictly positive probability, so

$$\overline{p}_{\beta_{\text{tail}},\lambda}(K_0) > 0. \tag{49}$$

Choose an integer $C \geq C_1$ so large that

$$C^{-1} \leq \overline{p}_{\beta_{\text{tail}},\lambda}(K_0),$$

and set $K_n = C^n K_0$. Since $K_n \geq K_1$ for every n and $C^{1-\beta_{\mathrm{tail}}\theta^2} \geq 1$, Lemma 3.4 gives

$$\overline{p}_{\beta_{\mathrm{tail}},\lambda}(K_{n+1}) \geq \min\{\overline{p}_{\beta_{\mathrm{tail}},\lambda}(K_n), C^{-1}\}.$$

The invariant is now a lower bound rather than an upper bound. At the initial scale, failure has positive probability because a finite cut can be closed. Choosing C^{-1} below that probability creates a floor. If $\overline{p}(K_n) \geq C^{-1}$, the minimum in the last display equals C^{-1}, and the positive exponent $1 - \beta_{\mathrm{tail}}\theta^2$ prevents the next-scale estimate from falling below that floor. Thus the recurrence does not claim that failures become more likely at every scale; it supplies exactly the uniform obstruction needed for the annulus argument. Induction therefore yields

$$\overline{p}_{\beta_{\mathrm{tail}},\lambda}(K_n) \geq C^{-1} \qquad (n \geq 0). \tag{50}$$

Define

$$A(K_n) := \{B_{3K_n} \leftrightarrow B^c_{9K_n}\},$$

and let $B(K_n)$ be the event that every edge of length strictly greater than K_n with at least one endpoint in B_{9K_n} is closed. The two side blocks are

$$B^{-2}_{3K_n} = [-9K_n, -3K_n), \qquad B^{2}_{3K_n} = [3K_n, 9K_n).$$

We claim the deterministic inclusion

$$\begin{aligned} B(K_n) \cap \{&B^{-2}_{3K_n} \text{ is not } K_n\text{-crossed}\} \\ &\cap \{B^{2}_{3K_n} \text{ is not } K_n\text{-crossed}\} \subset A(K_n)^c. \end{aligned} \tag{51}$$

To prove it, suppose instead that $A(K_n)$ occurs. Choose an open path $\gamma = (v_0, \dots, v_m)$ with $v_0 \in B_{3K_n}$, and stop it at its first exit $v_m \notin B_{9K_n}$. Thus

$$v_0, \dots, v_{m-1} \in B_{9K_n}.$$

On $B(K_n)$, every edge of this stopped path has length at most K_n, because each such edge has its initial endpoint in B_{9K_n}. If $v_m \geq 9K_n$, then $v_0 < 3K_n$, so the stopped path is a K_n-crossing of the right block $B^2_{3K_n}$. If $v_m < -9K_n$, reverse the stopped path: it then starts strictly to the left of $-9K_n$ and ends at $v_0 \geq -3K_n$, and hence is a K_n-crossing of the left block $B^{-2}_{3K_n}$. One of these two alternatives must occur, proving (51).

The event $B(K_n)$ uses only edge variables of length greater than K_n. Each of the two failed-crossing events in (51) uses only edge variables of length at most K_n. The product structure therefore makes $B(K_n)$ independent of the pair of failed-crossing events. The latter two events are decreasing, so

Harris–FKG and translation invariance give

$$\mathbb{P}_{\beta_{\mathrm{tail}},\lambda}\Big(\{B_{3K_n}^{-2} \text{ is not } K_n\text{-crossed}\} \cap \{B_{3K_n}^{2} \text{ is not } K_n\text{-crossed}\}\Big) \geq \overline{p}_{\beta_{\mathrm{tail}},\lambda}(K_n)^2.$$

No independence between the two side-block events is needed. Taking probabilities in (51) now yields

$$1 - \mathbb{P}_{\beta_{\mathrm{tail}},\lambda}[A(K_n)] \geq \mathbb{P}_{\beta_{\mathrm{tail}},\lambda}[B(K_n)]\, \overline{p}_{\beta_{\mathrm{tail}},\lambda}(K_n)^2. \tag{52}$$

The probability of $B(K_n)$ satisfies

$$\begin{aligned}\mathbb{P}_{\beta_{\mathrm{tail}},\lambda}[B(K_n)] &= \exp\left[-\beta_{\mathrm{tail}} \sum_{\substack{\{x,y\}:\ |x-y|>K_n \\ \{x,y\}\cap B_{9K_n}\neq\varnothing}} \frac{1}{|x-y|^2}\right] \\ &\geq \exp\left[-\beta_{\mathrm{tail}} |B_{9K_n}|\, 2 \sum_{r>K_n} \frac{1}{r^2}\right] \geq \mathrm{e}^{-36\beta_{\mathrm{tail}}} =: c_1(\beta_{\mathrm{tail}}) > 0.\end{aligned}$$

Combining this with (50) and (52) gives the uniform upper bound

$$\mathbb{P}_{\beta_{\mathrm{tail}},\lambda}[A(K_n)] \leq 1 - \frac{c_1(\beta_{\mathrm{tail}})}{C^2} < 1 \qquad \text{for every } n. \tag{53}$$

Let

$$\mathcal{I} = \{\text{there exists an infinite open cluster in } \mathbb{Z}\}.$$

This is a tail event for the countable independent family of edge variables: adding finitely many edges can join only finitely many finite clusters and cannot create an infinite cluster, while deleting finitely many edges from an infinite connected graph leaves at least one infinite component. Kolmogorov's 0-1 law gives

$$\mathbb{P}_{\beta_{\mathrm{tail}},\lambda}(\mathcal{I}) \in \{0, 1\}.$$

Since

$$\mathbb{P}_{\beta_{\mathrm{tail}},\lambda}(\mathcal{I}) \geq \mathbb{P}_{\beta_{\mathrm{tail}},\lambda}(0 \leftrightarrow \infty) = m > 0,$$

we have $\mathbb{P}_{\beta_{\mathrm{tail}},\lambda}(\mathcal{I}) = 1$.

Set

$$E_n = \{\text{some } x \in B_{K_n} \text{ belongs to an infinite cluster}\}.$$

The events E_n increase to $\mathcal{I}$, so continuity from below gives $\mathbb{P}_{\beta_{\mathrm{tail}},\lambda}(E_n) \to 1$. Since an infinite path starting in B_{K_n} must leave B_{9K_n}, one has $E_n \subset A(K_n)$. Hence $\mathbb{P}_{\beta_{\mathrm{tail}},\lambda}[A(K_n)] \to 1$, in contradiction with the uniform bound (53). The assumption was impossible, and

$$\theta(\beta_{\text{tail}}, \lambda) > 0 \quad \Longrightarrow \quad \beta_{\text{tail}}\theta(\beta_{\text{tail}}, \lambda)^2 \geq 1. \tag{54}$$

□

Remark (The same exponent in the two recurrences). The existence and density-gap proofs use the same inverse-square exponent in opposite ways. In the good-block argument, a defect at distance d from the nearer boundary creates two dense connected sets. Closing every edge between them has probability at most

$$\left(\frac{c_\star}{d}\right)^{\beta_{\text{tail}}\theta^2}.$$

The defect may occur at any distance, so the proof needs the series $\sum_d d^{-\beta_{\text{tail}}\theta^2}$ to converge. Establishing positive percolation density through this construction therefore uses $\beta_{\text{tail}}\theta^2 > 1$.

In the failed-crossing argument, one does not sum over an unbounded list of defect distances. Instead, a parent of scale CK contains order C candidate blocks, and one candidate is unbridged with probability of order $C^{-\beta_{\text{tail}}\theta^2}$. Their expected number is therefore of order

$$C^{1-\beta_{\text{tail}}\theta^2}.$$

To keep a positive supply of obstructions as the scale ratio grows, the proof uses $\beta_{\text{tail}}\theta^2 < 1$. The borderline value is the same because both estimates come from a logarithmic inverse-square energy; only the combinatorial question surrounding that energy has changed.

This also clarifies the logical division between the two halves of Theorem 1. The first half does not locate the critical point: for $\beta_{\text{tail}} > 1$, it makes the nearest-neighbour intensity large enough to start a contractive good-block iteration. The second half does not construct the infinite cluster: assuming it already exists, it rules out densities strictly below $\beta_{\text{tail}}^{-1/2}$. Together they exhibit the DCGT mechanism behind the jump. Dense components can be constructed when the disconnection costs are summable, and a hypothetical smaller positive density would force nonsummable crossing obstructions at arbitrarily large scales.

The failed-crossing proof itself has separated three layers that will be reused in the FK setting. Deterministically, the (s, t) construction turns a global crossing into a short local crossing or a bridge. Probabilistically, the long-edge exploration leaves local crossing events inside protected candidates, while the bridge estimate pays for two endpoint arms. The annulus argument converts a persistent local obstruction into a contradiction with percolation. The FK extension keeps these three geometric layers and changes only the conditional probability estimates.

3.4 Long-range FK, Ising and Potts models

The Bernoulli argument above uses independence in two conceptually different ways. In the good-block recursion, it is used to estimate the probability that two macroscopic clusters fail to merge. In the failed-crossing recursion, it is used after an exploration to factor the crossing events of several well-separated blocks. Neither factorisation remains valid for the FK random-cluster model when $q > 1$ [DCGT24].

Deterministic part. Good and bad blocks, dense clusters, defect zones, truncated crossings, candidate blocks and bridges are events of the underlying open-edge configuration. The overlap lemma for consecutive dense blocks, the two-defect/one-defect inclusion, the (s, t) path decomposition, and the annulus obstruction are therefore deterministic statements. Boundary wiring changes their probabilities, but it does not create an actual open edge or an actual crossing path. These pieces will be cited directly from the Bernoulli proof.

Loss of factorisation. Even when two blocks use disjoint edge sets, their badness events need not be independent under an FK measure: both interact through the cluster-count factor and the exterior boundary partition. Likewise, after revealing the long edges, the remaining short crossings are generally coupled. Direct product estimates from the Bernoulli proof cannot simply be copied.

FK replacements. The spatial Markov property turns every explored exterior configuration into an induced boundary partition on the unexplored graph. Worst-boundary probabilities give estimates uniform in that random partition; the single-edge conditional law controls open and closed long edges; and FKG replaces products of decreasing events by lower bounds. The FK proof below is organised to identify each replacement at the exact point where the Bernoulli proof used independence.

Remark (Proof architecture). The deterministic geometry of the Bernoulli renormalisation argument does not change. Only the probabilistic estimates must be replaced.

For the existence result, a mesoscopic open edge is first used to merge the two macroscopic clusters. Once that merger has occurred, all remaining edges between the two clusters again have their Bernoulli conditional law.

For the density-gap result, one never attempts to recover independence. Instead, every conditional crossing probability is bounded uniformly over the random boundary condition generated by the exploration, and products of decreasing events are controlled from below using FKG.

3.4.1 The FK specification and its basic properties

Let $S \subset T$ be finite subsets of $\mathbb{Z}$. Denote by $\mathfrak{B}(S, T)$ the finite set of partitions of $T \setminus S$; its elements are the admissible boundary conditions for the active set S in the ambient set T. For $\xi \in \mathfrak{B}(S, T)$, write

$$E(S,T) := \{\{i,j\} \subset T : \{i,j\} \cap S \neq \varnothing\}.$$

On configurations $\omega \in \{0,1\}^{E(S,T)}$, define

$$\mathbb{P}^{\xi}_{S,T,\beta_{\mathrm{tail}},\lambda,q}[\omega] = \frac{q^{k(\omega^{\xi})}}{Z^{\xi}_{S,T,\beta_{\mathrm{tail}},\lambda,q}} \prod_{\{i,j\}\in E(S,T)} p_{i,j}(\beta_{\mathrm{tail}},\lambda)^{\omega_{i,j}} \big(1-p_{i,j}(\beta_{\mathrm{tail}},\lambda)\big)^{1-\omega_{i,j}}. \tag{55}$$

Here $\omega_{i,j} = 1$ means that $\{i,j\}$ is open, ω^{ξ} is obtained by identifying all vertices belonging to the same element of ξ, and $k(\omega^{\xi})$ denotes the number of connected components after these identifications. The partition with a single boundary class is denoted by $\xi = 1$ and called the wired boundary condition; the partition into singletons is denoted by $\xi = 0$ and called the free boundary condition [FK72].

We use the following connectivity convention. A cluster *inside a block* is always computed from actual open edges with both endpoints in that block, and a K-crossing is always an actual open path in the underlying configuration ω. Boundary identifications in ω^{ξ} affect the cluster weight in (55) and the induced single-edge conditional law, but wiring is not counted as an open path when block goodness or block crossing is defined. We write $x \leftrightarrow y$ in ω^{ξ} only when connectivity in the quotient graph is intended explicitly.

Let $\mathfrak{B}(S)$ be the set of partitions of $\mathbb{Z} \setminus S$. For $\xi \in \mathfrak{B}(S)$, let $\mathbb{P}^{\xi}_{S,\beta_{\mathrm{tail}},\lambda,q}$ be the infinite-volume limit of $\mathbb{P}^{\xi_K}_{S,B_K,\beta_{\mathrm{tail}},\lambda,q}$, where ξ_K is the partition induced on $B_K \setminus S$. The wired infinite-volume FK measure is

$$\mathbb{P}^{1}_{\beta_{\mathrm{tail}},\lambda,q} = \lim_{K\to\infty} \mathbb{P}^{1}_{B_K,\beta_{\mathrm{tail}},\lambda,q},$$

and throughout the FK subsection we use the shorthand

$$\mathbb{P}^{\xi}_{K,\beta_{\mathrm{tail}},\lambda,q} := \mathbb{P}^{\xi}_{B_K,\beta_{\mathrm{tail}},\lambda,q}, \qquad \xi \in \mathfrak{B}(B_K). \tag{56}$$

Here and below $(\beta_{\mathrm{tail}},\lambda)$ are the DCGT edge-intensity parameters. They are kept distinct from the physical inverse temperatures introduced later. The wired percolation density is

$$\theta(q,\beta_{\mathrm{tail}},\lambda) := \mathbb{P}^{1}_{\beta_{\mathrm{tail}},\lambda,q}[0 \leftrightarrow \infty]. \tag{57}$$

When $q = 1$, the factor $q^{k(\omega^{\xi})}$ is identically one, and (55) is precisely the Bernoulli product measure. For $q \neq 1$, the cluster factor couples the edge states. Three properties describe how this dependence enters the proof. When a statement is uniform in the finite active graph and its boundary partition, we write ϕ^{ξ} for an arbitrary FK measure of the form (55).

1. The single-edge conditional law. Let $e = \{x,y\}$, write $p_e = p_{x,y}(\beta_{\mathrm{tail}},\lambda)$, and condition on the states of every edge except e. If x and y are already connected in $\omega^{\xi} \setminus \{e\}$, opening e does not change the number of clusters. Consequently,

$$\phi^\xi(\omega_e = 1 \mid \omega_{E\setminus\{e\}}) = p_e, \qquad \phi^\xi(\omega_e = 0 \mid \omega_{E\setminus\{e\}}) = 1 - p_e.$$

If x and y are not connected without e, opening e merges two clusters and therefore removes one factor q. In that case,

$$\phi^\xi(\omega_e = 1 \mid \omega_{E\setminus\{e\}}) = \frac{p_e}{p_e + q(1-p_e)},$$

and

$$\phi^\xi(\omega_e = 0 \mid \omega_{E\setminus\{e\}}) = \frac{q(1-p_e)}{p_e + q(1-p_e)}.$$

Thus

$$\phi^\xi(\omega_e = 1 \mid \omega_{E\setminus\{e\}}) = \begin{cases} p_e, & x \leftrightarrow y \text{ in } \omega^\xi \setminus \{e\}, \\ \dfrac{p_e}{p_e + q(1-p_e)}, & x \not\leftrightarrow y \text{ in } \omega^\xi \setminus \{e\}. \end{cases} \tag{58}$$

For $q \geq 1$, this gives the two inequalities

$$\phi^\xi(\omega_e = 1 \mid \omega_{E\setminus\{e\}}) \leq p_e, \qquad \phi^\xi(\omega_e = 0 \mid \omega_{E\setminus\{e\}}) \geq 1 - p_e. \tag{59}$$

The first inequality will be used to bound the probability that a long edge is a bridge. The second will be used to force collections of long edges to be closed.

For the existence proof, we also need an upper bound on the conditional probability that an edge is closed. Write

$$\tau_e := -\log(1 - p_e).$$

Thus $\tau_e = \lambda$ for a nearest-neighbour edge and $\tau_e = \beta_{\text{tail}} J_{x,y}$ for $|x - y| \geq 2$. For every $q > 0$,

$$\phi^\xi(\omega_e = 0 \mid \omega_{E\setminus\{e\}}) \leq w_q(\tau_e) := \mathrm{e}^{-\tau_e} \vee \frac{q\mathrm{e}^{-\tau_e}}{1 - \mathrm{e}^{-\tau_e} + q\mathrm{e}^{-\tau_e}}. \tag{60}$$

Moreover, with

$$c_q := \begin{cases} 1, & 0 < q \leq 1, \\ (2q)^{-1}, & q \geq 1, \end{cases}$$

one has

$$w_q(\tau) \leq \mathrm{e}^{-c_q \tau}, \qquad \tau \geq 0. \tag{61}$$

For $q \geq 1$,

$$\frac{q\mathrm{e}^{-\tau}}{1 - \mathrm{e}^{-\tau} + q\mathrm{e}^{-\tau}} = \frac{q}{\mathrm{e}^{\tau} + q - 1}.$$

The function

$$g_q(\tau) := \log(\mathrm{e}^\tau + q - 1) - \log q - \frac{\tau}{2q}$$

satisfies $g_q(0) = 0$, while

$$g_q'(\tau) = \frac{\mathrm{e}^\tau}{\mathrm{e}^\tau + q - 1} - \frac{1}{2q} \geq \frac{1}{2q} > 0.$$

Hence $q/(\mathrm{e}^\tau + q - 1) \leq \mathrm{e}^{-\tau/(2q)}$. For $0 < q \leq 1$, the second term in (60) is at most $\mathrm{e}^{-\tau}$. This proves (61). The estimate is uniform in the exterior configuration, the active graph, and the boundary partition. It is weaker than the Bernoulli value when $q > 1$, but remains strong enough for the existence proof, which therefore works for every $q > 0$.

A consequence of (58) is the following. If a conditioning has already connected all endpoints of a collection of unrevealed edges, then the cluster count no longer depends on those edge states. On that collection, the conditional FK measure therefore factorises exactly as a Bernoulli product measure. These single-edge facts and the spatial Markov property below are standard consequences of the random-cluster specification [FK72].

2. The spatial Markov property. Suppose that some collection of edges has been revealed. The conditional law of the remaining edges is again an FK measure with the same edge parameters, but with a boundary condition induced by the revealed open connections. In particular, all the dependence created by the exterior configuration is encoded by a random partition $\xi(\omega)$ of the boundary vertices.

Maxima or minima over all boundary conditions are introduced for this reason. After an exploration, the induced partition is random and may have arbitrary complexity, but a worst-boundary-condition estimate remains valid regardless of which partition occurs.

3. Monotonicity and FKG. For $q \geq 1$, FK measures are positively associated. Thus, for two increasing events A and B,

$$\phi^\xi(A \cap B) \geq \phi^\xi(A)\phi^\xi(B).$$

The same inequality holds when both events are decreasing.

Moreover, for increasing events, free and wired boundary conditions satisfy

$$\phi^0(A) \leq \phi^\xi(A) \leq \phi^1(A).$$

Consequently, the probability of a decreasing bad-block event is maximised by the free boundary condition, whereas the probability of an increasing crossing event is maximised by the wired boundary condition. DCGT define the relevant quantities by taking maxima over all boundary conditions and do not need to use the identity of these extremizers. These positive-association and boundary-monotonicity statements follow from the FKG lattice condition for $q \geq 1$ [FKG71; FK72].

Theorem 3.5 (DCGT Theorem 4, restated in our notation: FK case)**.** *For every $q \geq 1$, the following statements hold [DCGT24].*

(i) *If $\beta_{\text{tail}} > 1$, then*

$$\theta(q, \beta_{\text{tail}}, \lambda) > 0 \quad \textit{for all sufficiently large finite } \lambda. \tag{62}$$

(ii) *For every $\beta_{\text{tail}}, \lambda > 0$,*

$$\theta(q, \beta_{\text{tail}}, \lambda) > 0 \quad \Longrightarrow \quad \beta_{\text{tail}}\theta(q, \beta_{\text{tail}}, \lambda)^2 \geq 1. \tag{63}$$

3.4.2 The FK good-block recursion

We reconstruct the proof of Theorem 3.5(i) through the probabilistic steps in the FK good-block argument of DCGT [DCGT24]. Fix $\beta_{\text{tail}} > 1$. Choose

$$\theta_\infty \in (3/4, 1) \quad \text{and} \quad \delta \in (0, 1)$$

so that

$$\beta_{\text{tail}}\theta_\infty^2(1 - \delta) > 1. \tag{64}$$

The role of δ is to absorb the small loss in the exponent caused by the mesoscopic FK argument.

The target is the same next-scale recurrence as in the Bernoulli case. The bad parent is decomposed into the same two obstructions. The two-defect case is the easier one: reveal one block and use the worst boundary probability for the other. In the one-defect case, the geometry again produces two large connected sets, but their cross-edges are dependent. We first expose a mesoscopic edge whose opening merges the two sets in the FK connectivity relation. Conditional on that merger, the remaining cross-edges have their Bernoulli conditional law; before the merger, the uniform closed-edge bound controls the denominator. The inverse-square cross-energy is unchanged, while the parameter δ absorbs the bounded loss caused by the mesoscopic step.

Define the worst-boundary-condition bad-block probability by

$$p_{q,\beta_{\text{tail}},\lambda}(K, \theta) := \max_{\xi \in \mathfrak{B}(B_K)} \mathbb{P}^{\xi}_{K,\beta_{\text{tail}},\lambda,q}[B_K \text{ is } \theta\text{-bad}]. \tag{65}$$

We will prove the FK analogue of Lemma 3.2: after choosing C_0 sufficiently large,

$$p_{q,\beta_{\text{tail}},\lambda}\left(CK, \theta - \frac{C_0}{C}\right) \leq \frac{1}{100} p_{q,\beta_{\text{tail}},\lambda}(K, \theta) + 2C^2 p_{q,\beta_{\text{tail}},\lambda}(K, \theta)^2 \tag{66}$$

for $C \geq C_0$, $K \geq 2$, and $\theta \geq \theta_\infty$.

Fix these parameters and an arbitrary parent boundary condition $\zeta \in \mathfrak{B}(B_{CK})$. Until the maximum over ζ is taken at the end, every probability in the good-block proof is evaluated under $\mathbb{P}^{\zeta}_{CK,\beta_{\text{tail}},\lambda,q}$.

The deterministic two-defect/one-defect decomposition from the proof of Lemma 3.2 is unchanged. If the large block B_{CK} is bad, then either:

1. there are two disjoint bad K-blocks inside B_{CK}; or
2. there is one defective block B_K^i, while all blocks away from B_K^{i-1}, B_K^i, and B_K^{i+1} are good, but the two large clusters on the two sides of this defect fail to merge.

We treat these two possibilities separately.

Two disjoint bad blocks under arbitrary boundary conditions. Let D_i and D_j be the events that two disjoint K-blocks are bad. Reveal the complete edge configuration outside the second block B_K^j, and denote the resulting sigma-field by $\mathcal{R}_j$. Since $B_K^i \cap B_K^j = \varnothing$, all edge variables determining D_i have been revealed, so $D_i \in \mathcal{R}_j$. The spatial Markov property identifies the conditional law of the still-active edges in B_K^j with an FK measure having a random induced boundary condition $\xi_j(\omega) \in \mathfrak{B}(B_K^j)$. Therefore, almost surely,

$$\mathbb{P}^{\zeta}_{CK,\beta_{\mathrm{tail}},\lambda,q}(D_j \mid \mathcal{R}_j) \le p_{q,\beta_{\mathrm{tail}},\lambda}(K,\theta).$$

The same spatial Markov argument, now applied to B_K^i, gives $\mathbb{P}^{\zeta}_{CK,\beta_{\mathrm{tail}},\lambda,q}(D_i) \le p_{q,\beta_{\mathrm{tail}},\lambda}(K,\theta)$. The tower property now yields

$$\begin{aligned}\mathbb{P}^{\zeta}_{CK,\beta_{\mathrm{tail}},\lambda,q}(D_i \cap D_j) &= \mathbb{E}^{\zeta}_{CK,\beta_{\mathrm{tail}},\lambda,q}\left[\mathbf{1}_{D_i}\mathbb{P}^{\zeta}_{CK,\beta_{\mathrm{tail}},\lambda,q}(D_j \mid \mathcal{R}_j)\right] \\ &\le p_{q,\beta_{\mathrm{tail}},\lambda}(K,\theta)\mathbb{P}^{\zeta}_{CK,\beta_{\mathrm{tail}},\lambda,q}(D_i) \\ &\le p_{q,\beta_{\mathrm{tail}},\lambda}(K,\theta)^2.\end{aligned}$$

After a union bound over the possible pairs,

$$\mathbb{P}^{\zeta}_{CK,\beta_{\mathrm{tail}},\lambda,q}[\text{two disjoint bad } K\text{-blocks}] \le \binom{2C-1}{2} p_{q,\beta_{\mathrm{tail}},\lambda}(K,\theta)^2 \le 2C^2 p_{q,\beta_{\mathrm{tail}},\lambda}(K,\theta)^2. \tag{67}$$

This is the first place where the spatial Markov property and the maximum over boundary conditions replace Bernoulli independence.

The mesoscopic one-defect estimate. For $|i| \le C-1$, let E_i be the event that B_K^i is bad and that every K-block B_K^j with

$$j \in [-C+1, C-1] \setminus \{i-1, i, i+1\}$$

is good. Let

$$F_i := E_i \cap \left\{ B_{CK} \text{ is } \left(\theta - \frac{C_0}{C}\right)\text{-bad} \right\}.$$

Put

$$d_i := C - |i|, \qquad M_i := \left\lfloor \frac{K d_i}{2} \right\rfloor .$$

The defect-location statement in Lemma B.1 applies verbatim, so

$$F_i = \varnothing \qquad \text{whenever } |i| > C - C_0 \quad \text{or, equivalently, } d_i < C_0. \tag{68}$$

On E_i, define $\mathbf{C}^- = \mathbf{C}_i^-$ and $\mathbf{C}^+ = \mathbf{C}_i^+$ exactly as in the Bernoulli proof, using the same deterministic tie-breaking rule for a largest cluster in each good block. The overlap argument is deterministic, so both sets are connected. The same lemma gives

$$|\mathbf{C}^-|, |\mathbf{C}^+| \geq \frac{K}{2} d_i \geq M_i. \tag{69}$$

Write the vertices nearest the defect in the order

$$Ki > x_1 > x_2 > \cdots, \qquad Ki < y_1 < y_2 < \cdots,$$

where $x_a \in \mathbf{C}^-$ and $y_b \in \mathbf{C}^+$. The deterministic ordered-point estimate (15) gives

$$\theta(y_b - x_a) \leq 6K + a + b, \qquad 1 \leq a, b \leq M_i. \tag{70}$$

Consequently, Lemma B.2 yields

$$\begin{aligned} \sum_{x \in \mathbf{C}^-} \sum_{y \in \mathbf{C}^+} J_{x,y} &\geq \theta^2 \sum_{a=1}^{M_i} \sum_{b=1}^{M_i} \frac{1}{(6K + a + b)^2} \\ &\geq \theta^2 \log\left(\frac{d_i}{c_\star}\right), \qquad c_\star = 48. \end{aligned} \tag{71}$$

In the Bernoulli model, the probability that every edge between $\mathbf{C}^-$ and $\mathbf{C}^+$ is closed is therefore at most

$$\mathrm{e}^{-\beta_{\mathrm{tail}} \sum_{x \in \mathbf{C}^-} \sum_{y \in \mathbf{C}^+} J_{x,y}} \leq \left(\frac{c_\star}{d_i}\right)^{\beta_{\mathrm{tail}} \theta^2}.$$

For FK percolation, these cross-edges are neither independent of the conditioning nor independent of each other. This is the only genuinely new part of the existence proof [DCGT24].

Reduction to an FK measure on the cross-edges. Let $\mathcal{H}_i^{\mathrm{FK}}$ be the sigma-field generated by all edge variables internal to the K-blocks used to determine the events E_i, the distinguished clusters, and the unions $\mathbf{C}^-$ and $\mathbf{C}^+$. The deterministic tie-breaking rule makes both sets $\mathcal{H}_i^{\mathrm{FK}}$-measurable. As in the Bernoulli conditioning argument in the proof of Lemma 3.2, every edge joining $\mathbf{C}^-$ to $\mathbf{C}^+$ has length greater than $2K$, whereas an edge internal to a K-block has length at most $2K - 1$. No cross-edge therefore belongs to the determining family of $\mathcal{H}_i^{\mathrm{FK}}$.

Let G be the graph whose vertex set is $\mathbf{C}^- \cup \mathbf{C}^+$ and whose edge set consists of all edges $\{x, y\}$ with

$$x \in \mathbf{C}^-, \qquad y \in \mathbf{C}^+.$$

Condition further on the full configuration of every non-cross-edge, and call the enlarged sigma-field $\mathcal{G}_i^{\mathrm{FK}}$. This complete conditioning fixes every wiring relation induced outside the cross-edge graph. By the spatial Markov property, on every realisation of $\mathcal{G}_i^{\mathrm{FK}}$ the conditional law on G is an FK measure ϕ_G^ξ with an induced boundary partition ξ. The open paths already revealed inside $\mathbf{C}^-$ wire all vertices of that side together into one boundary class in ξ, and the same is true of $\mathbf{C}^+$.

If ξ already wires $\mathbf{C}^-$ to $\mathbf{C}^+$, then the cluster count is independent of every edge in G. The cross-edges are therefore independent Bernoulli edges and the preceding Bernoulli estimate applies without modification:

$$\phi_G^\xi[\text{all cross-edges are closed}] \le \left(\frac{c_\star}{d_i}\right)^{\beta_{\mathrm{tail}}\theta^2}. \tag{72}$$

Suppose from now on that the induced boundary partition does not wire the two sides together. Define the mesoscopic ratio

$$R_i^{\mathrm{mes}} := \left\lfloor d_i^\delta \right\rfloor.$$

After enlarging C_0, if necessary, we may and do assume that

$$R_i^{\mathrm{mes}} \ge 4, \qquad R_i^{\mathrm{mes}} \le \frac{d_i}{3} \qquad (d_i \ge C_0).$$

Let

$$I_i^{\mathrm{mes}} := [Ki - KR_i^{\mathrm{mes}}, Ki + KR_i^{\mathrm{mes}}).$$

Within the cross-edge graph G, define

- $\mathcal{A}_i$: every cross-edge whose two endpoints lie in I_i^{mes} is closed;
- $\mathcal{B}_i$: every remaining cross-edge in G is closed.

Thus

$$\mathcal{A}_i \cap \mathcal{B}_i = \{\text{no cross-edge joins } \mathbf{C}^- \text{ to } \mathbf{C}^+\}. \tag{73}$$

All events here involve finitely many edges, and every edge parameter lies strictly between zero and one. Finite energy gives $\phi_G^\xi(\mathcal{B}_i) > 0$ and $\phi_G^\xi(\mathcal{A}_i^c \cap \mathcal{B}_i) > 0$; in particular, $\phi_G^\xi(\mathcal{A}_i^c \mid \mathcal{B}_i) > 0$. Thus every conditional probability in the following Bayes manipulation is defined:

$$\phi_G^\xi(\mathcal{A}_i \cap \mathcal{B}_i) \le \phi_G^\xi(\mathcal{B}_i) = \frac{\phi_G^\xi(\mathcal{B}_i \mid \mathcal{A}_i^c)\phi_G^\xi(\mathcal{A}_i^c)}{\phi_G^\xi(\mathcal{A}_i^c \mid \mathcal{B}_i)} \le \frac{\phi_G^\xi(\mathcal{B}_i \mid \mathcal{A}_i^c)}{\phi_G^\xi(\mathcal{A}_i^c \mid \mathcal{B}_i)}. \tag{74}$$

We record the two deterministic energy estimates used below. Put

$$m_i := KR_i^{\mathrm{mes}} + 1, \qquad N_i := \lfloor \theta_\infty K(R_i^{\mathrm{mes}} - 4) \rfloor .$$

The distinct ordering of the vertices gives $x_a \leq Ki - a$ and $y_b \geq Ki + b$. Hence every cross-edge $\{x_a, y_b\}$ with $a, b \geq m_i$ belongs to the edge family defining $\mathcal{B}_i$. Using (70), and then integrating over the squares associated with the integer pairs, gives

$$\begin{aligned}\sum_{e \text{ tested by } \mathcal{B}_i} J_e &\geq \theta^2 \sum_{a=m_i}^{M_i} \sum_{b=m_i}^{M_i} \frac{1}{(6K + a + b)^2} \\ &\geq \theta^2 \log\left(\frac{(8K + m_i + M_i + 1)^2}{(8K + 2m_i)(8K + 2M_i + 2)}\right) \\ &\geq \theta^2 \log\left(\frac{d_i}{R_i^{\mathrm{mes}}}\right) - b_{\mathrm{num}}. \end{aligned} \tag{75}$$

Here and below $b_{\mathrm{num}} < \infty$ is a universal constant; the last line follows from $M_i \geq Kd_i/2 - 1$ and $R_i^{\mathrm{mes}} \leq d_i/3$.

For the inner edge family, the one-sided ordered-point bounds in Lemma B.1 show that $x_a, y_b \in I_i^{\mathrm{mes}}$ whenever $1 \leq a, b \leq N_i$. The integral evaluation in Lemma B.2 therefore gives a finite constant $b_{\mathrm{den}} = b_{\mathrm{den}}(\theta_\infty)$ such that

$$\begin{aligned}\sum_{e \text{ tested by } \mathcal{A}_i} J_e &\geq \theta^2 \sum_{a=1}^{N_i} \sum_{b=1}^{N_i} \frac{1}{(6K + a + b)^2} \\ &\geq \theta^2 \log\left(\frac{(8K + N_i)^2}{8K(8K + 2N_i)}\right) \\ &\geq \theta^2 \log R_i^{\mathrm{mes}} - b_{\mathrm{den}}. \end{aligned} \tag{76}$$

Increasing a fixed lower threshold R_0, if necessary, makes these estimates valid for every $R_i^{\mathrm{mes}} \geq R_0$. The constants are uniform in C, K, i, ζ, and the induced partition ξ.

We estimate the numerator and denominator in (74).

The numerator: one mesoscopic edge restores the Bernoulli law. Condition on the complete configuration of the mesoscopic cross-edges. On $\mathcal{A}_i^c$, at least one of them is open. Because each side has already been internally wired into one boundary class, that open cross-edge identifies the two classes; thereafter no remaining cross-edge can change the number of FK components. The cluster factor is therefore constant for every remaining cross-edge. Conditional on this complete mesoscopic configuration, the outer cross-edges factorise with closed probabilities $1 - p_e = \mathrm{e}^{-\beta_{\mathrm{tail}} J_e}$. Therefore (75) gives, uniformly over the conditioned mesoscopic configuration,

$$\begin{aligned}\phi_G^{\xi}(\mathcal{B}_i \mid \mathcal{A}_i^c) &\le \mathrm{e}^{-\beta_{\mathrm{tail}} \sum_{e \text{ tested by } \mathcal{B}_i} J_e} \\ &\le C_{\mathrm{num}} \left(\frac{R_i^{\mathrm{mes}}}{d_i}\right)^{\beta_{\mathrm{tail}}\theta^2},\end{aligned} \tag{77}$$

where $C_{\mathrm{num}} := \mathrm{e}^{\beta_{\mathrm{tail}} b_{\mathrm{num}}}$. The Bernoulli exponent $\beta_{\mathrm{tail}}\theta^2$ is recovered after the first open edge has merged the two clusters.

The denominator: the mesoscopic region is not completely closed. We have

$$\phi_G^{\xi}(\mathcal{A}_i^c \mid \mathcal{B}_i) = 1 - \phi_G^{\xi}(\mathcal{A}_i \mid \mathcal{B}_i).$$

Condition on $\mathcal{B}_i$, order the mesoscopic cross-edges deterministically, and reveal them sequentially as closed. At every step the exterior configuration and induced boundary partition may have changed, but (61) remains valid uniformly. The chain rule and (76) therefore give

$$\begin{aligned}\phi_G^{\xi}(\mathcal{A}_i \mid \mathcal{B}_i) &\le \mathrm{e}^{-c_q\beta_{\mathrm{tail}} \sum_{e \text{ tested by } \mathcal{A}_i} J_e} \\ &\le C_{\mathrm{den}} \left(R_i^{\mathrm{mes}}\right)^{-c_q\beta_{\mathrm{tail}}\theta^2},\end{aligned} \tag{78}$$

where

$$C_{\mathrm{den}} := \mathrm{e}^{c_q\beta_{\mathrm{tail}} b_{\mathrm{den}}}.$$

Choose $R_0 = R_0(q, \beta_{\mathrm{tail}}, \theta_\infty)$ so large that

$$C_{\mathrm{den}} R_0^{-c_q\beta_{\mathrm{tail}}\theta_\infty^2} \le \frac{1}{2},$$

and increase C_0 so that

$$R_i^{\mathrm{mes}} \ge R_0, \qquad R_i^{\mathrm{mes}} \le \frac{d_i}{3} \qquad \text{whenever } d_i \ge C_0.$$

Then

$$\phi_G^{\xi}(\mathcal{A}_i^c \mid \mathcal{B}_i) \ge \frac{1}{2}. \tag{79}$$

Combining (74), (77), and (79) gives

$$\phi_G^{\xi}(\mathcal{A}_i \cap \mathcal{B}_i) \le 2C_{\mathrm{num}} \left(\frac{R_i^{\mathrm{mes}}}{d_i}\right)^{\beta_{\mathrm{tail}}\theta^2} \le 2C_{\mathrm{num}} d_i^{-\beta_{\mathrm{tail}}\theta^2(1-\delta)}. \tag{80}$$

Together with the already-wired estimate (72), this yields, in both cases,

$$\phi_G^{\xi}[\text{all cross-edges are closed}] \leq C_{\mathrm{FK}} d_i^{-\beta_{\mathrm{tail}}\theta^2(1-\delta)}, \tag{81}$$

where

$$C_{\mathrm{FK}} := \max\{2C_{\mathrm{num}}, c_\star^{\beta_{\mathrm{tail}}}\}.$$

The constants $C_{\mathrm{num}}, C_{\mathrm{den}}$, and C_{FK} may depend on $q, \beta_{\mathrm{tail}}, \theta_\infty$, but not on C, K, i, ζ, or the induced partition ξ.

After integrating over all possible choices of $\mathbf{C}^-$, $\mathbf{C}^+$, and all previously revealed edges, (81) and the tower property give

$$\mathbb{P}^{\zeta}_{CK,\beta_{\mathrm{tail}},\lambda,q}(F_i) \leq \mathbb{P}^{\zeta}_{CK,\beta_{\mathrm{tail}},\lambda,q}(E_i) C_{\mathrm{FK}} d_i^{-\beta_{\mathrm{tail}}\theta^2(1-\delta)} \leq p_{q,\beta_{\mathrm{tail}},\lambda}(K,\theta) d_i^{-\beta_{\mathrm{tail}}\theta^2(1-\delta)} C_{\mathrm{FK}}. \tag{82}$$

For the last inequality, use $E_i \subset \{B_K^i \text{ is bad}\}$ and apply the spatial Markov property to the marginal in B_K^i.

By (64), the exponent is uniformly larger than one for $\theta \geq \theta_\infty$. Each value of $d_i = C - |i|$ occurs for at most two indices, and (68) removes every $d_i < C_0$. Increase C_0 once more so that

$$2C_{\mathrm{FK}} \sum_{d=C_0}^{\infty} d^{-\beta_{\mathrm{tail}}\theta_\infty^2(1-\delta)} \leq \frac{1}{100}. \tag{83}$$

Then

$$\sum_{i=-C+1}^{C-1} \mathbb{P}^{\zeta}_{CK,\beta_{\mathrm{tail}},\lambda,q}(F_i) \leq \frac{1}{100} p_{q,\beta_{\mathrm{tail}},\lambda}(K,\theta). \tag{84}$$

Together with the deterministic event decomposition and (67), this proves (66) under the arbitrary parent boundary condition ζ. Taking the maximum over $\zeta \in \mathfrak{B}(B_{CK})$ completes the proof of the recursion.

Initialisation and iteration. It remains to initialise the recursion uniformly over boundary conditions. For a nearest-neighbour edge,

$$1 - p_e = \mathrm{e}^{-\lambda}.$$

By the single-edge law,

$$\sup_{\xi, \omega_{E\setminus\{e\}}} \phi^{\xi}(\omega_e = 0 \mid \omega_{E\setminus\{e\}}) \leq \mathrm{e}^{-\lambda} \vee \frac{q\mathrm{e}^{-\lambda}}{1 - \mathrm{e}^{-\lambda} + q\mathrm{e}^{-\lambda}} \leq \mathrm{e}^{-c_q\lambda}.$$

If every nearest-neighbour edge in B_{C_1} is open, then B_{C_1} is θ_1-good for every fixed $\theta_1 < 1$. Sequentially exposing the at most $2C_1 - 1$ nearest-neighbour edges and using the uniform conditional estimate gives

$$p_{q,\beta_{\text{tail}},\lambda}(C_1, \theta_1) \le (2C_1 - 1)\mathrm{e}^{-c_q \lambda},$$

which can be made arbitrarily small by increasing λ.

Choose scales and densities by

$$C_{n+1} = (n+1)^3 C_1, \qquad K_{n+1} = C_{n+1} K_n, \qquad \theta_{n+1} = \theta_n - \frac{C_0}{C_{n+1}},$$

with $K_1 = C_1$, and choose $\theta_1 < 1$ and C_1 so that $\theta_n \ge \theta_\infty$ for every n. Setting

$$u_n := p_{q,\beta_{\text{tail}},\lambda}(K_n, \theta_n),$$

the recursion gives

$$u_{n+1} \le \frac{1}{100} u_n + 2C_{n+1}^2 u_n^2.$$

Set

$$v_n := C_n^2 u_n.$$

Since $C_{n+1}/C_n = ((n+1)/n)^3 \le 8$, the preceding recursion implies

$$v_{n+1} \le \frac{64}{100} v_n + 8192 v_n^2. \tag{85}$$

Choose

$$\delta_0 := \frac{1}{50000}.$$

Then

$$\frac{64}{100}\delta_0 + 8192\delta_0^2 = 0.0000160768 < 0.00002 = \delta_0.$$

Choose $\lambda < \infty$ so large that $v_1 \le \delta_0$. Equation (85) then gives inductively

$$v_n \le \delta_0, \qquad u_n \le \frac{\delta_0}{C_n^2} \qquad (n \ge 1).$$

The wired bad-block probability is bounded above by the worst-boundary quantity u_n. In particular,

$$\mathbb{P}^1_{\beta_{\text{tail}},\lambda,q}[B_{K_n} \text{ is } \theta_n\text{-good}] \ge 1 - u_n \ge \frac{1}{2}.$$

Since $\theta_n \ge \theta_\infty > 3/4$, a good block contains a cluster of cardinality at least $3K_n/2$. By translation invariance,

$$\frac{3K_n}{4} \le \mathbb{E}^1_{\beta_{\text{tail}},\lambda,q}\left[|\mathbf{C}(B_{K_n})|\mathbf{1}_{\{B_{K_n}\text{ is 3/4-good}\}}\right]$$
$$\le 2K_n\mathbb{P}^1_{\beta_{\text{tail}},\lambda,q}\left[0 \text{ belongs to a cluster of size at least } 3K_n/2\right].$$

It follows that

$$\mathbb{P}^1_{\beta_{\text{tail}},\lambda,q}\left[0 \text{ belongs to a cluster of size at least } 3K_n/2\right] \ge \frac{3}{8}.$$

Letting $n \to \infty$ proves

$$\theta(q, \beta_{\text{tail}}, \lambda) \ge \frac{3}{8} > 0.$$

This completes the reconstruction of Theorem 3.5(i). The argument up to this point did not use FKG; as observed by DCGT, the existence proof works for every $q > 0$.

The FK bad-block probability now obeys the same linear-plus-quadratic recurrence as its Bernoulli counterpart, uniformly over every boundary partition that an exterior configuration can induce. The deterministic dense-block geometry was reused verbatim; the only new work was to replace the two Bernoulli factorisations by spatial Markov conditioning and the mesoscopic merger estimate. The next subsection keeps the crossing and bridge geometry unchanged but needs both admissible conditional specifications and FKG to propagate failed crossings.

3.4.3 The FK failed-crossing recursion

We reconstruct the proof of Theorem 3.5(ii), conditional on the admissible-specification statement of DCGT recorded below. The density-gap proof is the FK modification of the failed-crossing recursion from Lemma 3.4 [DCGT24].

The goal is to keep a positive failed-crossing probability across scales under the wired FK law. The deterministic obstruction is exactly the Bernoulli one: a large crossing forces each candidate to be crossed or bridged. The new issue is probabilistic. An exploration produces a random active set and a random exterior partition, so the conditional crossing probability must be controlled uniformly over the admissible specifications generated by that exploration. The bridge estimate uses the FK single-edge upper bound and a worst-boundary two-arm probability; the abundance of unbridged blocks and the final annulus obstruction use FKG in place of independence. The inverse-square kernel enters through the same joining-edge and logarithmic spanning-edge sums as in the Bernoulli proof.

Imported input from DCGT. We use the admissible-specification statement that the conditional law generated by the sequential exploration belongs to the class entering the worst-boundary definition (86) [DCGT24, Section 3.3].

Concretely, when $S \subseteq B_{3K}$ and ξ is a boundary condition on the fixed exterior $\mathbb{Z} \setminus B_{3K}$, the shorthand $\mathbb{P}^{\xi}_{S,\beta_{\text{tail}},\lambda,q}$ denotes an admissible specification produced by that exploration. Information already revealed inside B_{3K} is inherited from the exploration; it is not an additional arbitrary partition of $\mathbb{Z} \setminus S$ over which the maximum below is taken. With this DCGT convention, define

$$\overline{p}_{q,\beta_{\text{tail}},\lambda}(K) := 1 - \max_{\substack{S \subseteq B_{3K} \\ \xi \text{ b.c. on } \mathbb{Z}\setminus B_{3K}}} \mathbb{P}^{\xi}_{S,\beta_{\text{tail}},\lambda,q}[B_{3K} \text{ is } K\text{-crossed}]. \tag{86}$$

Equivalently,

$$\overline{p}_{q,\beta_{\text{tail}},\lambda}(K) = \min_{\substack{S \subseteq B_{3K} \\ \xi \text{ b.c. on } \mathbb{Z}\setminus B_{3K}}} \mathbb{P}^{\xi}_{S,\beta_{\text{tail}},\lambda,q}[B_{3K} \text{ is not } K\text{-crossed}]. \tag{87}$$

The quantity in (86) is the one used in [DCGT24, Section 3.3]. Here the boundary condition is imposed on the fixed exterior $\mathbb{Z} \setminus B_{3K}$; it must not be interpreted as an arbitrary partition of $\mathbb{Z} \setminus S$. DCGT observe that the maximum is attained for $S = B_{3K}$ with wired exterior boundary. Consequently,

$$1 - \overline{p}_{q,\beta_{\text{tail}},\lambda}(K) = \mathbb{P}^{1}_{3K,\beta_{\text{tail}},\lambda,q}[B_{3K} \text{ is } K\text{-crossed}]. \tag{88}$$

The worst-boundary formulation is retained precisely for the admissible specifications generated by that exploration.

We also need the elementary strict bound

$$\theta(q, \beta_{\text{tail}}, \lambda) < 1. \tag{89}$$

Indeed, enumerate the edges incident to the origin and close the first N of them sequentially. The conditional lower bound in (59) gives

$$\mathbb{P}^{1}_{\beta_{\text{tail}},\lambda,q}[\text{the first } N \text{ incident edges are closed}] \geq \prod_{m=1}^{N} (1 - p_{e_m}).$$

Letting $N \to \infty$, continuity from above and summability of the inverse-square kernel yield

$$\mathbb{P}^{1}_{\beta_{\text{tail}},\lambda,q}[\text{every edge incident to 0 is closed}] \geq \mathrm{e}^{-2\lambda - 2\beta_{\text{tail}} \sum_{r\geq 2} r^{-2}} > 0.$$

On this event the origin has no actual open path to infinity, irrespective of boundary wiring, proving (89).

Assume, for contradiction, that

$$\theta_0 := \theta(q, \beta_{\text{tail}}, \lambda) > 0, \qquad \beta_{\text{tail}}\theta_0^2 < 1.$$

Fix a number ϑ satisfying

$$\theta_0 < \vartheta < \min\{1, \beta_{\text{tail}}^{-1/2}\}. \tag{90}$$

The FK analogue of Lemma 3.4 states that there are thresholds $C_1, K_1 < \infty$ and a constant

$$c_{\text{gap}} = c_{\text{gap}}(q, \beta_{\text{tail}}, \lambda, \vartheta) > 0$$

such that, for every $C \geq C_1$ and $K \geq K_1$,

$$\overline{p}_{q,\beta_{\text{tail}},\lambda}(CK) \geq c_{\text{gap}} C^{1-\beta_{\text{tail}}\vartheta^2} \min\left\{\overline{p}_{q,\beta_{\text{tail}},\lambda}(K), C^{-1}\right\}. \tag{91}$$

The multiplicative constant remains visible; only in the final iteration will one fixed C be chosen so that $c_{\text{gap}} C^{1-\beta_{\text{tail}}\vartheta^2} \geq 1$.

Short edges, long edges, and bridges. Let R_{arm} be the endpoint-arm radius chosen below, with $R_{\text{arm}} < K/2$. For the remainder of the FK gap proof, put

$$E^{(\leq CK)} := \{\{x, y\} \subset \mathbb{Z} : |x - y| \leq CK\}, \qquad \omega^{(\leq CK)} := \omega|_{E^{(\leq CK)}}.$$

Every FK arm, bridge, bridged-block, unbridged-block, and revealing event below is evaluated in $\omega^{(\leq CK)}$. The truncation does not change a CK-crossing, which already uses only edges of length at most CK. Call an edge *short* if $|e| \leq K$, and *long* if $K < |e| \leq CK$; no edge longer than CK enters the construction.

A long edge $e = \{x, y\}$ is a *bridge* if it is open in $\omega^{(\leq CK)}$ and, after deleting e, each endpoint has an actual open arm leaving its translate of $B_{R_{\text{arm}}}$. Define

$$\mathcal{I}_C^{\text{cand}} := \{i \in 3\mathbb{Z} : B_{3K}^i \subset B_{CK}\}.$$

For $i \in \mathcal{I}_C^{\text{cand}}$, put

$$c_i := 3Ki, \qquad \ell_i := c_i - 3K, \qquad r_i := c_i + 3K,$$

and

$$I_i := [c_i - 4K, c_i + 4K), \qquad J_i := [c_i - 5K, c_i + 5K).$$

A candidate block B_{3K}^i is *bridged* if either

(a) a bridge has one endpoint strictly to the left of ℓ_i and the other at or to the right of r_i; or

(b) an open long edge has an endpoint in J_i.

Otherwise it is *unbridged*. Define the random set

$$\mathbf{U} := \{B_{3K}^i : i \in \mathcal{I}_C^{\text{cand}} \text{ and } B_{3K}^i \text{ is unbridged in } \omega^{(\leq CK)}\}.$$

Distinct candidate centres are separated by at least $9K$.

Lemma B.3 gives the unchanged deterministic inclusion: if B_{3CK} is CK-crossed, then every block in $\mathbf{U}$ must be K-crossed. By (88) and the DLR property of the wired measure, therefore

$$1 - \overline{p}_{q,\beta_{\mathrm{tail}},\lambda}(CK) \leq \mathbb{P}^1_{\beta_{\mathrm{tail}},\lambda,q}[\text{every } B \in \mathbf{U} \text{ is } K\text{-crossed}]. \tag{92}$$

Conditional crossing estimates after exploration (DCGT (12)). For a short edge $f = \{u, v\}$ and a vertex z, set

$$\mathrm{dist}(f, z) := \min\{|u - z|, |v - z|\}.$$

The truncated configuration is exposed in two stages. First reveal every long edge, namely every edge with $K < |e| \leq CK$. Then, for each revealed open long edge $e = \{x, y\}$, reveal every short edge f satisfying

$$\min\{\mathrm{dist}(f, x), \mathrm{dist}(f, y)\} \leq R_{\mathrm{arm}}.$$

Let $\mathcal{F}_{\mathrm{FK}}$ be the sigma-field generated by all edge states exposed by this procedure.

This sigma-field determines all bridge statuses. To test the arm at one endpoint of an open long edge, stop a candidate path at its first exit from the corresponding translate of $B_{R_{\mathrm{arm}}}$. Every long edge on the stopped path was exposed in the first stage, and every short edge before the exit was exposed in the second. Hence each bridge event, each bridged-block event, and the random set $\mathbf{U}$ are $\mathcal{F}_{\mathrm{FK}}$-measurable.

For later conditioning, define the local short-edge family

$$\mathcal{E}_i^{\mathrm{loc}} := \big\{\{x, y\} : x, y \in I_i,\ |x - y| \leq K\big\}.$$

The deterministic localisation in Lemma B.3 applies verbatim: the event

$$X_i := \{B^i_{3K} \text{ is } K\text{-crossed}\}$$

is measurable with respect to the variables in $\mathcal{E}_i^{\mathrm{loc}}$. If $B^i_{3K} \in \mathbf{U}$, no open long edge has an endpoint in J_i. Moreover,

$$\mathrm{dist}(I_i, J_i^c) \geq K, \qquad R_{\mathrm{arm}} < K/2.$$

Thus none of the edges in $\mathcal{E}_i^{\mathrm{loc}}$ was exposed in the second stage. Distinct candidate centres are at distance at least $9K$, so the corresponding intervals I_i, and hence their localised edge families, are pairwise disjoint. This is precisely the buffered localisation used in the Bernoulli proof.

Fix a realisation of $\mathcal{F}_{\mathrm{FK}}$, and write the realised unbridged blocks from left to right as

$$\mathbf{U} = \{D_1, \ldots, D_m\}, \qquad D_j = B^{i_j}_{3K}, \quad i_1 < \cdots < i_m.$$

Reveal the *complete* localised configuration of D_1, followed by those of $D_2, \ldots, D_m$. Before revealing the j-th one, the available information is

$$\mathcal{G}_{j-1} := \mathcal{F}_{\mathrm{FK}} \vee \sigma\left(\omega_f : f \in \bigcup_{h<j} \mathcal{E}^{\mathrm{loc}}_{i_h}\right).$$

The sequential exposure is the exploration used in the FK failed-crossing argument of [DCGT24, Section 3.3]. By the domain Markov property, the conditional law of the unrevealed crossing-relevant edges is an admissible specification entering the worst-boundary quantity in (86). This specification step is imported from DCGT; no arbitrary partition of the complement of a random active set is being optimised here. Therefore, for every realisation of $\mathcal{G}_{j-1}$,

$$\mathbb{P}^1_{\beta_{\mathrm{tail}},\lambda,q}[X_{i_j} \mid \mathcal{G}_{j-1}] \le 1 - \overline{p}_{q,\beta_{\mathrm{tail}},\lambda}(K). \tag{93}$$

The conditioning records complete edge configurations. Recording only the abstract events that earlier blocks are crossed would not determine the conditional FK specification. Repeatedly applying the tower property to the indicators of the X_{i_j}'s and using (93) yields

$$\mathbb{P}^1_{\beta_{\mathrm{tail}},\lambda,q}[\text{every } B \in \mathbf{U} \text{ is } K\text{-crossed} \mid \mathcal{F}_{\mathrm{FK}}] \le \left(1 - \overline{p}_{q,\beta_{\mathrm{tail}},\lambda}(K)\right)^{|\mathbf{U}|}. \tag{94}$$

This is the FK replacement for the Bernoulli conditional product: no conditional independence is asserted.

Combining (92) and (94) gives

$$\overline{p}_{q,\beta_{\mathrm{tail}},\lambda}(CK) \ge 1 - \mathbb{E}^1_{\beta_{\mathrm{tail}},\lambda,q}\left[\left(1 - \overline{p}_{q,\beta_{\mathrm{tail}},\lambda}(K)\right)^{|\mathbf{U}|}\right]. \tag{95}$$

Set

$$t := \min\left\{\overline{p}_{q,\beta_{\mathrm{tail}},\lambda}(K), C^{-1}\right\}.$$

Since $|\mathbf{U}| \le C$, one has $t|\mathbf{U}| \le 1$, and hence

$$(1-t)^{|\mathbf{U}|} \le \mathrm{e}^{-t|\mathbf{U}|} \le 1 - \mathrm{e}^{-1} t |\mathbf{U}|.$$

It follows from (95) that

$$\overline{p}_{q,\beta_{\mathrm{tail}},\lambda}(CK) \ge \mathrm{e}^{-1}\mathbb{E}^1_{\beta_{\mathrm{tail}},\lambda,q}[|\mathbf{U}|] \min\left\{\overline{p}_{q,\beta_{\mathrm{tail}},\lambda}(K), C^{-1}\right\}. \tag{96}$$

It remains to obtain an explicit lower bound on $\mathbb{E}^1_{\beta_{\mathrm{tail}},\lambda,q}[|\mathbf{U}|]$.

The FK bridge estimate (DCGT (14)). For an integer $R \geq 1$, define the worst-boundary arm probability

$$\alpha_R := \max_{\xi \text{ b.c. on } \mathbb{Z}\setminus B_R} \mathbb{P}^{\xi}_{B_R,\beta_{\text{tail}},\lambda,q}[0 \leftrightarrow \mathbb{Z} \setminus B_R \text{ by an actual open path}]. \tag{97}$$

By boundary-condition monotonicity for increasing events, the maximum is attained by wired boundary conditions. Hence

$$\alpha_R = \mathbb{P}^1_{R,\beta_{\text{tail}},\lambda,q}[0 \leftrightarrow \mathbb{Z} \setminus B_R], \qquad \alpha_R \downarrow \theta(q, \beta_{\text{tail}}, \lambda).$$

The analogous arm probability in the CK-truncated graph is no larger than α_R under the admissible specification produced by the DCGT exploration.

By (90), choose R_{arm} and numbers ρ, η such that

$$\alpha^2_{R_{\text{arm}}} < \rho < \eta < \vartheta^2. \tag{98}$$

We subsequently require $K > 2R_{\text{arm}} + 1$.

Fix a long edge $e = \{x, y\}$, so $K < |x - y| \leq CK$, and let $\omega^{(\leq CK)\setminus e}$ be the truncated configuration with e deleted. Put

$$\Lambda_x := x + B_{R_{\text{arm}}}, \qquad \Lambda_y := y + B_{R_{\text{arm}}},$$

and define the endpoint-arm events

$$A_x := \{x \leftrightarrow \mathbb{Z} \setminus \Lambda_x \text{ in } \omega^{(\leq CK)\setminus e}\}, \qquad A_y := \{y \leftrightarrow \mathbb{Z} \setminus \Lambda_y \text{ in } \omega^{(\leq CK)\setminus e}\}.$$

The boxes are disjoint. Let

$$\mathcal{J}_{x,y} := \{\{u, v\} \in E^{(\leq CK)} \setminus \{e\} : u \in \Lambda_x,\ v \in \Lambda_y\}$$

and let $G_{x,y}$ be the event that some edge of $\mathcal{J}_{x,y}$ is open. The candidate edge e is explicitly excluded. By the conditional open-edge bound (59) and a union bound,

$$\begin{aligned} \mathbb{P}^1_{\beta_{\text{tail}},\lambda,q}(G_{x,y}) &\leq |B_{R_{\text{arm}}}|^2 \left(1 - \mathrm{e}^{-\beta_{\text{tail}}/(K-2R_{\text{arm}})^2}\right) \\ &\leq \frac{\beta_{\text{tail}} |B_{R_{\text{arm}}}|^2}{(K - 2R_{\text{arm}})^2} =: \varepsilon_{R_{\text{arm}},K}. \end{aligned} \tag{99}$$

On $G^c_{x,y}$, reveal completely the finite edge family that decides A_x, then the one that decides A_y. The common interbox edges have already been fixed closed. At each reveal the spatial Markov property gives the full arm block with a boundary condition on its fixed exterior. The conditional arm probability is therefore at most $\alpha_{R_{\mathrm{arm}}}$. In conditional expectation form,

$$\begin{aligned}\mathbb{P}^1_{\beta_{\mathrm{tail}},\lambda,q}&(A_x \cap A_y \cap G^c_{x,y}) \\ &\le \alpha_{R_{\mathrm{arm}}} \mathbb{P}^1_{\beta_{\mathrm{tail}},\lambda,q}(A_x \cap G^c_{x,y}) \le \alpha^2_{R_{\mathrm{arm}}}.\end{aligned} \tag{100}$$

It follows from (99) and (100) that

$$\mathbb{P}^1_{\beta_{\mathrm{tail}},\lambda,q}(A_x \cap A_y) \le \alpha^2_{R_{\mathrm{arm}}} + \varepsilon_{R_{\mathrm{arm}},K}. \tag{101}$$

Increase the threshold K_1 so that this last quantity is at most ρ for every $K \ge K_1$.

The event $A_x \cap A_y$ is measurable without the state of e. Thus the tower property and the conditional single-edge law give

$$\begin{aligned}\mathbb{P}^1_{\beta_{\mathrm{tail}},\lambda,q}[e \text{ is a bridge}] &= \mathbb{E}^1_{\beta_{\mathrm{tail}},\lambda,q}\left[\mathbf{1}_{A_x \cap A_y} \mathbb{P}^1_{\beta_{\mathrm{tail}},\lambda,q}(\omega_e = 1 \mid \omega_{E\setminus\{e\}})\right] \\ &\le p_e\, \mathbb{P}^1_{\beta_{\mathrm{tail}},\lambda,q}(A_x \cap A_y) \le \rho p_e < \vartheta^2 p_e,\end{aligned} \tag{102}$$

where $p_e = 1 - \mathrm{e}^{-\beta_{\mathrm{tail}}/|e|^2}$. This is the required strict slack; unlike the Bernoulli proof, no independence of e from its environment has been used.

Abundance of unbridged blocks (DCGT (13)). For $i \in \mathcal{I}^{\mathrm{cand}}_C$, introduce the two finite edge families

$$\mathcal{E}^{\mathrm{jump}}_i := \{\{x,y\} : x < \ell_i,\ y \ge r_i,\ K < y - x \le CK\}$$

and

$$\mathcal{E}^{\mathrm{adj}}_i := \{\{x,y\} : \{x,y\} \cap J_i \ne \varnothing,\ K < |x - y| \le CK\}.$$

Every bridge and arm in these definitions is evaluated in $\omega^{(\le CK)}$. The definition of an unbridged block is now the exact finite intersection

$$\{B^i_{3K} \text{ is unbridged}\} = \bigcap_{e \in \mathcal{E}^{\mathrm{jump}}_i} \{e \text{ is not a bridge}\} \cap \bigcap_{f \in \mathcal{E}^{\mathrm{adj}}_i} \{f \text{ is closed}\}. \tag{103}$$

The event that a fixed edge is a bridge is increasing: opening additional edges preserves both endpoint arms after that edge is deleted. Hence its complement is decreasing, as is the event that a fixed edge is closed. Applying FK–FKG to the finite family in (103), then using (59) and (102), gives

$$\begin{aligned}\mathbb{P}^1_{\beta_{\text{tail}},\lambda,q}[B^i_{3K} \text{ is unbridged}] &\geq \prod_{e\in\mathcal{E}_i^{\text{jump}}} \mathbb{P}^1_{\beta_{\text{tail}},\lambda,q}[e \text{ is not a bridge}] \prod_{f\in\mathcal{E}_i^{\text{adj}}} \mathbb{P}^1_{\beta_{\text{tail}},\lambda,q}[f \text{ is closed}] \\ &\geq \prod_{e\in\mathcal{E}_i^{\text{jump}}} (1-\vartheta^2 p_e) \prod_{f\in\mathcal{E}_i^{\text{adj}}} (1-p_f). \end{aligned} \tag{104}$$

An edge may occur in both finite families; FKG is then applied to the two corresponding decreasing events.

The choice (90) ensures $0 < \vartheta^2 < 1$. This restriction is needed in the convexity estimate

$$1 - a(1-\mathrm{e}^{-t}) = (1-a) + a\mathrm{e}^{-t} \geq \mathrm{e}^{-at}, \qquad 0 \leq a \leq 1, \quad t \geq 0.$$

With $a = \vartheta^2$ and $t = \beta_{\text{tail}}/|e|^2$, it follows that

$$1 - \vartheta^2 p_e \geq \mathrm{e}^{-\beta_{\text{tail}}\vartheta^2/|e|^2}.$$

The deterministic kernel estimates in Lemma B.4 apply without change. Thus there is a universal constant $b_{\text{jump}} < \infty$ such that

$$\sum_{e\in\mathcal{E}_i^{\text{jump}}} \frac{1}{|e|^2} \leq \log C + b_{\text{jump}}, \qquad \sum_{f\in\mathcal{E}_i^{\text{adj}}} \frac{1}{|f|^2} \leq 20.$$

Consequently,

$$\mathbb{P}^1_{\beta_{\text{tail}},\lambda,q}[B^i_{3K} \text{ is unbridged}] \geq c_{\mathrm{u}} C^{-\beta_{\text{tail}}\vartheta^2}, \qquad c_{\mathrm{u}} := \mathrm{e}^{-\beta_{\text{tail}}(\vartheta^2 b_{\text{jump}}+20)}. \tag{105}$$

The constant $c_{\mathrm{u}} > 0$ is uniform in C, K, i; the thresholds used above may depend on $q, \beta_{\text{tail}}, \lambda, \vartheta$.

For all $C \geq 30$, the candidate count in Lemma B.4 gives $|\mathcal{I}_C^{\text{cand}}| \geq C/6$. Hence, by linearity of expectation alone,

$$\mathbb{E}^1_{\beta_{\text{tail}},\lambda,q}[|\mathbf{U}|] \geq \frac{c_{\mathrm{u}}}{6} C^{1-\beta_{\text{tail}}\vartheta^2}. \tag{106}$$

Substituting this estimate into (96) proves (91) with, for example,

$$c_{\text{gap}} := \frac{\mathrm{e}^{-1} c_{\mathrm{u}}}{6}.$$

Iteration and the annulus contradiction. Choose an integer $K_0 \geq K_1$. To verify that the initial failure probability is strictly positive, consider the finite cut

$$\mathcal{C}_{K_0} := \{\{x,y\} : x \leq -1,\ y \geq 0,\ |x-y| \leq K_0\}.$$

Every actual K_0-crossing of B_{3K_0} uses an edge of this cut at its first passage from a negative to a nonnegative vertex. Boundary wiring does not count as a path. Sequential use of (59) under the full wired specification gives

$$\mathbb{P}^1_{3K_0,\beta_{\mathrm{tail}},\lambda,q}[\omega_e = 0 \text{ for every } e \in \mathcal{C}_{K_0}] \geq \prod_{e\in\mathcal{C}_{K_0}} (1-p_e) > 0.$$

Together with (88), this proves

$$\overline{p}_{q,\beta_{\mathrm{tail}},\lambda}(K_0) > 0. \tag{107}$$

Fix one integer $C \geq \max\{C_1, 30\}$ sufficiently large that

$$c_{\mathrm{gap}} C^{1-\beta_{\mathrm{tail}}\vartheta^2} \geq 1, \qquad C^{-1} \leq \overline{p}_{q,\beta_{\mathrm{tail}},\lambda}(K_0),$$

and set $K_n := C^n K_0$. The recursion (91) then gives inductively

$$\overline{p}_{q,\beta_{\mathrm{tail}},\lambda}(K_n) \geq C^{-1}, \qquad n \geq 0. \tag{108}$$

Let

$$\mathcal{A}_n := \{B_{3K_n} \leftrightarrow B^c_{9K_n} \text{ by an actual open path}\}.$$

To avoid double-counting, define the unordered edge family

$$\mathcal{E}^{\mathrm{out}}_n := \{\{x,y\} : \{x,y\} \cap B_{9K_n} \neq \varnothing,\ |x-y| > K_n\}$$

and the closure event

$$\mathcal{L}_n := \{\omega_e = 0 \text{ for every } e \in \mathcal{E}^{\mathrm{out}}_n\}.$$

Also put

$$\mathcal{N}^-_n := \{B^{-2}_{3K_n} \text{ is not } K_n\text{-crossed}\}, \qquad \mathcal{N}^+_n := \{B^2_{3K_n} \text{ is not } K_n\text{-crossed}\}.$$

The deterministic annulus obstruction (51) applies verbatim:

$$\mathcal{L}_n \cap \mathcal{N}^-_n \cap \mathcal{N}^+_n \subseteq \mathcal{A}^c_n. \tag{109}$$

The DLR property and the worst-boundary minimum (87) imply, for each translated side block,

$$\mathbb{P}^1_{\beta_{\mathrm{tail}},\lambda,q}(\mathcal{N}^-_n) \wedge \mathbb{P}^1_{\beta_{\mathrm{tail}},\lambda,q}(\mathcal{N}^+_n) \geq \overline{p}_{q,\beta_{\mathrm{tail}},\lambda}(K_n) \geq C^{-1}. \tag{110}$$

A uniform lower bound for $\mathcal{L}_n$ is obtained by taking, for $M > 9K_n$, let

$$\mathcal{E}^{\mathrm{out}}_{n,M} := \{e \in \mathcal{E}^{\mathrm{out}}_n : e \subset B_M\}.$$

This is finite. Closing its edges one at a time and using the conditional lower bound in (59) yields

$$\begin{aligned}
&\mathbb{P}^1_{\beta_{\mathrm{tail}},\lambda,q}[\omega_e = 0 \text{ for every } e \in \mathcal{E}^{\mathrm{out}}_{n,M}] \\
&\quad\geq \exp\left(-\beta_{\mathrm{tail}} \sum_{e\in\mathcal{E}^{\mathrm{out}}_{n,M}} \frac{1}{|e|^2}\right) \\
&\quad\geq \exp\left(-\beta_{\mathrm{tail}}|B_{9K_n}|\, 2 \sum_{r>K_n} \frac{1}{r^2}\right) \geq \mathrm{e}^{-36\beta_{\mathrm{tail}}}.
\end{aligned} \tag{111}$$

Here $|B_{9K_n}| = 18K_n$ and $\sum_{r>K_n} r^{-2} \leq K_n^{-1}$. The finite closure events decrease to $\mathcal{L}_n$ as $M \to \infty$. Continuity from above therefore gives

$$\mathbb{P}^1_{\beta_{\mathrm{tail}},\lambda,q}(\mathcal{L}_n) \geq \mathrm{e}^{-36\beta_{\mathrm{tail}}}. \tag{112}$$

uniformly in n.

The three events $\mathcal{L}_n, \mathcal{N}_n^-, \mathcal{N}_n^+$ are decreasing. FK–FKG, rather than independence, together with (109)– (112), gives

$$\begin{aligned}
1 - \mathbb{P}^1_{\beta_{\mathrm{tail}},\lambda,q}(\mathcal{A}_n) &\geq \mathbb{P}^1_{\beta_{\mathrm{tail}},\lambda,q}(\mathcal{L}_n \cap \mathcal{N}_n^- \cap \mathcal{N}_n^+) \\
&\geq \mathbb{P}^1_{\beta_{\mathrm{tail}},\lambda,q}(\mathcal{L}_n)\mathbb{P}^1_{\beta_{\mathrm{tail}},\lambda,q}(\mathcal{N}_n^-)\mathbb{P}^1_{\beta_{\mathrm{tail}},\lambda,q}(\mathcal{N}_n^+) \\
&\geq \mathrm{e}^{-36\beta_{\mathrm{tail}}} C^{-2}.
\end{aligned} \tag{113}$$

On the other hand, the extremal wired infinite-volume FK state is translation ergodic; this is the standard ergodic property of extremal translation-invariant Gibbs states [Geo11]. Since $\theta_0 > 0$, the spatial ergodic theorem implies that expanding boxes meet the infinite cluster with probability tending to one. If B_{3K_n} meets that cluster, then $\mathcal{A}_n$ occurs. Therefore

$$\mathbb{P}^1_{\beta_{\mathrm{tail}},\lambda,q}(\mathcal{A}_n) \longrightarrow 1,$$

contradicting (113). The assumption $\beta_{\mathrm{tail}}\theta_0^2 < 1$ is impossible, and hence

$$\theta(q, \beta_{\mathrm{tail}}, \lambda) > 0 \quad\Longrightarrow\quad \beta_{\mathrm{tail}}\theta(q, \beta_{\mathrm{tail}}, \lambda)^2 \geq 1.$$

The use of FKG in (104) and (113) is the reason that this part of the theorem is stated for $q \geq 1$.

Both Bernoulli recurrences survive dependence. Their deterministic geometry did not change, but every product estimate was replaced visibly: spatial Markov conditioning and a mesoscopic merger for the good-block recursion, admissible worst-boundary crossing probabilities and FKG for the failed-crossing recursion. Consequently the wired FK density has the same quantitative gap $\theta > 0 \Rightarrow \beta_{\text{tail}}\theta^2 \geq 1$. The remaining step is not a new renormalisation argument: Edwards–Sokal identifies this geometric density with the physical Potts, and in particular Ising, order parameter.

3.5 Edwards–Sokal coupling and the Potts magnetisation

Let $q \geq 2$ be an integer. Under the wired Edwards–Sokal coupling, the boundary cluster has colour (1) and every other FK cluster receives an independent uniform colour [ES88]. Thus

$$\mu^1_{\beta_{\text{tail}},\lambda,q}(s_0 = 1) = \frac{1}{q} + \frac{q-1}{q}\mathbb{P}^1_{\beta_{\text{tail}},\lambda,q}(0 \leftrightarrow \infty).$$

For the normalised Potts magnetisation $m = (q\mu^1(s_0 = 1) - 1)/(q-1)$, this is the exact identity

$$m(q, \beta_{\text{tail}}, \lambda) = \theta(q, \beta_{\text{tail}}, \lambda). \tag{114}$$

Corollary 3.6 (DCGT: Potts magnetisation)**.** *For every integer $q \geq 2$, the following hold.*

(i) *For every $\beta_{\text{tail}} > 1$, there exists $\lambda_0 = \lambda_0(q, \beta_{\text{tail}}) < \infty$ such that*

$$m(q, \beta_{\text{tail}}, \lambda) > 0 \qquad \textit{for every } \lambda \geq \lambda_0.$$

(ii) *For every $\beta_{\text{tail}}, \lambda > 0$,*

$$m(q, \beta_{\text{tail}}, \lambda) > 0 \quad \Longrightarrow \quad \beta_{\text{tail}} m(q, \beta_{\text{tail}}, \lambda)^2 \geq 1.$$

Proof. Equation (114) identifies the Potts magnetisation with wired FK density. The two assertions are therefore Theorem 3.5(i)–(ii), with stochastic monotonicity in λ extending the existence statement from λ_0 to every $\lambda \geq \lambda_0$. □

3.5.1 The physical Ising ray

The two parameters $(\beta_{\text{tail}}, \lambda)$ appearing in Theorem 3.5 are FK edge-intensity parameters. They are not, in general, equal to the physical inverse temperature of an Ising or Potts Hamiltonian. To identify the physical Ising family inside the DCGT parameter plane, recall the Edwards–Sokal normalisation.

For a q-state Potts Hamiltonian

$$H^{\text{Potts}}(s) = -\sum_{i<j} K_{i,j} \mathbf{1}_{\{s_i = s_j\}}$$

at physical inverse temperature β_{P}, the identity

$$\exp\Big(\beta_{\mathrm{P}} K_{i,j} \mathbf{1}_{\{s_i=s_j\}}\Big) = 1 + (\mathrm{e}^{\beta_{\mathrm{P}} K_{i,j}} - 1)\mathbf{1}_{\{s_i=s_j\}}$$

shows that the Edwards–Sokal edge parameter is

$$p_{i,j} = 1 - \mathrm{e}^{-\beta_{\mathrm{P}} K_{i,j}}.$$

For the ± 1-valued Ising Hamiltonian fixed in Section 1.2,

$$H^{\text{Ising}}(\sigma) = -\sum_{i<j} J_{i,j}\sigma_i\sigma_j,$$

at physical inverse temperature β_{I}, one has

$$\exp(\beta_{\mathrm{I}} J_{i,j}\sigma_i\sigma_j) = \mathrm{e}^{-\beta_{\mathrm{I}} J_{i,j}} \left[1 + (\mathrm{e}^{2\beta_{\mathrm{I}} J_{i,j}} - 1)\mathbf{1}_{\{\sigma_i=\sigma_j\}}\right].$$

The prefactor is independent of the spin configuration. Consequently, the associated $q = 2$ FK edge parameter is

$$p_{i,j} = 1 - \mathrm{e}^{-2\beta_{\mathrm{I}} J_{i,j}}.$$

Equivalently, under the recoding

$$s_i = 1 \longleftrightarrow \sigma_i = +1, \qquad s_i = 2 \longleftrightarrow \sigma_i = -1,$$

a Potts coupling $K_{i,j} = 2J_{i,j}$ satisfies

$$-K_{i,j}\mathbf{1}_{\{s_i=s_j\}} = -J_{i,j}\sigma_i\sigma_j - J_{i,j}.$$

Thus it differs from the Ising interaction only by an additive constant.

Now consider the fixed Ising couplings

$$J(r) = \frac{c}{r^2} \quad (r \geq 2), \qquad J(1) = J_1 > 0.$$

The DCGT model has edge probabilities

$$p_{i,j} = 1 - \exp\left(-\frac{\beta_{\text{tail}}}{|i-j|^2}\right), \qquad |i-j| \geq 2,$$

and

$$p_{i,i+1} = 1 - \mathrm{e}^{-\lambda_{\mathrm{DCGT}}}.$$

Matching these probabilities with the physical Ising probabilities gives the ray

$$\beta_{\text{tail}} = 2\beta_{\text{I}}c, \qquad \lambda_{\text{DCGT}} = 2\beta_{\text{I}}J_1. \tag{115}$$

For the exact inverse-square kernel

$$J(r) = \frac{c}{r^2} \qquad (r \geq 1),$$

one has $J_1 = c$, and the physical family lies on the diagonal ray

$$\lambda_{\text{DCGT}} = \beta_{\text{tail}} = 2\beta_{\text{I}}c.$$

For $q = 2$, finite FK clusters receive independent signs, while the wired cluster receives sign $+1$. Hence the normalised Potts magnetisation is the usual plus-state Ising magnetisation:

$$m(2, \beta_{\text{tail}}, \lambda) = 2\mu^1_{\beta_{\text{tail}},\lambda,2}(s_0 = 1) - 1 = \mathbb{E}_{\mu^1_{\beta_{\text{tail}},\lambda,2}}[\sigma_0].$$

Combining this observation with (114) and (115), we obtain

$$m^+(\beta_{\text{I}}) = \theta\left(2, 2\beta_{\text{I}}c, 2\beta_{\text{I}}J_1\right). \tag{116}$$

Thus changing the physical inverse temperature changes both DCGT parameters. The physical phase transition is not a fixed-λ transition or a fixed-β_{tail} transition in the DCGT plane. This does not prevent us from applying Theorem 3.5: part (ii) is a pointwise statement that can be applied at every point of the physical ray, while part (i), together with monotonicity in both coordinates, implies that the ray eventually enters the ordered region.

3.5.2 Existence of a finite critical point on the physical ray

Define

$$\beta_{\text{I},c} := \inf\{\beta_{\text{I}} > 0 : m^+(\beta_{\text{I}}) > 0\}.$$

Theorem 3.5 also gives

$$0 < \beta_{\text{I},c} < \infty.$$

Suppose that

$$\beta_{\text{I}} < \frac{1}{2c}.$$

If $m^+(\beta_{\text{I}}) > 0$, then (116) and Theorem 3.5(ii) would imply

$$1 \leq 2\beta_{\text{I}}c \cdot m^+(\beta_{\text{I}})^2 \leq 2\beta_{\text{I}}c < 1,$$

where we used $m^+(\beta_{\mathrm{I}}) \le 1$. This is impossible. Therefore

$$m^+(\beta_{\mathrm{I}}) = 0 \qquad \text{for } \beta_{\mathrm{I}} < \frac{1}{2c},$$

and hence

$$\beta_{\mathrm{I},c} \ge \frac{1}{2c} > 0. \tag{117}$$

To prove that $\beta_{\mathrm{I},c} < \infty$, fix any auxiliary parameter

$$\overline{\beta_{\mathrm{tail}}} > 1.$$

By Theorem 3.5(i), there exists $\bar\lambda < \infty$ such that

$$\theta(2, \overline{\beta_{\mathrm{tail}}}, \bar\lambda) > 0.$$

Choose

$$\beta_{\mathrm{I}}^\star \ge \max\left\{\frac{\overline{\beta_{\mathrm{tail}}}}{2c}, \frac{\bar\lambda}{2J_1}\right\}.$$

Then the physical point corresponding to $\beta_{\mathrm{I}}^\star$ satisfies

$$2\beta_{\mathrm{I}}^\star c \ge \overline{\beta_{\mathrm{tail}}}, \qquad 2\beta_{\mathrm{I}}^\star J_1 \ge \bar\lambda.$$

By stochastic monotonicity of the wired FK measure in both edge-intensity parameters,

$$\begin{aligned} m^+(\beta_{\mathrm{I}}^\star) &= \theta\left(2, 2\beta_{\mathrm{I}}^\star c, 2\beta_{\mathrm{I}}^\star J_1\right) \\ &\ge \theta(2, \overline{\beta_{\mathrm{tail}}}, \bar\lambda) > 0. \end{aligned}$$

Consequently,

$$\beta_{\mathrm{I},c} \le \beta_{\mathrm{I}}^\star < \infty. \tag{118}$$

This argument identifies the precise role of Theorem 3.5(i) for the physical model. The theorem first produces an ordered point somewhere in the two-parameter DCGT plane. A sufficiently distant point on the physical ray dominates that ordered point in both coordinates and is therefore ordered as well.

3.5.3 The magnetisation gap and the Thouless jump

The function

$$\beta_{\mathrm{I}} \longmapsto m^+(\beta_{\mathrm{I}})$$

is nondecreasing. This follows either from the Griffiths inequalities for the Ising model or directly from (116), since both $2\beta_{\mathrm{I}}c$ and $2\beta_{\mathrm{I}}J_1$ are increasing and the wired FK measure is stochastically increasing in its edge parameters.

It follows from the definition of $\beta_{\mathrm{I},c}$ and monotonicity that

$$m^+(\beta_{\mathrm{I}}) = 0 \qquad \text{for } \beta_{\mathrm{I}} < \beta_{\mathrm{I},c},$$

and

$$m^+(\beta_{\mathrm{I}}) > 0 \qquad \text{for } \beta_{\mathrm{I}} > \beta_{\mathrm{I},c}.$$

Indeed, if $\beta_{\mathrm{I}} > \beta_{\mathrm{I},c}$, the definition of the infimum provides some $\beta'_{\mathrm{I}} \in (\beta_{\mathrm{I},c}, \beta_{\mathrm{I}})$ with $m^+(\beta'_{\mathrm{I}}) > 0$, and monotonicity then gives

$$m^+(\beta_{\mathrm{I}}) \geq m^+(\beta'_{\mathrm{I}}) > 0.$$

For every $\beta_{\mathrm{I}} > \beta_{\mathrm{I},c}$, we may therefore apply Theorem 3.5(ii) at the corresponding point of the physical ray. Using (116), we obtain

$$2\beta_{\mathrm{I}}c \cdot m^+(\beta_{\mathrm{I}})^2 \geq 1.$$

Equivalently,

$$m^+(\beta_{\mathrm{I}}) \geq \frac{1}{\sqrt{2\beta_{\mathrm{I}}c}}, \qquad \beta_{\mathrm{I}} > \beta_{\mathrm{I},c}. \tag{119}$$

Thus, throughout the ordered phase, the magnetisation cannot lie in the interval

$$\left(0, \frac{1}{\sqrt{2\beta_{\mathrm{I}}c}}\right).$$

In particular, it cannot approach zero continuously as $\beta_{\mathrm{I}} \downarrow \beta_{\mathrm{I},c}$.

It remains to verify that the lower bound survives at the critical point itself. Let

$$\Lambda_n \uparrow \mathbb{Z}$$

be an increasing sequence of finite intervals, and let

$$m^+_{\Lambda_n}(\beta_{\mathrm{I}}) := \mathbb{E}^+_{\mu_{\Lambda_n,\beta_{\mathrm{I}}}}[\sigma_0]$$

be the corresponding finite-volume plus magnetisation. Ferromagnetic domain monotonicity gives

$$m^+_{\Lambda_n}(\beta_{\mathrm{I}}) \downarrow m^+(\beta_{\mathrm{I}}) \qquad \text{as } n \to \infty,$$

and hence

$$m^+(\beta_{\mathrm{I}}) = \inf_n m^+_{\Lambda_n}(\beta_{\mathrm{I}}).$$

For each fixed n, the function

$$\beta_{\mathrm{I}} \longmapsto m^{+}_{\Lambda_n}(\beta_{\mathrm{I}})$$

is continuous. Indeed, Λ_n contains only finitely many spin variables, and the inverse-square interaction is absolutely summable, so the contribution of the fixed plus boundary defines finite boundary fields. The finite-volume expectation is therefore a ratio of finite sums of continuous, in fact analytic, functions of β_{I}.

An infimum of continuous functions is upper semicontinuous. More explicitly, for every $\beta_{\mathrm{I},0} > 0$,

$$\begin{aligned}
\limsup_{\beta_{\mathrm{I}} \to \beta_{\mathrm{I},0}} m^{+}(\beta_{\mathrm{I}}) &= \limsup_{\beta_{\mathrm{I}} \to \beta_{\mathrm{I},0}} \inf_n m^{+}_{\Lambda_n}(\beta_{\mathrm{I}}) \\
&\le \inf_n \limsup_{\beta_{\mathrm{I}} \to \beta_{\mathrm{I},0}} m^{+}_{\Lambda_n}(\beta_{\mathrm{I}}) \\
&= \inf_n m^{+}_{\Lambda_n}(\beta_{\mathrm{I},0}) \\
&= m^{+}(\beta_{\mathrm{I},0}).
\end{aligned}$$

Applying this at $\beta_{\mathrm{I},0} = \beta_{\mathrm{I},c}$ gives

$$m^{+}(\beta_{\mathrm{I},c}) \ge \limsup_{\beta_{\mathrm{I}} \downarrow \beta_{\mathrm{I},c}} m^{+}(\beta_{\mathrm{I}}).$$

On the other hand, letting $\beta_{\mathrm{I}} \downarrow \beta_{\mathrm{I},c}$ in (119) yields

$$\liminf_{\beta_{\mathrm{I}} \downarrow \beta_{\mathrm{I},c}} m^{+}(\beta_{\mathrm{I}}) \ge \frac{1}{\sqrt{2\beta_{\mathrm{I},c} c}}.$$

Combining the last two inequalities,

$$\begin{aligned}
m^{+}(\beta_{\mathrm{I},c}) &\ge \limsup_{\beta_{\mathrm{I}} \downarrow \beta_{\mathrm{I},c}} m^{+}(\beta_{\mathrm{I}}) \\
&\ge \liminf_{\beta_{\mathrm{I}} \downarrow \beta_{\mathrm{I},c}} m^{+}(\beta_{\mathrm{I}}) \\
&\ge \frac{1}{\sqrt{2\beta_{\mathrm{I},c} c}}.
\end{aligned}$$

Thus

$$m^{+}(\beta_{\mathrm{I},c}) \ge \frac{1}{\sqrt{2\beta_{\mathrm{I},c} c}} > 0. \tag{120}$$

Since

$$m^{+}(\beta_{\mathrm{I}}) = 0 \qquad \text{for every } \beta_{\mathrm{I}} < \beta_{\mathrm{I},c},$$

we have

$$\lim_{\beta_{\mathrm{I}} \uparrow \beta_{\mathrm{I},c}} m^{+}(\beta_{\mathrm{I}}) = 0,$$

whereas

$$m^+(\beta_{\mathrm{I},c}) \geq \frac{1}{\sqrt{2\beta_{\mathrm{I},c}c}} > 0.$$

Consequently,

$$m^+(\beta_{\mathrm{I},c}) - \lim_{\beta_\mathrm{I}\uparrow\beta_{\mathrm{I},c}} m^+(\beta_\mathrm{I}) \geq \frac{1}{\sqrt{2\beta_{\mathrm{I},c}c}},$$

which is the Thouless jump of the physical Ising magnetisation.

The logical structure of the argument is therefore

$$\begin{aligned}
\text{Edwards–Sokal coupling} \quad &\Longrightarrow \quad m^+ = \theta \quad \text{on the physical ray,}\\
\text{Theorem 3.5(i) plus monotonicity} \quad &\Longrightarrow \quad \beta_{\mathrm{I},c} < \infty,\\
\text{Theorem 3.5(ii)} \quad &\Longrightarrow \quad m^+ > 0 \implies m^+ \geq (2\beta_\mathrm{I}c)^{-1/2},\\
\text{finite-volume domain monotonicity} \quad &\Longrightarrow \quad \text{the lower bound persists at } \beta_{\mathrm{I},c}.
\end{aligned}$$

DCGT succeeds here because, after Edwards–Sokal, FK connectivity is itself the Ising order parameter: a density gap for the infinite cluster is exactly a magnetisation gap. The Discrete Gaussian Chain has no corresponding cluster-density identity, so the argument cannot simply be transferred. This motivates a second graphical comparison. Chapter 4 uses random currents to test which finite-volume algebraic identities survive long-range interactions and which part, if any, survives in the DGC moment-weighted expansion.

4 From long-range Ising random currents to the Discrete Gaussian Chain

Finite-volume random-current algebra does not require a finite interaction range. This chapter proves the current expansion and switching lemma on an arbitrary finite ferromagnetic weighted graph. It then states the imported infinite-volume theorems of Aizenman, Duminil-Copin and Sidoravicius (ADCS) and reconstructs the pair-connectivity, LRO–percolation and plus/free estimates in their continuity argument. The final sections test the same algebra on the DGC. The moment-weighted expansion and the obstruction to the canonical Ising path switch are derived here. DGC heights are not identified with Ising currents.

Two distinctions organise the chapter. At finite volume, long range only makes the Ising interaction graph dense; at infinite volume, summability, boundary conditions and current-cluster geometry enter the proof. The DGC changes a different part of the expansion. Ising spin sums retain only the parity of the incident degree, whereas DGC sums produce a moment for each even degree. Thus interaction range does not break the finite-volume Ising switch, but degree-dependent DGC weights do.

4.1 Finite long-range interaction graphs

For a finite set Λ, define the interaction graph

$$G_\Lambda = (\Lambda, E_\Lambda), \qquad E_\Lambda := \{\{x,y\} \subset \Lambda : J_{x,y} > 0\}.$$

If the interaction is finite range, each vertex has only nearby neighbours. For a long-range kernel, E_Λ may instead contain every unordered pair of vertices. It is nevertheless a finite edge set, so the Taylor expansion can be performed edge by edge and the resulting current sums are absolutely convergent. In particular, no truncation of long edges is needed for the finite-volume algebra.

Remark (Finite-volume algebra and thermodynamic control). The finite-volume correlation expansion, the source constraint $\partial\mathbf{n}$, and the switching lemma hold on any finite ferromagnetic weighted graph. The infinite-volume construction is a separate analytic problem: it requires a thermodynamic limit, here under $\sum_y J_{0,y} < \infty$, and any argument based on locality, short paths or Euclidean crossing geometry must be reconsidered.

For example, a d-dimensional power law $J_{0,x} \asymp |x|^{-(d+s)}$ with $s > 0$ is summable. In the one-dimensional notation of this report, this is $J(r) \asymp r^{-\alpha}$ with $\alpha = 1+s > 1$. Thus the long-range regimes $1 < \alpha \leq 2$, including the inverse-square model, fall within the summable setting considered by ADCS. Long edges therefore alter connectivity geometry, not the parity algebra of currents.

4.2 Current expansion and parity sources

For the finite interaction graph $G_\Lambda = (\Lambda, E_\Lambda)$ above, set

$$\Omega_\Lambda := \mathbb{N}_0^{E_\Lambda} = \{\mathbf{n} : E_\Lambda \longrightarrow \mathbb{N}_0\}.$$

Here $\mathbb{N}_0 = \{0, 1, 2, \ldots\}$, and for $e = \{x, y\}$ we abbreviate $J_e = J_{x,y}$. The source set and current weight are

$$\partial\mathbf{n} := \left\{x \in \Lambda : \sum_{e \ni x} n_e \text{ is odd}\right\}, \qquad w_{\beta_\mathrm{I}}(\mathbf{n}) := \prod_{e \in E_\Lambda} \frac{(\beta_\mathrm{I} J_e)^{n_e}}{n_e!}.$$

For $A \subset \Lambda$, define

$$\mathcal{Z}_\Lambda(A) := \sum_{\partial\mathbf{n} = A} w_{\beta_\mathrm{I}}(\mathbf{n}), \qquad \mathbf{P}^A_{\Lambda,\beta_\mathrm{I}}(\mathbf{n}) := \frac{\mathbf{1}_{\{\partial\mathbf{n} = A\}} w_{\beta_\mathrm{I}}(\mathbf{n})}{\mathcal{Z}_\Lambda(A)},$$

whenever $\mathcal{Z}_\Lambda(A) > 0$. The support is $\mathrm{supp}(\mathbf{n}) := \{e \in E_\Lambda : n_e > 0\}$.

Recall the Hamiltonian convention fixed in Section 1.2:

$$H^{\mathrm{Ising},0}_\Lambda(\sigma) = -\sum_{\{x,y\} \in E_\Lambda} J_{x,y}\sigma_x\sigma_y.$$

Expanding each Boltzmann factor gives

$$\mathrm{e}^{\beta_\mathrm{I} J_{xy}\sigma_x\sigma_y} = \sum_{n_{xy} \geq 0} \frac{(\beta_\mathrm{I} J_{xy})^{n_{xy}}}{n_{xy}!}(\sigma_x\sigma_y)^{n_{xy}}.$$

After multiplication over edges, the exponent of σ_x is $\sum_{e \ni x} n_e$. Summing over $\sigma_x = \pm 1$ annihilates a term unless this exponent is even. Consequently,

$$Z^0_{\Lambda,\beta_\mathrm{I}} = 2^{|\Lambda|}\mathcal{Z}_\Lambda(\varnothing). \tag{121}$$

Inserting $\prod_{x \in A}\sigma_x$ reverses the required parity precisely at the vertices of A, and therefore

$$\sum_{\sigma \in \{-1,+1\}^\Lambda} \left(\prod_{x \in A}\sigma_x\right) \mathrm{e}^{-\beta_\mathrm{I} H^{\mathrm{Ising},0}_\Lambda(\sigma)} = 2^{|\Lambda|}\mathcal{Z}_\Lambda(A). \tag{122}$$

Dividing the last two identities yields

$$\left\langle \prod_{x \in A}\sigma_x \right\rangle^0_{\Lambda,\beta_\mathrm{I}} = \frac{\mathcal{Z}_\Lambda(A)}{\mathcal{Z}_\Lambda(\varnothing)}. \tag{123}$$

If $|A|$ is odd, the handshake lemma gives $\mathcal{Z}_\Lambda(A) = 0$, so the correlation is zero.

Thus a spin correlation is a ratio of weighted parity constraints. The derivation uses neither a metric nor planarity, a maximum edge length, or a bounded-degree assumption. Long range only enlarges

E_Λ and changes the factors J_e [Dum18]. Combining two expansions introduces support connectivity [Aiz82; GHS70]; source parity in each replica must therefore be distinguished from connectivity in the support of their sum.

4.3 Switching is independent of interaction range

Multiplying two current expansions allows the source constraints to be redistributed without changing the total current. For $\mathbf{n} \in \Omega_H$, let $\widehat{\mathbf{n}} \in \{0,1\}^{E_H}$ be its support configuration,

$$\widehat{n}_e = \mathbf{1}_{\{n_e>0\}}.$$

If $G \subset H$ and $x, y \in G$, the notation

$$x \overset{\widehat{\mathbf{n}}}{\longleftrightarrow} y \text{ in } G$$

means that x and y are joined by a path whose vertices lie in G and whose edges are open in $\widehat{\mathbf{n}}$.

The switching lemma states this redistribution exactly. In what follows, $G \subset H$ denotes a nested pair of finite vertex sets, each identified with its induced interaction graph. We use the nested-volume formulation of [ADCS15, Lemma 2.2].

Lemma 4.1 (Switching lemma)**.** *For any nested pair of finite vertex sets $G \subset H$, any $x, y \in G$, any $A \subset H$, and any function $F : \Omega_H \to \mathbb{R}$ that is bounded,*

$$\begin{aligned} &\sum_{\substack{\mathbf{n}_1\in\Omega_G:\,\partial\mathbf{n}_1=\{x,y\}\\ \mathbf{n}_2\in\Omega_H:\,\partial\mathbf{n}_2=A}} F(\mathbf{n}_1+\mathbf{n}_2)w_{\beta_\mathrm{I}}(\mathbf{n}_1)w_{\beta_\mathrm{I}}(\mathbf{n}_2) \\ &\quad= \sum_{\substack{\mathbf{n}_1\in\Omega_G:\,\partial\mathbf{n}_1=\varnothing\\ \mathbf{n}_2\in\Omega_H:\,\partial\mathbf{n}_2=A\triangle\{x,y\}}} F(\mathbf{n}_1+\mathbf{n}_2)w_{\beta_\mathrm{I}}(\mathbf{n}_1)w_{\beta_\mathrm{I}}(\mathbf{n}_2)\mathbf{1}\left[x \overset{\widehat{\mathbf{n}_1+\mathbf{n}_2}}{\longleftrightarrow} y \text{ in } G\right]. \end{aligned} \tag{124}$$

Here a current in Ω_G is extended by zero on $E_H \setminus E_G$ when it is added to a current in Ω_H, and $\triangle$ denotes symmetric difference. Both sides are absolutely convergent.

Proof. Indeed, the absolute value of either side is bounded by

$$\|F\|_\infty \exp\left(\beta_\mathrm{I} \sum_{e\in E_G} J_e\right) \exp\left(\beta_\mathrm{I} \sum_{e\in E_H} J_e\right) < \infty.$$

Fix a total current $\mathbf{N} = \mathbf{n}_1 + \mathbf{n}_2 \in \Omega_H$ with $\partial\mathbf{N} = A\triangle\{x,y\}$. For every admissible choice of the first current, write $\mathbf{n}_1 \le \mathbf{N}$ when $n_{1,e} \le N_e$ for every edge. Then

$$w_{\beta_\mathrm{I}}(\mathbf{n}_1)w_{\beta_\mathrm{I}}(\mathbf{N}-\mathbf{n}_1) = w_{\beta_\mathrm{I}}(\mathbf{N}) \prod_{e\in E_G} \binom{N_e}{n_{1,e}}.$$

Regard the N_e parallel copies of each edge as individually labelled. The binomial product counts their assignments to the two replicas; every copy of an edge outside E_G must belong to the second replica. Moreover, $\partial\mathbf{n}_2 = \partial\mathbf{N}\triangle\partial\mathbf{n}_1$. Thus changing $\partial\mathbf{n}_1$ from $\{x,y\}$ to $\varnothing$ changes $\partial\mathbf{n}_2$ from A to $A\triangle\{x,y\}$, exactly as in the two sides of (124).

It remains to count assignments on E_G. If x and y are not connected by $\widehat{\mathbf{N}}$ inside G, no subgraph of the corresponding multigraph can have exactly x and y as its odd-degree vertices: every connected component contains an even number of odd-degree vertices.

If they are connected, fix an ordering of all finite labelled paths and let $\gamma(\mathbf{N})$ be the first x-to-y path contained in the total-current multigraph over G. Toggle the replica assignment of the selected labelled copy of every path edge. This operation is an involution on labelled assignments. It changes the source set of the first replica from $\varnothing$ to $\{x,y\}$, or conversely, while preserving the total current and hence $F(\mathbf{N})w_{\beta_{\mathrm{I}}}(\mathbf{N})$. Summing first over labelled assignments and then over $\mathbf{N}$ proves the identity. □

Sources can be switched only inside a component containing both x and y, which accounts for the connectivity indicator. Taking $G = H = \Lambda$, $A = \{x,y\}$, and $F \equiv 1$ gives the correlation-connectivity identity

$$\left(\langle\sigma_x\sigma_y\rangle^0_{\Lambda,\beta_{\mathrm{I}}}\right)^2 = \mathbf{P}^{\varnothing}_{\Lambda,\beta_{\mathrm{I}}} \otimes \mathbf{P}^{\varnothing}_{\Lambda,\beta_{\mathrm{I}}}(x \leftrightarrow y \text{ in } \operatorname{supp}(\mathbf{n}_1+\mathbf{n}_2)). \tag{125}$$

The tensor product means that $\mathbf{n}_1$ and $\mathbf{n}_2$ are sampled independently from the two displayed current laws. The proof took place entirely in the multigraph determined by the total current. A long interaction edge is just another edge in this multigraph, so the path involution and the identity remain valid without a finite-range assumption.

4.4 Boundary conditions and infinite-volume current laws

For the infinite-volume application, ADCS work on $\mathbb{Z}^d$ under the assumptions [ADCS15]:

C1. $J_{x,y} = J_{0,y-x}$ (translation invariance);

C2. $J_{x,y} \geq 0$ (ferromagnetism);

C3. $\sum_x J_{0,x} < \infty$ (summability);

C4. the graph with edge set $\{\{x,y\} : J_{x,y} > 0\}$ is connected (the condition called *aperiodicity* in the paper).

The finite-volume algebra above is exact for arbitrary interaction range. The genuinely analytic step is now to construct infinite-volume current laws. Here summability in **C3**, rather than finite range, controls the total coupling leaving a site and the thermodynamic limit. Free boundary conditions use currents on Λ. Plus boundary conditions are encoded by adding a ghost vertex $\mathfrak{g}$ with coupling

$$J_{x,\mathfrak{g}} = \sum_{y \notin \Lambda} J_{x,y}.$$

Let $\mathbf{P}^0_{\Lambda,\beta_{\mathrm{I}}}$ be the sourceless law on the ordinary induced graph. For an augmented current $\mathbf{n}$ on $\Lambda \cup \{\mathfrak{g}\}$, ADCS record only the ordinary sources,

$$\partial_\Lambda \mathbf{n} := \left\{ x \in \Lambda : \sum_{e \ni x} n_e \text{ is odd} \right\}.$$

The ghost is not listed in this source set, and no independent source constraint is recorded there. Define

$$\mathcal{Z}^{+,\mathfrak{g}}_\Lambda(A) := \sum_{\partial_\Lambda \mathbf{n} = A} w_{\beta_{\mathrm{I}}}(\mathbf{n}), \qquad A \subset \Lambda,$$

and let $\mathbf{P}^{+,\mathfrak{g}}_{\Lambda,\beta_{\mathrm{I}}}$ be the normalised augmented law with $\partial_\Lambda \mathbf{n} = \varnothing$. Its projection onto ordinary edges is denoted by $\widehat{\mathbf{P}}^+_{\Lambda,\beta_{\mathrm{I}}}$. The finite-volume plus correlation is represented by the augmented sums:

$$\langle \sigma_x \sigma_y \rangle^+_{\Lambda,\beta_{\mathrm{I}}} = \frac{\mathcal{Z}^{+,\mathfrak{g}}_\Lambda(\{x,y\})}{\mathcal{Z}^{+,\mathfrak{g}}_\Lambda(\varnothing)}.$$

Projection can create odd ordinary-edge degree at physical vertices because the removed ghost edges contributed to their augmented parity.

Theorem 4.2 (ADCS Theorem 2.3: infinite-volume current limits)**.** *Under assumptions **C1–C4**, for every $\beta_{\mathrm{I}} > 0$, the restrictions of $\mathbf{P}^0_{\Lambda_L,\beta_{\mathrm{I}}}$ and $\widehat{\mathbf{P}}^+_{\Lambda_L,\beta_{\mathrm{I}}}$, where $\Lambda_L = [-L,L]^d \cap \mathbb{Z}^d$, to any fixed finite set of ordinary lattice edges converge as $L \to \infty$. The limiting laws $\mathbf{P}^0_{\beta_{\mathrm{I}}}$ and $\mathbf{P}^+_{\beta_{\mathrm{I}}}$ on ordinary-edge currents are translation invariant. Each limiting law is also ergodic under lattice translations [ADCS15, Theorem 2.3].*

Remark (Why summability replaces finite range). The theorem is imported rather than fully reproved here. Its proof architecture conditions first on edge-parity variables. Given those parities, multiplicities are independent Poisson variables conditioned to be even or odd. Finite-dimensional parity probabilities converge because they can be written through finite-volume Ising correlations. Translation invariance and ergodicity then follow from the corresponding limits and the mixing of even spin observables. Summability controls these thermodynamic steps; it was not needed for the finite-volume algebra in Sections 4.2–4.3.

Thus $\mathbf{P}^+_{\beta_{\mathrm{I}}}$ always denotes the infinite-volume limit of the projected plus currents. The ghost remains a finite-volume device.

Let $\mathbb{P}_{\mathrm{supp},\beta_{\mathrm{I}}}$ denote the induced law of the support of $\mathbf{n}_1 + \mathbf{n}_2$, where $\mathbf{n}_1 \sim \mathbf{P}^0_{\beta_{\mathrm{I}}}$ and $\mathbf{n}_2 \sim \mathbf{P}^+_{\beta_{\mathrm{I}}}$ are independent, and let $\mathbb{E}_{\mathrm{supp},\beta_{\mathrm{I}}}$ denote expectation under this support law. The support has the following almost-sure uniqueness property.

Theorem 4.3 (ADCS Theorem 2.5: uniqueness of the infinite current cluster)**.** *Under assumptions **C1–C4**, the support of* $\mathbf{n}_1 + \mathbf{n}_2$ *has at most one infinite cluster,* $\mathbb{P}_{\mathrm{supp},\beta_{\mathrm{I}}}$*-almost surely, for every* $\beta_{\mathrm{I}} \geq 0$ *[ADCS15].*

Proof sketch. This is an imported Burton–Keane-type argument. Ordinary FKG is unavailable for current supports. ADCS replace it by insertion tolerance: adding multiplicity 2 to allowed edges in a fixed box opens those support edges while preserving source parity. Ergodicity excludes any deterministic finite number of infinite clusters larger than one. If infinitely many infinite clusters existed, a local modification would create trifurcations with positive density. Amenability, together with summability of J, bounds the expected number of exits from a large box by a boundary-order quantity and contradicts that density [ADCS15, Theorem 2.5 and Lemma 2.6]. □

4.5 The ADCS continuity criterion

The preceding current algebra and infinite-volume construction are applied to the spontaneous magnetisation defined in Section 1.2. The free-state long-range-order parameter is

$$M_{\mathrm{f}}^{\mathrm{LRO}}(\beta_{\mathrm{I}})^2 = \inf_{\substack{B \Subset \mathbb{Z}^d \\ 0<|B|<\infty}} \frac{1}{|B|^2} \sum_{x,y \in B} \langle \sigma_x \sigma_y \rangle^0_{\beta_{\mathrm{I}}} = \inf_{\substack{B \Subset \mathbb{Z}^d \\ 0<|B|<\infty}} \left\langle \left(\frac{1}{|B|} \sum_{x \in B} \sigma_x \right)^2 \right\rangle^0_{\beta_{\mathrm{I}}}. \tag{126}$$

Here B is finite and nonempty. The free state is spin-flip symmetric, so its one-point function vanishes even when two-point long-range order is present. The quantity in (126) is instead the second moment of the block-averaged magnetisation.

Theorem 4.4 (ADCS Theorem 1.2)**.** *Under assumptions **C1–C4**,*

$$M_{\mathrm{f}}^{\mathrm{LRO}}(\beta_{\mathrm{I},c}) = 0 \quad \Longrightarrow \quad m^+(\beta_{\mathrm{I},c}) = 0.$$

In this case the Gibbs state at $\beta_{\mathrm{I},c}$ *is unique, and the Gibbs states are continuous there with respect to* β_{I}*, meaning convergence of the expectation of every local observable for any choice of boundary conditions [ADCS15, Theorem 1.2].*

The function m^+ is nondecreasing in β_{I}, vanishes for $\beta_{\mathrm{I}} < \beta_{\mathrm{I},c}$, and is upper semicontinuous. Hence

$$m^+(\beta_{\mathrm{I},c}) = \lim_{\beta_{\mathrm{I}} \downarrow \beta_{\mathrm{I},c}} m^+(\beta_{\mathrm{I}}),$$

so the theorem gives continuity from the ordered, low-temperature side; the disordered-side limit $\beta_{\mathrm{I}} \uparrow \beta_{\mathrm{I},c}$ is zero by the definition of $\beta_{\mathrm{I},c}$. The proof below uses switching, uniqueness of the infinite current cluster, averaging and Cauchy–Schwarz. Switching alone is not the continuity argument.

The critical magnetisation implication follows from three estimates. They are reconstructed because, unlike the imported thermodynamic theorems, they form the operative random-current part of the continuity proof.

Claim (Current connectivity and free correlations; ADCS (3.2)–(3.3))**.** *For* $x, y \in \mathbb{Z}^d$,

$$\mathbb{P}_{\mathrm{supp},\beta_{\mathrm{I}}}(x \leftrightarrow y) \le \langle \sigma_x \sigma_y \rangle^0_{\beta_{\mathrm{I}}}. \tag{127}$$

Proof. In Λ_L, apply Lemma 4.1 with $G = \Lambda_L$, $H = \Lambda_L \cup \{\mathfrak{g}\}$ and $A = \{x, y\}$. The first current has sources $\{x, y\}$ on the left and no sources on the right; the augmented second current has sources $\{x, y\}$ on the left and no recorded ordinary sources on the right. After normalisation,

$$\begin{aligned}&\mathbf{P}^0_{\Lambda_L,\beta_{\mathrm{I}}} \otimes \mathbf{P}^{+,\mathfrak{g}}_{\Lambda_L,\beta_{\mathrm{I}}}(x \leftrightarrow y \text{ through ordinary edges inside } \Lambda_L)\\ &\quad= \langle \sigma_x \sigma_y \rangle^0_{\Lambda_L,\beta_{\mathrm{I}}} \langle \sigma_x \sigma_y \rangle^+_{\Lambda_L,\beta_{\mathrm{I}}} \le \langle \sigma_x \sigma_y \rangle^0_{\Lambda_L,\beta_{\mathrm{I}}}.\end{aligned} \tag{128}$$

For a fixed radius R, connection by ordinary edges inside Λ_R is a cylinder event. Theorem 4.2 permits $L \to \infty$; these events then increase to $\{x \leftrightarrow y\}$ as $R \to \infty$. Monotone convergence proves (127) [ADCS15, (3.2)–(3.3)]. □

Likewise, $\{x \leftrightarrow \infty\}$ is understood as the decreasing limit of $\{x \leftrightarrow \Lambda_R^c\}$, each approximated by paths in a larger finite box. This convention is used below for every nonlocal connection event.

Claim (Vanishing free LRO excludes doubled-current percolation; ADCS (3.5))**.** *For every* $\beta_{\mathrm{I}} \ge 0$,

$$\mathbb{P}_{\mathrm{supp},\beta_{\mathrm{I}}}(0 \leftrightarrow \infty) \le M_{\mathrm{f}}^{\mathrm{LRO}}(\beta_{\mathrm{I}}). \tag{129}$$

Proof. For finite nonempty $B \subset \mathbb{Z}^d$, let

$$X_B := \sum_{x \in B} \mathbf{1}_{\{x \leftrightarrow \infty\}}.$$

Translation invariance and Cauchy–Schwarz give

$$\left(|B| \mathbb{P}_{\mathrm{supp},\beta_{\mathrm{I}}}(0 \leftrightarrow \infty)\right)^2 = \left(\mathbb{E}_{\mathrm{supp},\beta_{\mathrm{I}}}[X_B]\right)^2 \le \mathbb{E}_{\mathrm{supp},\beta_{\mathrm{I}}}[X_B^2].$$

By Theorem 4.3, two vertices connected to infinity belong to the same infinite cluster and hence are connected. Using (127),

$$\begin{aligned}\mathbb{P}_{\mathrm{supp},\beta_{\mathrm{I}}}(0 \leftrightarrow \infty)^2 &\le \frac{1}{|B|^2} \sum_{x,y \in B} \mathbb{P}_{\mathrm{supp},\beta_{\mathrm{I}}}(x \leftrightarrow y)\\ &\le \frac{1}{|B|^2} \sum_{x,y \in B} \langle \sigma_x \sigma_y \rangle^0_{\beta_{\mathrm{I}}}.\end{aligned}$$

Taking the infimum over B proves the claim [ADCS15, (3.5)]. Infinite-cluster uniqueness replaces the

FKG step available in independent or FK percolation. □

Lemma 4.5 (Plus/free correlation comparison; ADCS (3.11))**.** *Let* $\beta_\mathrm{I} > 0$. *For* $x, y \in \mathbb{Z}^d$, *fix an interaction path* $x = x_0, x_1, \ldots, x_m = y$ *with* $J_{x_j,x_{j+1}} > 0$, *and set*

$$\Gamma_{x,y} := \prod_{j=0}^{m-1} \min\left\{ \frac{\sinh(\beta_\mathrm{I} J_{x_j,x_{j+1}})}{\cosh(\beta_\mathrm{I} J_{x_j,x_{j+1}})}, \frac{\cosh(\beta_\mathrm{I} J_{x_j,x_{j+1}}) - 1}{\sinh(\beta_\mathrm{I} J_{x_j,x_{j+1}})} \right\} = \prod_{j=0}^{m-1} \tanh\Big(\frac{\beta_\mathrm{I} J_{x_j,x_{j+1}}}{2}\Big) > 0.$$

Then

$$0 \le \langle \sigma_x \sigma_y \rangle^+_{\beta_\mathrm{I}} - \langle \sigma_x \sigma_y \rangle^0_{\beta_\mathrm{I}} \le \Gamma^{-1}_{x,y} \mathbb{P}_{\mathrm{supp},\beta_\mathrm{I}}(x \leftrightarrow \infty). \tag{130}$$

Proof. Take L large enough that the chosen path lies in Λ_L, and abbreviate $\mathcal{Z}^0(A) = \mathcal{Z}_{\Lambda_L}(A)$ and $\mathcal{Z}^+(A) = \mathcal{Z}^{+,\mathfrak{g}}_{\Lambda_L}(A)$. The two current expansions give

$$\begin{aligned} &\langle \sigma_x \sigma_y \rangle^+_{\Lambda_L,\beta_\mathrm{I}} - \langle \sigma_x \sigma_y \rangle^0_{\Lambda_L,\beta_\mathrm{I}} \\ &\quad = \frac{\mathcal{Z}^0(\varnothing)\mathcal{Z}^+(\{x,y\}) - \mathcal{Z}^0(\{x,y\})\mathcal{Z}^+(\varnothing)}{\mathcal{Z}^0(\varnothing)\mathcal{Z}^+(\varnothing)}. \end{aligned}$$

Apply Lemma 4.1 to the second product in the numerator. Both products can then be summed over $\partial \mathbf{n}_1 = \varnothing$ and $\partial_{\Lambda_L} \mathbf{n}_2 = \{x, y\}$, and their difference becomes

$$\frac{\sum w_{\beta_\mathrm{I}}(\mathbf{n}_1) w_{\beta_\mathrm{I}}(\mathbf{n}_2) \mathbf{1}_{\{x \not\leftrightarrow y \text{ inside } \Lambda_L\}}}{\mathcal{Z}^0(\varnothing)\mathcal{Z}^+(\varnothing)}. \tag{131}$$

Here and below in this proof, the sum is over these two source conditions.

If the augmented second current has ordinary sources x, y, but the two vertices are not connected through ordinary edges, the parity rule on their distinct ordinary components forces both components to meet the ghost. Thus the numerator in (131) is bounded by the same sum with $\mathbf{1}_{\{x \leftrightarrow \mathfrak{g}\}}$.

Classify current pairs by every variable away from the path and by the parities of $n_{2,e}$ on its edges. Flip each path parity in the second current, requiring the new multiplicity to be at least one. This one-to-many map changes $\partial_{\Lambda_L} \mathbf{n}_2 = \{x, y\}$ into $\partial_{\Lambda_L} \mathbf{n}'_2 = \varnothing$. Since every path edge remains present, the connection from x to the ghost in the combined support is preserved. Comparing the even and odd Poisson series edge by edge gives the uniform cost explicitly. For one path edge, write $t = \beta_\mathrm{I} J_e > 0$. Its three relevant parity sums are

$$\sum_{\substack{n \ge 0 \\ n \text{ even}}} \frac{t^n}{n!} = \cosh t, \qquad \sum_{\substack{n \ge 1 \\ n \text{ odd}}} \frac{t^n}{n!} = \sinh t, \qquad \sum_{\substack{n \ge 2 \\ n \text{ even}}} \frac{t^n}{n!} = \cosh t - 1. \tag{132}$$

If the original multiplicity is even, its positive odd images have relative mass $\sinh t / \cosh t = \tanh t$. If it is odd, its positive even images have relative mass

$$\frac{\cosh t - 1}{\sinh t} = \tanh\left(\frac{t}{2}\right).$$

Since $\tanh(t/2) < \tanh t$ for $t > 0$, the edgewise lower cost is $\tanh(t/2)$. Multiplication over the fixed path gives precisely $\Gamma_{x,y}$, and the sourceful sum is therefore at most $\Gamma_{x,y}^{-1}$ times its source-free image sum. Hence

$$\begin{aligned}&\langle \sigma_x \sigma_y \rangle^{+}_{\Lambda_L,\beta_{\mathrm{I}}} - \langle \sigma_x \sigma_y \rangle^{0}_{\Lambda_L,\beta_{\mathrm{I}}} \\ &\qquad \le \Gamma_{x,y}^{-1} \mathbf{P}^{0}_{\Lambda_L,\beta_{\mathrm{I}}} \otimes \mathbf{P}^{+,\mathfrak{g}}_{\Lambda_L,\beta_{\mathrm{I}}}(x \leftrightarrow \mathfrak{g}).\end{aligned}$$

The lower bound follows from ferromagnetic boundary-condition monotonicity. Approximate the connection on the right by finite-radius events, project the plus current onto ordinary edges, and let $L \to \infty$. This proves (130), reconstructing ADCS (3.6)–(3.11) [ADCS15, (3.6)–(3.11)]. □

If $\beta_{\mathrm{I},c} = 0$, then $m^{+}(\beta_{\mathrm{I},c}) = m^{+}(0) = 0$, so the desired conclusion is immediate. We may therefore assume $\beta_{\mathrm{I},c} > 0$, in which case Lemma 4.5 applies at $\beta_{\mathrm{I}} = \beta_{\mathrm{I},c}$. Then (129) and $M_{\mathrm{f}}^{\mathrm{LRO}}(\beta_{\mathrm{I},c}) = 0$ imply $\mathbb{P}_{\mathrm{supp},\beta_{\mathrm{I},c}}(0 \leftrightarrow \infty) = 0$. Lemma 4.5 then identifies the plus and free two-point functions. The Ising FKG inequality gives

$$m^{+}(\beta_{\mathrm{I},c})^2 \le \langle \sigma_x \sigma_y \rangle^{+}_{\beta_{\mathrm{I},c}} = \langle \sigma_x \sigma_y \rangle^{0}_{\beta_{\mathrm{I},c}}.$$

Averaging over $x, y \in B$ and taking the infimum over finite nonempty B proves $m^{+}(\beta_{\mathrm{I},c}) = 0$. This reconstructs the critical-magnetisation implication. Uniqueness of the Gibbs state and continuity of every local observable are the additional conclusions of ADCS Theorem 1.2 and its thermodynamic argument, in particular Proposition B.1; they are not claimed to follow from these three estimates alone [ADCS15].

The inverse-square Ising chain does not satisfy the vanishing-LRO hypothesis: the Thouless jump gives $m^{+}(\beta_{\mathrm{I},c}) > 0$, so the contrapositive of Theorem 4.4 yields $M_{\mathrm{f}}^{\mathrm{LRO}}(\beta_{\mathrm{I},c}) > 0$.

Finite-volume switching, infinite-volume current laws and support connectivity together give a precise conditional mechanism: if the free state has no long-range order at the critical point, doubled-current percolation disappears, plus and free correlations coincide, and critical magnetisation vanishes. The next subsection checks the only missing input for the inverse-square model. Its failure there limits the continuity criterion, but it does not invalidate any of the current identities just proved.

4.6 Failure of the infrared criterion at inverse-square decay

For reflection-positive interactions, which is an additional assumption at this stage, ADCS verify $M_{\mathrm{f}}^{\mathrm{LRO}}(\beta_{\mathrm{I},c}) = 0$ through an infrared bound. Set

$$E(p) = \sum_{x \in \mathbb{Z}^d} (1 - \cos(p \cdot x)) J_{0,x}.$$

Here $p \in [-\pi, \pi]^d$ is the Fourier variable and $p \cdot x$ is the Euclidean scalar product.

The relevant condition is

$$\int_{[-\pi,\pi]^d} \frac{dp}{(2\pi)^d} \frac{1}{E(p)} < \infty.$$

The same integral is the transience criterion for the random walk whose jump probabilities are proportional to $J_{x,y}$. Consequently, reflection positivity and transience imply continuity of the spontaneous magnetisation at $\beta_{\mathrm{I},c}$ [ADCS15, Corollaries 1.4–1.5]. The criterion includes nearest-neighbour models in $d > 2$ and reflection-positive one-dimensional power-law kernels, such as the exact interaction $J(r) = cr^{-\alpha}$, with $1 < \alpha < 2$. The mere two-sided asymptotic relation $J(r) \asymp r^{-\alpha}$ does not by itself imply reflection positivity, so this application is not asserted for every comparable kernel.

For the exact one-dimensional power-law interaction $J(r) = cr^{-\alpha}$, the small-momentum behaviour is $E(p) \asymp |p|^{\alpha-1}$ for $1 < \alpha < 2$. The integral is finite in that range. At $\alpha = 2$, one has $E(p) \asymp |p|$. This borderline estimate can be computed directly and identifies the analytic obstruction. Up to the fixed factor $2c$,

$$E(p) = \sum_{r \geq 1} \frac{1 - \cos(pr)}{r^2}.$$

For the upper bound, split the sum at $L = \lfloor |p|^{-1} \rfloor$. On $r \leq L$, the inequality $1 - \cos t \leq t^2/2$ gives

$$\sum_{r \leq L} \frac{1 - \cos(pr)}{r^2} \leq \frac{p^2}{2} L = O(|p|).$$

On the tail, $1 - \cos(pr) \leq 2$ and $\sum_{r>L} r^{-2} = O(L^{-1}) = O(|p|)$. Thus $E(p) \lesssim |p|$.

For the matching lower bound, take integers r in an interval $[a|p|^{-1}, b|p|^{-1}]$, where $0 < a < b < \pi$ are fixed and chosen so that $1 - \cos t \geq c_{a,b} > 0$ for $t \in [a, b]$. For all sufficiently small $|p|$,

$$E(p) \geq c_{a,b} \sum_{a/|p| \leq r \leq b/|p|} \frac{1}{r^2} \gtrsim |p|.$$

Hence $E(p) \asymp |p|$ without appealing to a general Fourier asymptotic. The contribution of a neighbourhood of the origin to the infrared integral is therefore comparable to

$$\int_0^{\varepsilon} \frac{dp}{p},$$

which diverges logarithmically. The infrared criterion therefore gives no continuity conclusion at the inverse-square exponent, where the Thouless jump occurs. This is a failure of the estimate used to verify the vanishing-LRO hypothesis, not a failure of the random-current representation or of the switching lemma. Those identities remain exact at $\alpha = 2$.

4.7 From Ising currents to the DGC

The ADCS criterion does not resolve the inverse-square critical Ising point: its required free-state LRO hypothesis fails there. Nevertheless, the finite-volume expansion and switching algebra remain exact and therefore provide an informative transfer test. In the Ising argument, a nonnegative expansion produces parity sources, the switching lemma turns a source constraint into a connectivity event and the doubled-current geometry controls a spin observable. We therefore test whether an analogous algebra exists for the DGC. Its single-site sum and observable are different, so each step must be checked separately.

Table 1 records the two graphical mechanisms used in this comparison. The DCGT column uses the inverse-square tail parameter β_{tail}, whereas the ADCS column uses the physical Ising inverse temperature β_{I}.

	DCGT	**ADCS**
random object	Bernoulli percolation or a wired FK random-cluster configuration	ordinary-edge support of the sum of independent free and projected-plus infinite-volume currents
order parameter	$\theta(q, \beta_{\text{tail}}, \lambda) = \mathbb{P}^1_{\beta_{\text{tail}},\lambda,q}[0 \leftrightarrow \infty]$	$m^+(\beta_{\text{I}})$, controlled through $M_{\text{f}}^{\text{LRO}}$
main tool	block renormalisation	switching and uniqueness of the infinite cluster
decisive estimate	$\theta > 0 \Rightarrow \beta_{\text{tail}}\theta^2 \geq 1$	$\mathbb{P}_{\text{supp},\beta_{\text{I}}}(0 \leftrightarrow \infty) \leq M_{\text{f}}^{\text{LRO}}(\beta_{\text{I}})$
role here	inverse-square density gap and Ising jump	what switching proves when free LRO vanishes

Table 1: The DCGT and ADCS graphical mechanisms used as transfer tests, with their model-specific parameters β_{tail} and β_{I}.

The Ising current formalism shows what becomes possible when a positive expansion, parity sources and a weight-preserving switch coexist. It leads to three transfer questions:

Q1. Does the DGC admit a nonnegative current-type expansion?

Q2. Do field insertions produce parity-source constraints?

Q3. Is there a weight-preserving source-switching operation?

The DGC expansion is derived directly from its Gibbs weight and tested against **Q1–Q3**. It has nonnegative weights; field insertions retain part of the parity-source structure; and the canonical Ising path switch fails to preserve the DGC weights. These statements do not resolve critical localisation or delocalisation.

From this point onward, β_{D} denotes the inverse temperature of the DGC; it is distinct from both β_{I} and β_{tail}.

Remark (Kernel scope). The moment-weighted expansion is algebraic and applies to a fixed nonnegative summable kernel whenever the corresponding finite-volume Dirichlet matrix is positive definite. The positive-tail inverse-square kernels used in the main application satisfy this condition through a direct exterior-mass lower bound. For finite-range kernels, the same Fubini argument uses the smallest eigenvalue of the full Dirichlet matrix rather than a pointwise direct coupling to the exterior. Garban's small-β_{D} logarithmic variance bounds hold for every nonnegative kernel $J_2(r) \asymp r^{-2}$. His full invariance principle and identification of the effective temperature are proved for the special extension kernels constructed in that work. Finiteness of a localisation threshold is asserted only for kernels covered by a sufficiently large-β_{D} localisation theorem [Gar23; FZ91].

4.7.1 Garban's problem and the DGC observable

Garban's Open Problem 4 asks whether, at $\alpha = 2$, DGC delocalisation is discontinuous [Gar23]. The relevant observable is the growth of a height variance rather than a spin magnetisation. We fix the model before separating the established small- and large-β_{D} regimes from the unknown endpoint.

Let $\Lambda_N = \{-N, \dots, N\}$, and extend $\varphi \in \mathbb{Z}^{\Lambda_N}$ by $\varphi_i = 0$ outside Λ_N. Fix a nonnegative translation-invariant kernel

$$J_\alpha : \mathbb{N} \longrightarrow [0, \infty), \qquad J_\alpha(r) \asymp r^{-\alpha}.$$

Consider

$$H^{\mathrm{DGC}}_{N,\alpha}(\varphi) = \frac{1}{2} \sum_{\substack{i,j \in \mathbb{Z} \\ i \neq j \\ \{i,j\} \cap \Lambda_N \neq \varnothing}} J_\alpha(|i-j|)(\varphi_i - \varphi_j)^2$$

and

$$\mu^{\mathrm{DGC}}_{N,\beta_{\mathrm{D}},\alpha}(\varphi) = \frac{1}{Z_{N,\beta_{\mathrm{D}},\alpha}} \exp\{-\beta_{\mathrm{D}} H^{\mathrm{DGC}}_{N,\alpha}(\varphi)\}.$$

Here $Z_{N,\beta_{\mathrm{D}},\alpha}$ is the partition function. We use $\mathbb{E}^{\mathrm{DGC}}_{N,\beta_{\mathrm{D}},\alpha}$ and $\mathrm{Var}^{\mathrm{DGC}}_{N,\beta_{\mathrm{D}},\alpha}$ for expectation and variance under this probability measure. The factor $1/2$ compensates for summing over ordered pairs. Each height φ_i is unbounded, unlike an Ising spin. Magnetisation is therefore replaced by the growth of height fluctuations.

From now on, $\alpha = 2$ and J_2 is fixed; all thresholds refer to this kernel.

The established small- and large-β_{D} regimes are consistent with a BKT-type scenario, but the $T = T_c$ behaviour in Garban's formulation is not known [Gar23, Figure 1 and Open Problem 4]. Slurink and Hilhorst related the inverse-square height chain to a plasma of logarithmically interacting charges. The modern high-temperature analysis uses a Coulomb-gas expansion in the spirit of the Fröhlich–Spencer proof of the BKT transition [FS81; SH83; Gar23]. These Coulomb-gas methods concern the integer-valued height field; they do not produce an Edwards–Sokal-type identity with the Ising model.

For periodic boundary conditions, Kjaer and Hilhorst derived an exact variance identity at $\beta_{\mathrm{D}} = 1$ for the special kernel

$$J(r) = \frac{1}{r^2 - \frac{1}{4}},$$

which in particular implies logarithmic divergence of the height variance [KH82]. Fröhlich and Zegarlinski proved large-β_{D} localisation for the kernel class treated in their work [FZ91]. Garban proved the general sufficiently-small-β_{D} logarithmic bounds for nonnegative kernels comparable to r^{-2}, together with the stronger invariance principle for his extension kernels [Gar23, Theorem 1.1]. The two estimates used here can be displayed as

$$\begin{aligned} c_{\beta_{\mathrm{D}}} \log N \le \mathrm{Var}^{\mathrm{DGC}}_{N,\beta_{\mathrm{D}},2}(\varphi_0) \le C_{\beta_{\mathrm{D}}} \log N, &\quad \beta_{\mathrm{D}} \ll 1, \quad N \ge 2, \\ \sup_{N\ge 1} \mathrm{Var}^{\mathrm{DGC}}_{N,\beta_{\mathrm{D}},2}(\varphi_0) \le C'_{\beta_{\mathrm{D}}} < \infty, &\quad \beta_{\mathrm{D}} \gg 1. \end{aligned} \tag{133}$$

The regime-only meaning of $\beta_{\mathrm{D}} \ll 1$ and $\beta_{\mathrm{D}} \gg 1$ is fixed in Section 1; this notation does not locate the critical point. Garban proved the first line for every nonnegative $J_2(r) \asymp r^{-2}$ [Gar23, Theorem 1.1]. The second line is a bounded-variance estimate for kernels covered by the localisation theorem, and we do not extend it to every kernel in that wider comparison class. For a particular class of inverse-square kernels arising from his extension construction, the rescaled integer-valued chain has the same Gaussian limit and effective temperature as the corresponding real-valued chain. Garban calls this the *invisibility of the integers* [Gar23, Theorem 1.1].

Both models therefore have a marginal phase diagram at $\alpha = 2$, but the analogy stops at that level. Their microscopic variables, Gibbs measures and observables differ. The Ising transition is described by $m^+(\beta_{\mathrm{I}})$; DGC delocalisation is measured by the growth of the height variance. These order parameters are not identified with one another.

The open endpoint and the report-specific proxy. Garban asks whether DGC delocalisation is discontinuous at $\alpha = 2$. One motivation is the numerical prediction of Slurink and Hilhorst: the integers should be invisible for $T > T_c$, while $T = T_c$ should display intermediate behaviour [SH83; Gar23]. Neither source states this problem as the equality of thresholds called $\beta^{\log}_{\mathrm{D,deloc}}$ and $\beta_{\mathrm{D,loc}}$.

The report-specific quantities below give a weaker finite-volume version of the question. Since convergence of the normalised variance is not known, set

$$\rho_-(\beta_{\mathrm{D}}) = \liminf_{N\to\infty} \frac{\mathrm{Var}^{\mathrm{DGC}}_{N,\beta_{\mathrm{D}},2}(\varphi_0)}{\log N}, \qquad \rho_+(\beta_{\mathrm{D}}) = \limsup_{N\to\infty} \frac{\mathrm{Var}^{\mathrm{DGC}}_{N,\beta_{\mathrm{D}},2}(\varphi_0)}{\log N}. \tag{134}$$

These are the lower and upper delocalisation coefficients. If they agree, their common value is denoted by $\rho(\beta_{\mathrm{D}})$. The known high-temperature estimates give

$$0 < \rho_-(\beta_{\mathrm{D}}) \le \rho_+(\beta_{\mathrm{D}}) < \infty$$

for sufficiently small β_{D}. For a kernel covered by a large-β_{D} localisation theorem, $\rho_+(\beta_{\mathrm{D}}) = 0$ for every sufficiently large β_{D}.

Definition 4.6 (Two report-specific threshold parameters)**.** For the fixed kernel J_2, set

$$\beta_{\mathrm{D,deloc}}^{\log} := \sup\{\beta_{\mathrm{D}} > 0 : \rho_-(\beta_{\mathrm{D}}) > 0\}, \tag{135}$$

$$\beta_{\mathrm{D,loc}} := \inf\left\{\beta_{\mathrm{D}} > 0 : \sup_{N\geq 1} \mathrm{Var}^{\mathrm{DGC}}_{N,\beta_{\mathrm{D}},2}(\varphi_0) < \infty\right\}. \tag{136}$$

Both quantities take values in the extended interval $[0,\infty]$, with the convention that the infimum of the empty set is ∞. The small-β_{D} bound implies $\beta_{\mathrm{D,deloc}}^{\log} > 0$. If bounded-variance localisation holds for every sufficiently large β_{D}, then both $\beta_{\mathrm{D,deloc}}^{\log}$ and $\beta_{\mathrm{D,loc}}$ are finite.

Remark (Monotonicity in the inverse temperature)*.* For every fixed N, the map

$$\beta_{\mathrm{D}} \longmapsto \mathrm{Var}^{\mathrm{DGC}}_{N,\beta_{\mathrm{D}},2}(\varphi_0)$$

is nonincreasing. Indeed, increasing β_{D} increases every conductance of the associated integer-valued Gaussian free field, and the height variance is nonincreasing in the conductances [CDL26, Proposition 2.4]. Consequently, both ρ_- and ρ_+ are nonincreasing functions of β_{D}.

The two parameters describe different finite-volume properties. Bounded-variance localisation implies $\rho_+(\beta_{\mathrm{D}}) = 0$, whereas $\rho_-(\beta_{\mathrm{D}}) = 0$ is also compatible with a variance that diverges more slowly than $\log N$.

By monotonicity in β_{D}, the set

$$\{\beta_{\mathrm{D}} > 0 : \rho_-(\beta_{\mathrm{D}}) > 0\}$$

is an initial interval, while

$$\left\{\beta_{\mathrm{D}} > 0 : \sup_{N\geq 1} \mathrm{Var}^{\mathrm{DGC}}_{N,\beta_{\mathrm{D}},2}(\varphi_0) < \infty\right\}$$

is a terminal interval. In particular,

$$\beta_{\mathrm{D,deloc}}^{\log} \leq \beta_{\mathrm{D,loc}}$$

in the extended-real sense. What remains open is whether the two thresholds coincide, whether either endpoint belongs to the corresponding regime, and what the precise fluctuation scale is at the endpoint. These are additional questions introduced by this reformulation rather than Garban's stated open problem [Gar23].

Remark (A report-specific endpoint proxy)*.* Whenever $\beta_{\mathrm{D,deloc}}^{\log} < \infty$, one weaker question suggested by Garban's discontinuity problem is whether

$$\rho_-(\beta_{\mathrm{D,deloc}}^{\log}) > 0?$$

If the normalised variance converges there, what is its limit? For kernels in Garban's extension class, does it agree with the corresponding Gaussian coefficient? The separate equality $\beta_{\mathrm{D,deloc}}^{\log} = \beta_{\mathrm{D,loc}}$ is meaningful under the definitions above, but it is an additional question and is not asserted here.

The endpoint inequality controls only the order of the variance. It gives neither an invariance principle nor the effective temperature, and it does not identify either threshold with a unique critical point. It is therefore weaker than the proposed BKT-type roughening and discontinuity scenario.

4.7.2 The moment-weighted current expansion

The DGC has a finite-volume current expansion that shows which parts of the Ising construction survive. Translation invariance gives the site-independent diagonal coefficient

$$a := \sum_{j \neq i} J_2(|i-j|) = 2 \sum_{r \geq 1} J_2(r) \in (0, \infty).$$

Let

$$E_N := \{\{i,j\} \subset \Lambda_N : J_2(|i-j|) > 0\}.$$

Because the field is zero outside Λ_N, every interaction with an exterior site contributes only to the diagonal term. Expanding the squares in the ordered-pair Hamiltonian therefore gives

$$H^{\mathrm{DGC}}_{N,2}(\varphi) = a \sum_{i \in \Lambda_N} \varphi_i^2 - 2 \sum_{\{i,j\} \in E_N} J_2(|i-j|)\varphi_i \varphi_j.$$

For $k \in \mathbb{N}_0$, define the one-site moments

$$\mathfrak{m}_{\beta_{\mathrm{D}}}(k) := \sum_{m \in \mathbb{Z}} m^k \mathrm{e}^{-\beta_{\mathrm{D}} a m^2}.$$

A current is now $\mathbf{n} \in \mathbb{N}_0^{E_N}$, with degree $d_{\mathbf{n}}(i) = \sum_{e \ni i} n_e$. For an insertion vector $\mathbf{s} \in \mathbb{N}_0^{\Lambda_N}$, put

$$W^{(N)}_{\beta_{\mathrm{D}},\mathbf{s}}(\mathbf{n}) := \prod_{e=\{i,j\} \in E_N} \frac{(2\beta_{\mathrm{D}} J_2(|i-j|))^{n_e}}{n_e!} \prod_{i \in \Lambda_N} \mathfrak{m}_{\beta_{\mathrm{D}}}(d_{\mathbf{n}}(i) + s_i).$$

The coordinate s_i is the power of φ_i inserted in the observable, and $\mathbf{0}$ denotes the all-zero insertion vector.

Proposition 4.7 (Moment-weighted DGC expansion)**.** *For every finite N whose finite-volume Dirichlet matrix is positive definite, every $\beta_{\mathrm{D}} > 0$, and every $\mathbf{s} \in \mathbb{N}_0^{\Lambda_N}$,*

$$\mathbb{E}^{\mathrm{DGC}}_{N,\beta_{\mathrm{D}},2}\left[\prod_{i \in \Lambda_N} \varphi_i^{s_i}\right] = \frac{\sum_{\mathbf{n} \in \mathbb{N}_0^{E_N}} W^{(N)}_{\beta_{\mathrm{D}},\mathbf{s}}(\mathbf{n})}{\sum_{\mathbf{n} \in \mathbb{N}_0^{E_N}} W^{(N)}_{\beta_{\mathrm{D}},\mathbf{0}}(\mathbf{n})}. \tag{137}$$

Every summand is nonnegative. A nonzero term satisfies

$$d_{\mathbf{n}}(i) + s_i \equiv 0 \pmod 2 \qquad (i \in \Lambda_N).$$

Proof. For each internal edge, expand

$$e^{2\beta_{\mathrm{D}} J_2(|i-j|)\varphi_i\varphi_j} = \sum_{n_{ij}\geq 0} \frac{(2\beta_{\mathrm{D}} J_2(|i-j|))^{n_{ij}}}{n_{ij}!} \varphi_i^{n_{ij}} \varphi_j^{n_{ij}}.$$

Define the finite-volume Dirichlet matrix by

$$(L_N^{\mathrm{D}})_{ij} = \begin{cases} a, & i = j, \\ -J_2(|i-j|), & i \neq j, \end{cases} \qquad i, j \in \Lambda_N.$$

Then

$$H_{N,2}^{\mathrm{DGC}}(\psi) = \langle \psi, L_N^{\mathrm{D}} \psi \rangle, \qquad \psi \in \mathbb{R}^{\Lambda_N}.$$

By the positive-definiteness hypothesis,

$$\kappa_N := \lambda_{\min}(L_N^{\mathrm{D}}) > 0.$$

Consequently,

$$H_{N,2}^{\mathrm{DGC}}(|\varphi|) = \langle |\varphi|, L_N^{\mathrm{D}} |\varphi| \rangle \geq \kappa_N \|\varphi\|_2^2.$$

For the positive-tail inverse-square kernels considered in the main application, the decomposition into internal-gradient and exterior terms also gives the sufficient lower bound

$$\kappa_N \geq \min_{i\in\Lambda_N} \sum_{j\notin\Lambda_N} J_2(|i-j|) > 0.$$

After taking absolute values and summing each exponential series, the total absolute sum is

$$\sum_{\varphi\in\mathbb{Z}^{\Lambda_N}} \prod_{i\in\Lambda_N} |\varphi_i|^{s_i} e^{-\beta_{\mathrm{D}} H_{N,2}^{\mathrm{DGC}}(|\varphi|)} \\ \leq \sum_{\varphi\in\mathbb{Z}^{\Lambda_N}} \prod_{i\in\Lambda_N} |\varphi_i|^{s_i} e^{-\beta_{\mathrm{D}}\kappa_N \|\varphi\|_2^2} < \infty.$$

No lower bound on κ_N uniform in N is required for this finite-volume application of Fubini's theorem. Summing the field variable at each vertex yields the displayed moment factors. Since $\mathfrak{m}_{\beta_{\mathrm{D}}}(k) = 0$ for odd k and $\mathfrak{m}_{\beta_{\mathrm{D}}}(k) > 0$ for even k. Together with $J_2 \geq 0$, this proves nonnegativity and the parity constraint. $\square$

This proves **Q1**: the DGC has a nonnegative finite-volume *current-type* expansion. Unlike the Ising random-current representation, its vertex factors retain the full incident degree.

4.7.3 Sources versus degree defects

For $x \neq y$, taking $\mathbf{s} = \mathbf{1}_{\{x\}} + \mathbf{1}_{\{y\}}$, where $\mathbf{1}_{\{x\}}$ is one at coordinate x and zero elsewhere, forces

$$\partial\mathbf{n} := \{i \in \Lambda_N : d_{\mathbf{n}}(i) \text{ is odd}\} = \{x, y\}.$$

This resembles the Ising source constraint, but fixing $\partial\mathbf{n}$ does not fix the local factors: the numerator contains $\mathfrak{m}_{\beta_{\mathrm{D}}}(d_{\mathbf{n}}(x)+1)\mathfrak{m}_{\beta_{\mathrm{D}}}(d_{\mathbf{n}}(y)+1)$, while the denominator contains the degree-dependent factors $\mathfrak{m}_{\beta_{\mathrm{D}}}(d_{\mathbf{n}}(i))$.

Normalise the zero-insertion weights by

$$\mathbb{Q}^{\mathrm{DGC}}_{N,\beta_{\mathrm{D}}}(\mathbf{n}) := \frac{W^{(N)}_{\beta_{\mathrm{D}},\mathbf{0}}(\mathbf{n})}{\sum_{\mathbf{m}\in\mathbb{N}_0^{E_N}} W^{(N)}_{\beta_{\mathrm{D}},\mathbf{0}}(\mathbf{m})}. \tag{138}$$

The Gibbs law is invariant under the global sign change $\varphi \mapsto -\varphi$, hence $\mathbb{E}^{\mathrm{DGC}}_{N,\beta_{\mathrm{D}},2}[\varphi_0] = 0$. Proposition 4.7 therefore gives the exact degree-defect identity

$$\mathrm{Var}^{\mathrm{DGC}}_{N,\beta_{\mathrm{D}},2}(\varphi_0) = \mathbb{E}_{\mathbb{Q}^{\mathrm{DGC}}_{N,\beta_{\mathrm{D}}}}\left[\frac{\mathfrak{m}_{\beta_{\mathrm{D}}}(d_{\mathbf{n}}(0)+2)}{\mathfrak{m}_{\beta_{\mathrm{D}}}(d_{\mathbf{n}}(0))}\right].$$

The ratio is evaluated on the support of $\mathbb{Q}^{\mathrm{DGC}}_{N,\beta_{\mathrm{D}}}$, where every degree is even and the denominator is positive. This insertion creates no odd source; instead it replaces the local factor $\mathfrak{m}_{\beta_{\mathrm{D}}}(d_{\mathbf{n}}(0))$ by $\mathfrak{m}_{\beta_{\mathrm{D}}}(d_{\mathbf{n}}(0)+2)$. This ratio, rather than source connectivity, is the observable that a graphical argument would have to control.

The answer to **Q2** is only partial. A two-point insertion produces the familiar parity-source set $\{x, y\}$, but the observable in Garban's problem is φ_0^2, whose insertion leaves every source parity even. Parity alone therefore does not turn the relevant height variance into a source-connectivity probability. One power at each of two vertices changes two parity constraints; two powers at the same vertex change its moment index without changing parity. The variance is therefore a local degree ratio under $\mathbb{Q}^{\mathrm{DGC}}_{N,\beta_{\mathrm{D}}}$. An estimate for Garban's problem must control that ratio.

4.7.4 Obstruction to the canonical Ising switch

The expansion retains the full degree in each vertex weight. For Ising spins, $\sum_{\sigma=\pm1}\sigma^k$ depends only on the parity of k; the even DGC moments retain more information. This difference obstructs the specific labelled-path involution used in Lemma 4.1.

For two insertion vectors $\mathbf{s}_1, \mathbf{s}_2$, define the two-replica weight

$$W^{(2,N)}_{\beta_{\mathrm{D}},\mathbf{s}_1,\mathbf{s}_2}(\mathbf{n}_1, \mathbf{n}_2) := W^{(N)}_{\beta_{\mathrm{D}},\mathbf{s}_1}(\mathbf{n}_1) W^{(N)}_{\beta_{\mathrm{D}},\mathbf{s}_2}(\mathbf{n}_2).$$

Fix a total current $\mathbf{N} = \mathbf{n}_1 + \mathbf{n}_2$, and write $J_e = J_2(|i-j|)$ for $e = \{i, j\}$. On each edge,

$$\frac{(2\beta_{\mathrm{D}} J_e)^{n_{1,e}}}{n_{1,e}!} \frac{(2\beta_{\mathrm{D}} J_e)^{n_{2,e}}}{n_{2,e}!} = \frac{(2\beta_{\mathrm{D}} J_e)^{N_e}}{N_e!} \binom{N_e}{n_{1,e}}. \tag{139}$$

Thus the binomial factor counts assignments of the N_e labelled copies to the two replicas. A canonical path transfer toggles the replica assignment of one labelled copy of every edge along a chosen path. It preserves the total current and the fixed-total-current edge bookkeeping in (139). The new ingredient is the product of vertex moments, which need not be preserved.

Proposition 4.8 (Obstruction to the canonical Ising path-switching involution)**.** *The canonical transfer of labelled path lines between two replicas does not, in general, preserve the product of DGC vertex weights. The obstruction already occurs when the local replica degrees change from* $(4, 0)$ *to* $(2, 2)$*: total degree and parity are preserved, but* $\mathfrak{m}_{\beta_{\mathrm{D}}}(4)\mathfrak{m}_{\beta_{\mathrm{D}}}(0) \neq \mathfrak{m}_{\beta_{\mathrm{D}}}(2)^2$*. Consequently, the standard Ising labelled-path proof does not directly yield a DGC switching identity. This conclusion concerns only that canonical operation.*

Proof. Consider distinct vertices $x, v, y, z \in \Lambda_N$ for which the interaction edges $\{x, v\}$, $\{v, y\}$, and $\{v, z\}$ have positive weight. This configuration is available for the positive inverse-square kernel. Let

$$n_{1,xv} = n_{1,vy} = 1, \qquad n_{1,vz} = 2, \qquad \mathbf{n}_2 = \mathbf{0},$$

and set every other multiplicity to zero. With insertion vectors $\mathbf{s}_1 = \mathbf{1}_{\{x\}} + \mathbf{1}_{\{y\}}$ and $\mathbf{s}_2 = \mathbf{0}$, all one-site moment indices are even, so the complete two-replica weight is positive. At v, the initial degree pair is $(4, 0)$.

Transfer the labelled copies on the path $x - v - y$ from replica (1) to replica (2), and compare the resulting pair with insertion vectors $\mathbf{s}_1' = \mathbf{0}$ and $\mathbf{s}_2' = \mathbf{1}_{\{x\}} + \mathbf{1}_{\{y\}}$. The endpoint moment products are merely exchanged between replicas, the factors at z are unchanged, and the edge factors are preserved by (139). At (v), however, the degree pair is now $(2, 2)$. Writing $\nu_{\beta_{\mathrm{D}}}(m) := \mathrm{e}^{-\beta_{\mathrm{D}} a m^2}$, strict Cauchy–Schwarz gives

$$\mathfrak{m}_{\beta_{\mathrm{D}}}(2)^2 = \left(\sum_{m\in\mathbb{Z}} m^2 \nu_{\beta_{\mathrm{D}}}(m)\right)^2 < \left(\sum_{m\in\mathbb{Z}} m^4 \nu_{\beta_{\mathrm{D}}}(m)\right)\left(\sum_{m\in\mathbb{Z}} \nu_{\beta_{\mathrm{D}}}(m)\right) = \mathfrak{m}_{\beta_{\mathrm{D}}}(4)\mathfrak{m}_{\beta_{\mathrm{D}}}(0), \tag{140}$$

because m^2 is not constant on the support of $\nu_{\beta_{\mathrm{D}}}$. Hence the complete two-replica weight changes, even though the total current, the source bookkeeping and the factorial edge contribution have the canonical switched form. □

Remark (Component exchange). For zero insertion vectors, choose a connected component of $\mathrm{supp}(\mathbf{n}_1 + \mathbf{n}_2)$ and exchange $n_{1,e}$ with $n_{2,e}$ on every edge of that component. At every incident vertex this swaps $(d_{\mathbf{n}_1}(i), d_{\mathbf{n}_2}(i))$ with $(d_{\mathbf{n}_2}(i), d_{\mathbf{n}_1}(i))$. The symmetric edge factors and the product of one-site moments are therefore preserved. This symmetry does not, by itself, produce a useful source-switching connectivity identity for the DGC variance.

The proposition answers **Q3** only for the canonical Ising switch. It does not rule out a different resummation, a component-exchange identity, a quantitative defect inequality, or another graphical representation.

Limits of the transfer. The DCGT and random-current mechanisms do not pass directly to the DGC for three related reasons.

1. No known Edwards–Sokal-type identity identifies the DGC height variance with an infinite-cluster density, and the expansion above is not parity-only. Its degree-dependent vertex moments obstruct the canonical switch that turns Ising correlations into a bare connectivity event.
2. The DCGT recursion bounds the probability that all inverse-square edges between two dense clusters are closed. No analogous independent-edge event is presently available in this moment-weighted expansion.
3. For the real-valued Gaussian chain, variance is a Green-function or effective-resistance quantity. After restricting the field to integer values, that exact Gaussian resolvent identity no longer applies directly; controlling the effect of the restriction is precisely the hard part near criticality.

A transfer argument would have to relate

$$\frac{\mathrm{Var}^{\mathrm{DGC}}_{N,\beta_{\mathrm{D}},2}(\varphi_0)}{\log N}$$

to a multiscale geometric or energetic quantity while controlling the degree-dependent factors $\mathfrak{m}_{\beta_{\mathrm{D}}}(d_{\mathbf{n}}(i))$.

4.7.5 The remaining multiscale target

A switching, cut, or decoupling inequality for the moment-weighted expansion would have to control its degree-dependent defect across scales. For general nonnegative $J_2(r) \asymp r^{-2}$, the sourced result presently used here is Garban's logarithmic variance estimate at sufficiently small β_{D}. For his extension kernels, the stronger invariance principle also identifies the coefficient with that of the corresponding Gaussian chain. Neither result is an endpoint estimate.

Assuming $\beta^{\log}_{\mathrm{D,deloc}} < \infty$, an endpoint estimate of interest is

$$\mathrm{Var}^{\mathrm{DGC}}_{N,\beta^{\log}_{\mathrm{D,deloc}},2}(\varphi_0) \geq c_0 \log N$$

for some $c_0 > 0$ and all sufficiently large N. This is exactly the positivity of $\rho_-(\beta^{\log}_{\mathrm{D,deloc}})$. An effective-resistance comparison stable under the integer constraint, a defect inequality, a resummation of the moment weights, or a multiscale estimate excluding continuous decay of the logarithmic coefficient could provide such a bound. It would prove neither an invariance principle nor $\beta^{\log}_{\mathrm{D,deloc}} = \beta_{\mathrm{D,loc}}$. No such endpoint estimate is proved in this report.

The expansion has positive weights, and two-point insertions still produce parity sources. The variance insertion is instead a degree defect, and the canonical Ising path switch does not preserve its two-replica weights. A proof of the logarithmic lower bound above would require control of this defect across scales, without assuming an Ising–DGC equivalence.

The three transfer questions now have precise answers. The DGC has a nonnegative moment-weighted expansion; two-point insertions retain parity sources, whereas the variance insertion changes a local degree weight; and the canonical labelled-path Ising switch fails because those degree-dependent moment factors are not invariant. The component-exchange symmetry nevertheless preserves part of the graphical algebra, so the obstruction concerns the canonical path switch rather than every possible switching operation. The unresolved step is to turn the positive expansion into a quantitative multiscale estimate for the degree defect at the report-specific endpoint proxy.

5 Conclusion and perspectives

The Ising reference model. The inverse-square Ising chain is an example of a one-dimensional model at marginal decay whose critical order parameter is discontinuous. Its droplet energy is logarithmic and its plus-state magnetisation satisfies the Thouless jump $m^+(\beta_{\mathrm{I},c}) > 0$. This gives a rigorous point of comparison for Garban's Open Problem 4, but does not solve it. Ising magnetisation and DGC height variance are different observables, and no coupling identifies their Gibbs laws. Only the mechanisms that prevent continuous decay can be compared.

The DCGT density gap. The DCGT proof uses two recurrences. The good-block estimate separates two defects from a single localised defect. In the latter case, the inverse-square interaction between two dense sets produces a logarithmic cross-energy, and the condition $\beta_{\mathrm{tail}}\theta_\infty^2 > 1$ makes the defect locations summable. Iteration establishes positive percolation density. In the opposite direction, the failed-crossing recurrence uses unbridged blocks, long-edge bridge estimates and an annulus obstruction. If $\beta_{\mathrm{tail}}\theta^2 < 1$, failed crossings persist at arbitrarily large scales, contradicting positive percolation. Hence

$$\theta > 0 \quad \Longrightarrow \quad \beta_{\mathrm{tail}}\theta^2 \geq 1.$$

For FK measures, the deterministic geometry stays the same; spatial Markov conditioning, worst-boundary estimates and FKG replace Bernoulli factorisation. DCGT yields an Ising jump because the Edwards–Sokal coupling identifies wired FK connectivity with magnetisation. No such identification is available for the DGC.

Random currents at long range. On every finite ferromagnetic weighted graph, including a dense long-range graph, the Ising Taylor expansion, parity-source rule and switching lemma are unchanged. Maximum interaction range enters the infinite-volume geometry, not the finite-volume algebra. The ADCS argument exploits this algebra to exclude doubled-current percolation when free-state long-range order vanishes. That hypothesis fails at the inverse-square critical Ising point, so the criterion gives no conclusion there even though switching remains exact.

For the DGC, we obtained a nonnegative moment-weighted current expansion. A two-point insertion retains an odd-source constraint, whereas the variance insertion is a local degree defect. Under the normalised DGC current law,

$$\mathrm{Var}^{\mathrm{DGC}}_{N,\beta_{\mathrm{D}}}(\varphi_0) = \mathbb{E}_{\mathbb{Q}^{\mathrm{DGC}}_{N,\beta_{\mathrm{D}}}}\left[\frac{\mathfrak{m}_{\beta_{\mathrm{D}}}(d_{\mathbf{n}}(0)+2)}{\mathfrak{m}_{\beta_{\mathrm{D}}}(d_{\mathbf{n}}(0))}\right].$$

The expansion therefore retains positivity and part of the parity structure, but its weights depend on the full degree at each vertex.

The DGC obstruction and the open endpoint. The canonical Ising path switch is not weight preserving for the DGC. It can replace local replica degrees $(4,0)$ by $(2,2)$, changing $\mathfrak{m}_{\beta_{\mathrm{D}}}(4)\mathfrak{m}_{\beta_{\mathrm{D}}}(0)$ into the strictly smaller $\mathfrak{m}_{\beta_{\mathrm{D}}}(2)^2$. This calculation rules out that canonical switch. It does not rule out a component exchange, a different resummation, a quantitative defect inequality, or every possible DGC switching identity. Garban's Open Problem 4 therefore remains open.

The remaining mathematical target is to control the degree-dependent defect across scales. Whenever $\beta^{\log}_{\mathrm{D,deloc}} < \infty$, a concrete first objective is to prove at the endpoint proxy that, for some $c_0 > 0$,

$$\mathrm{Var}^{\mathrm{DGC}}_{N,\beta^{\log}_{\mathrm{D,deloc}},2}(\varphi_0) \geq c_0 \log N$$

for all sufficiently large N. Such a bound would require a multiscale comparison that remains valid under the integer constraint and controls the degree-dependent moment weights.

A Model overview and notation map

This appendix lists the models, graphical representations and model-specific symbols used in the report. Each inverse-temperature symbol has one meaning. Definitions and proofs remain in the sections cited in the last column.

A.1 Models and representations at a glance

Figure 5 distinguishes exact graphical relations from structural comparisons. Bernoulli percolation, FK, the spin systems and the DGC are separate probability models. Random currents give an exact Ising representation. The inverse-square Ising chain is a structural reference for the DGC, and its current expansion supplies the algebraic identities tested in the DGC moment-current expansion. These comparisons do not identify the two Gibbs laws or their observables.

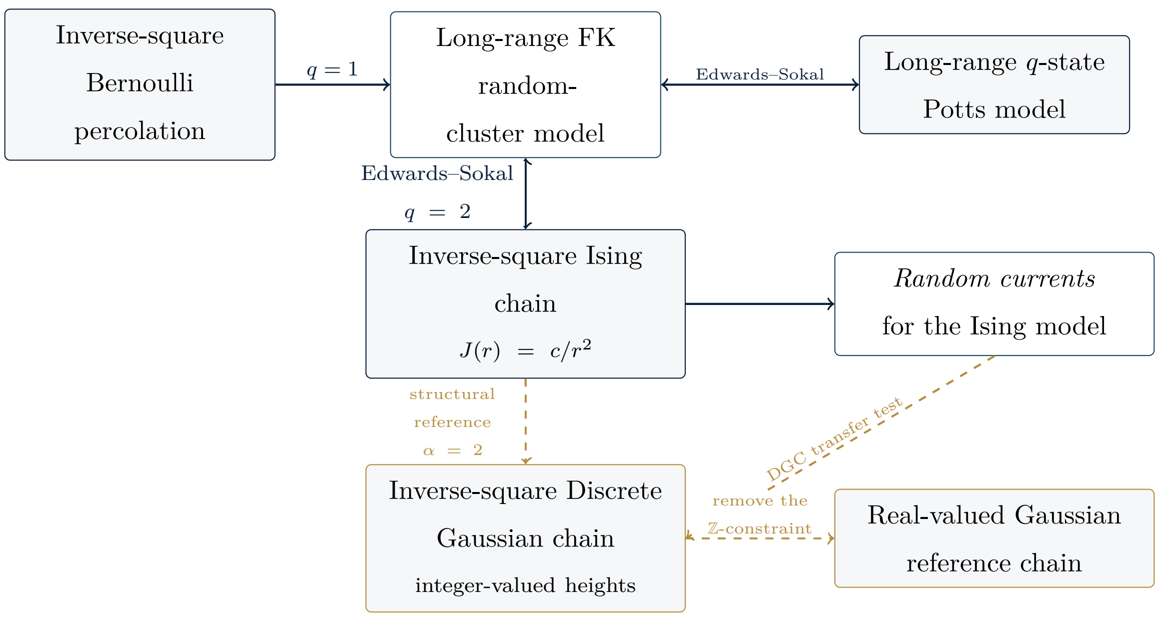

Figure 5: Exact graphical relations and transfer tests used in the report. Solid navy arrows mark exact specialisations, Edwards–Sokal couplings or the random-current representation. Dashed gold arrows mark structural comparisons or transfer tests only. In particular, the arrow from random currents to the DGC records the test of positivity, parity sources and source switching; it does not identify Gibbs laws, configurations or observables. The final dashed arrow gives the real-valued Gaussian reference obtained by removing the integer constraint.

Table 2: Models, representations and transfer roles in the report.

Model or representation	Configuration or random object	Parameters and convention	Observable or exact relation	Role in the report
Long-range Bernoulli percolation	Independent indicators $\omega_{i,j} \in \{0,1\}$	DCGT tail intensity β_{tail} and nearest-neighbour intensity λ	$\theta(\beta_{\text{tail}}, \lambda) = \mathbb{P}_{\beta_{\text{tail}},\lambda}(0 \leftrightarrow \infty)$, with $\theta > 0 \Rightarrow \beta_{\text{tail}}\theta^2 \geq 1$	The $q = 1$ setting for the reconstruction of the DCGT block renormalisation and its two recursions. See Section 3.
FK random-cluster model	Bond configuration $\omega \in \{0,1\}^E$, weighted by $q^{k(\omega)}$	$q \geq 1$, DCGT parameters $(\beta_{\text{tail}}, \lambda)$, and free or wired boundary condition	$\theta(q, \beta_{\text{tail}}, \lambda) = \mathbb{P}^1_{\beta_{\text{tail}},\lambda,q}(0 \leftrightarrow \infty)$	Extends the DCGT reconstruction beyond independent edges. At $q = 2$, the wired model is coupled exactly to Ising spins by Edwards–Sokal; for integer $q \geq 2$, the same coupling gives the Potts model. See Section 3.
Long-range Potts model	Colours $s_i \in \{1, \ldots, q\}$, for integer $q \geq 2$	Potts/FK normalisation with parameters $(q, \beta_{\text{tail}}, \lambda)$	Normalised magnetisation $m(q, \beta_{\text{tail}}, \lambda) = \theta(q, \beta_{\text{tail}}, \lambda)$	The Edwards–Sokal coupling transfers the FK density gap to Potts magnetisation. The Ising model is the $q = 2$ case. See Section 3.
One-dimensional long-range Ising chain	Spins $\sigma_i \in \{-1, +1\}$ with $J(r) \asymp r^{-\alpha}$	Physical inverse temperature β_{I}	$m^+(\beta_{\text{I}})$; at $J(r) = c/r^2$, $m^+(\beta_{\text{I},c}) > 0$	The spin reference model. At inverse-square decay, Edwards–Sokal transfers the DCGT density gap to the Thouless jump, while random currents give the exact algebraic representation used in the transfer chapter. See Sections 2, 3 and 4.
One-dimensional nearest-neighbour Ising chain	Spins $\sigma_i \in \{-1, +1\}$ with only $J(1) \neq 0$	Physical inverse temperature β_{I}	Plus-state magnetisation $m^+(\beta_{\text{I}})$	A background comparison, omitted from Figure 5: in one dimension it has no phase transition at positive temperature. See Section 2.
Random currents for the Ising model	Multiplicities $\mathbf{n} : E \to \mathbb{N}_0$; ADCS study the support of an independent free current plus a projected-plus current	Physical Ising inverse temperature β_{I}	$M_{\text{f}}^{\text{LRO}}(\beta_{\text{I}})$, $m^+(\beta_{\text{I}})$, and connectivity under $\mathbb{P}_{\text{supp},\beta_{\text{I}}}$	An exact Ising representation. Its positive expansion, parity sources and switching identity are separated from the geometric estimates used by ADCS, then tested on the DGC. See Section 4.
Discrete Gaussian chain (DGC)	$\varphi : \mathbb{Z} \to \mathbb{Z}$, with $\varphi_i = 0$ for $i \notin \Lambda_N$	DGC inverse temperature β_{D}, decay exponent α, and fixed inverse-square kernel J_2	$\text{Var}^{\text{DGC}}_{N,\beta_{\text{D}},2}(\varphi_0)$ and the coefficients $\rho_-(\beta_{\text{D}}), \rho_+(\beta_{\text{D}})$	A separate integer-valued height model. The moment-current expansion preserves positivity and part of the parity structure, but the canonical Ising path switch is not weight preserving. Critical discontinuity remains open. See Subsection 4.7.

Continued on the next page

Table 2 (continued)

Model or representation	**Configuration or random object**	**Parameters and convention**	**Observable or exact relation**	**Role in the report**
Real-valued Gaussian height chain	A real height field with the quadratic interaction obtained by removing the integer constraint	Inverse temperature β_{D} and the kernel J_α	Height variance, equivalently a Gaussian Green-function or effective-resistance quantity	The Gaussian reference obtained from the DGC energy after relaxing the integer-valued state space. It supports the "invisibility of the integers" comparison and is not an Ising representation. See Subsection 4.7.

A.2 Model-specific notation map

Model-specific inverse temperatures. Throughout the report, β_{tail} denotes the DCGT inverse-square edge intensity, β_{I} the physical Ising inverse temperature, and β_{D} the DGC inverse temperature. These parameters are not identified across models.

Table 3: Model-specific notation map.

Symbol	Meaning and convention	Scope or first definition
Common graph and Ising notation		
$G = (V, E)$, $J_{x,y}$	Interaction graph and ferromagnetic coupling. In the translation-invariant chain, $J_{x,y} = J(\lvert x-y\rvert)$.	Section 1
σ_i	Ising spin in $\{-1, +1\}$.	Section 1
α	Power-law decay exponent in $J(r) \asymp r^{-\alpha}$. The value $\alpha = 2$ is the inverse-square, marginal case.	Section 1
β_{I}	Physical Ising inverse temperature.	Section 1
$\mu^{\xi}_{\Lambda,\beta_{\mathrm{I}}}$, $\langle f\rangle^{\xi}_{\Lambda,\beta_{\mathrm{I}}}$	Finite-volume Ising Gibbs law and expectation. Here $\xi \in \{+, -, 0\}$; 0 means free boundary, not zero exterior spins.	Equation (1)
$\mu^{+}_{\beta_{\mathrm{I}}}, \mu^{-}_{\beta_{\mathrm{I}}}, \mu^{0}_{\beta_{\mathrm{I}}}$	Selected plus, minus and free thermodynamic limits.	Equation (2)
$m^{+}(\beta_{\mathrm{I}})$	Spontaneous magnetisation in the plus state.	Equation (3)
$\beta_{\mathrm{I},c}$	Critical physical Ising inverse temperature. It is not one of the report-specific DGC thresholds.	Equation (4)
$\mathbb{P}^{\xi}_{S,T,\beta_{\mathrm{tail}},\lambda,q}$	Finite-volume DCGT FK specification on $E(S,T)$ with exterior partition ξ.	Equation (55)
$p_e = 1 - e^{-2\beta_{\mathrm{I}} J_e}$	Edwards–Sokal bond parameter for the $\{-1,+1\}$-valued Ising Hamiltonian.	Section 3
DCGT Bernoulli and FK notation		
$\omega_{i,j}$	Open-edge indicator in a Bernoulli or FK configuration.	Section 3
$p_{i,j}(\beta_{\mathrm{tail}}, \lambda)$	DCGT edge-open probability: β_{tail} controls the inverse-square tail and λ controls nearest-neighbour edges.	Equation (5)
β_{tail}	Inverse-square long-edge intensity. It is not the physical Ising inverse temperature β_{I}.	Section 3
λ	Nearest-neighbour edge intensity in the DCGT Bernoulli and FK models. It is unrelated to the DGC coercivity constant κ_N.	Equation (5)
$\mathbb{P}_{\beta_{\mathrm{tail}},\lambda}$	Independent DCGT Bernoulli product law.	Section 3
$\theta(\beta_{\mathrm{tail}}, \lambda)$	Bernoulli percolation density $\mathbb{P}_{\beta_{\mathrm{tail}},\lambda}(0 \leftrightarrow \infty)$.	Equation (6)
θ, θ_∞	In the existence proof, the bare θ is a block-goodness level and θ_∞ is its fixed scale-independent lower bound. Neither symbol alone denotes a new thermodynamic order parameter.	Section 3
q	FK cluster weight: $q = 1$ is Bernoulli percolation and $q = 2$ is the Ising case.	Section 3
$\mathbb{P}^{1}_{\beta_{\mathrm{tail}},\lambda,q}$	Infinite-volume wired DCGT FK law.	Section 3
$\theta(q, \beta_{\mathrm{tail}}, \lambda)$	Wired FK density $\mathbb{P}^{1}_{\beta_{\mathrm{tail}},\lambda,q}(0 \leftrightarrow \infty)$.	Equation (57)
$(\beta_{\mathrm{tail}}, \lambda) = (2\beta_{\mathrm{I}} c, 2\beta_{\mathrm{I}} J_1)$	Physical Ising ray in the DCGT parameter plane. For the exact kernel $J(r) = c/r^2$, one has $J_1 = c$ and hence $\lambda = \beta_{\mathrm{tail}}$.	Equation (115)
$m(q, \beta_{\mathrm{tail}}, \lambda)$	Normalised Potts magnetisation, equal to $\theta(q, \beta_{\mathrm{tail}}, \lambda)$ under Edwards–Sokal.	Section 3

Continued on the next page

Table 3 (continued)

Symbol	**Meaning and convention**	**Scope or first definition**
ADCS *random-current* notation		
$\mathbf{n} : E \to \mathbb{N}_0$	Edge-multiplicity current.	Section 4
$\partial\mathbf{n}$	Source set: the vertices of odd incident current degree.	Section 4
$w_{\beta_\mathrm{I}}(\mathbf{n})$	Ising current weight $\prod_e(\beta_\mathrm{I} J_e)^{n_e}/n_e!$.	Section 4
Ω_Λ, $\mathcal{Z}_\Lambda(A)$, $\mathbf{P}^A_{\Lambda,\beta_\mathrm{I}}$	Finite current space, source-constrained partition sum and current law with $\partial\mathbf{n} = A$.	Subsection 4.2
$\widehat{\mathbf{n}} = \mathrm{supp}(\mathbf{n})$	Ordinary-edge support $\{e : n_e > 0\}$, used for connectivity after multiplicities are discarded.	Section 4
$\mathbf{P}^{+,\mathfrak{g}}_{\Lambda,\beta_\mathrm{I}}$, $\widehat{\mathbf{P}}^{+}_{\Lambda,\beta_\mathrm{I}}$	Ghost-augmented plus-current law and its projection onto ordinary edges, respectively. The ghost is not recorded in the ordinary source set.	Subsection 4.4
$\mathbf{P}^0_{\beta_\mathrm{I}}, \mathbf{P}^+_{\beta_\mathrm{I}}$	Infinite-volume free current law and projected-plus current law. The superscripts are boundary-law labels here, not source sets.	Subsection 4.4
$\mathbb{P}_{\mathrm{supp},\beta_\mathrm{I}}$	Induced law of $\mathrm{supp}(\mathbf{n}_1 + \mathbf{n}_2)$, where $\mathbf{n}_1 \sim \mathbf{P}^0_{\beta_\mathrm{I}}$ and $\mathbf{n}_2 \sim \mathbf{P}^+_{\beta_\mathrm{I}}$ are independent.	Subsection 4.4
$M^{\mathrm{LRO}}_{\mathrm{f}}(\beta_\mathrm{I})$	Free-state long-range-order parameter obtained from averaged two-point functions.	Equation (126)

Continued on the next page

Table 3 (continued)

Symbol	Meaning and convention	Scope or first definition
DGC notation		
$\Lambda_N = \{-N, \dots, N\}$	Finite interval on which the DGC heights fluctuate.	Subsection 4.7
$\varphi : \mathbb{Z} \to \mathbb{Z}$	Integer height field, extended by $\varphi_i = 0$ for $i \notin \Lambda_N$.	Subsection 4.7
J_α, J_2	Nonnegative DGC kernel with $J_\alpha(r) \asymp r^{-\alpha}$; J_2 is the fixed inverse-square kernel. It is not automatically the Ising kernel c/r^2.	Subsection 4.7
β_{D}	DGC inverse temperature. It is unrelated to the DCGT tail intensity except through a qualitative comparison of phase diagrams.	Subsection 4.7
$H^{\mathrm{DGC}}_{N,\alpha}, \mu^{\mathrm{DGC}}_{N,\beta_{\mathrm{D}},\alpha}$	DGC Hamiltonian and finite-volume Gibbs law with zero exterior boundary condition.	Subsection 4.7
$\mathbb{E}^{\mathrm{DGC}}_{N,\beta_{\mathrm{D}},\alpha}, \mathrm{Var}^{\mathrm{DGC}}_{N,\beta_{\mathrm{D}},\alpha}$	Expectation and variance under the DGC law.	Subsection 4.7
$\rho_-(\beta_{\mathrm{D}}), \rho_+(\beta_{\mathrm{D}})$	Liminf and limsup coefficients of $\mathrm{Var}^{\mathrm{DGC}}_{N,\beta_{\mathrm{D}},2}(\varphi_0)/\log N$. If they agree, their common value is $\rho(\beta_{\mathrm{D}})$.	Equation (134)
$\beta^{\log}_{\mathrm{D,deloc}}$	Report-specific delocalisation threshold proxy.	Equation (135)
$\beta_{\mathrm{D,loc}}$	Report-specific localisation threshold proxy defined through bounded variance.	Equation (136)
$E_N, a, \mathfrak{m}_{\beta_{\mathrm{D}}}(k)$, $d_{\mathbf{n}}(i), \mathbf{s}$, $W^{(N)}_{\beta_{\mathrm{D}},\mathbf{s}}(\mathbf{n})$	Internal edges, diagonal coefficient, one-site moments, current degree, insertion vector and degree-dependent weight in the DGC moment expansion. Here $\mathbf{n}$ is a DGC expansion variable, not an ADCS current law.	Equation (137)
$\mathbb{Q}^{\mathrm{DGC}}_{N,\beta_{\mathrm{D}}}$	Normalised zero-insertion DGC moment-current law. Under this law the height variance is the expectation of a local degree-defect ratio.	Equation (138)
κ_N	Smallest eigenvalue of the finite-volume Dirichlet matrix, used as the finite-volume coercivity constant in the proof of the DGC expansion. For positive-tail kernels it is bounded below by the minimum exterior mass. No lower bound uniform in N is used.	Subsection 4.7
$\nu_{\beta_{\mathrm{D}}}(m) = \mathrm{e}^{-\beta_{\mathrm{D}} a m^2}$	One-site Gaussian weight used in the strict Cauchy–Schwarz estimate.	Subsection 4.7

B Technical details for the DCGT reconstruction

This appendix collects the deterministic interval checks and numerical estimates suppressed from the main reconstruction of Section 3. No result here is new: the arguments verify the corresponding steps of DCGT Lemmas 2–3 [DCGT24]. Keeping them here leaves the two renormalisation arguments in the main chapter focused on their geometric and probabilistic steps.

B.1 Dense runs and the one-defect geometry

Lemma B.1 (Dense-run geometry)**.** *Let $\theta > 3/4$. If N consecutive K-blocks are θ-good, their chosen large clusters belong to one connected set of cardinality at least θKN. In the one-defect event used in the proof of Lemma 3.2, put $d_i = C - |i|$. If the parent block is θ'-bad, then $d_i \geq C_0$, the connected sets on both sides of the defect contain at least $Kd_i/2$ vertices, and their ordered vertices satisfy*

$$\theta(y_b - x_a) \leq 6K + a + b, \qquad 1 \leq a, b \leq \left\lfloor \frac{Kd_i}{2} \right\rfloor .$$

Proof. Two consecutive good blocks have union of size $3K$, whereas two disjoint large clusters would have total size at least $4\theta K > 3K$. Thus the clusters overlap. Since each vertex belongs to at most two blocks,

$$\left| \bigcup_{j=a}^{b} C_j \right| \geq \frac{1}{2} \sum_{j=a}^{b} |C_j| \geq \theta K(b - a + 1).$$

Applying this to the runs on either side of the defect gives the stated size bounds. If $d_i < C_0$, the longer run alone has at least $2\theta' CK$ vertices, contradicting badness of the parent.

For the ordered-point estimate, select every other good block on the right. These blocks are disjoint, and the first $\ell_b = \lceil b/(2K\theta) \rceil$ of them contain at least b points of C_i^+. The inequalities $b \leq Kd_i/2$, $\theta \geq 3/4$, and $d_i \geq C_0 \geq 48$ ensure that all selected indices remain in the good run. Hence

$$y_b \leq Ki + 3K + \frac{b}{\theta}.$$

The symmetric selection on the left gives $x_a \geq Ki - 3K - a/\theta$. Subtraction and $\theta \leq 1$ prove the claim. □

Lemma B.2 (Inverse-square cross-energy)**.** *For $d \geq 48$, $K \geq 2$, and $M = \lfloor Kd/2 \rfloor$,*

$$\sum_{a,b=1}^{M} \frac{1}{(6K + a + b)^2} \geq \log\left(\frac{d}{48}\right).$$

Consequently, the probability that every Bernoulli edge between the two dense sets of Lemma B.1 is closed is at most $(48/d)^{\beta_{\mathrm{tail}}\theta^2}$.

Proof. On each unit square $[a-1,a]\times[b-1,b]$, $(6K+a+b)^{-2}$ dominates $(8K+x+y)^{-2}$. Therefore

$$\sum_{a,b=1}^{M}\frac{1}{(6K+a+b)^2}\geq\int_0^M\int_0^M\frac{dx\,dy}{(8K+x+y)^2}=\log\left(\frac{(8K+M)^2}{8K(8K+2M)}\right).$$

Since $M\geq Kd/3$, the last expression is at least

$$\log\left(\frac{(d+24)^2}{48(d+12)}\right)\geq\log\left(\frac{d}{48}\right).$$

The ordered-point inequality gives $(y_b-x_a)^{-2}\geq\theta^2(6K+a+b)^{-2}$. Independence and $1-p_{x,y}=\exp[-\beta_{\mathrm{tail}}/(y-x)^2]$ then give the probability bound. □

The permanent constants in the good-block proof may now be chosen once: fix $\theta_\infty>3/4$ with $\alpha_0=\beta_{\mathrm{tail}}\theta_\infty^2>1$, and take $C_0\geq 48$ such that

$$2\sum_{d\geq C_0}(48/d)^{\alpha_0}\leq 1/100.$$

This single choice supplies the overlap margin, the ordered-point estimate, and the summability of all one-defect locations at every scale.

B.2 Crossing localisation and bridge bookkeeping

Lemma B.3 (Localisation of an unbridged crossing)**.** *Use the notation of the failed-crossing proof. A path made of edges of length at most K which crosses B^i_{3K} contains a subpath lying in $[c_i-4K,c_i+4K)$ and measurable from the short edges internal to that interval. Moreover, a CK-crossing which meets an unbridged candidate block forces such a K-crossing of that block.*

Proof. For the first assertion, take the first path vertex at or to the right of the block and the last earlier vertex strictly to its left. All intermediate vertices lie between the two sides, and the step bound K places both endpoints inside the stated buffer.

For the second assertion, apply the same first/last-index construction to the large crossing. If the resulting segment contains only short edges, it is the required local crossing. Otherwise take its first long edge. If an endpoint lies within the prescribed $5K$-neighbourhood, the block is bridged by definition. If neither endpoint does, the portions of the path before and after that edge supply the two R-arms, so the long edge is a bridge spanning the block. Both alternatives contradict the assumption that the block is unbridged. □

Lemma B.4 (Unbridged-block count)**.** *Assume the choices $q_R^2<\rho<\theta^2$ and $q_R^2+\varepsilon_{R,K}\leq\rho$ from the proof of Lemma 3.4. After increasing K_1 and then C_1, uniformly for $K\geq K_1$ and $C\geq C_1$, every candidate block satisfies*

$$\mathbb{P}_{\beta_{\mathrm{tail}},\lambda}(B^i_{3K}\text{ is unbridged})\geq 6e\,C^{-\beta_{\mathrm{tail}}\theta^2}.$$

Since there are at least $C/6$ candidate blocks, $\mathbb{E}[|\mathbf{U}|] \geq eC^{1-\beta_{\text{tail}}\theta^2}$.

Proof. The unbridged event is the intersection of the decreasing events that every spanning long edge is not a bridge and every long edge meeting the local $10K$-window is closed. Harris–FKG and the bridge estimate give a product lower bound. Using $-\log(1-u) \leq u/(1-u)$ after taking K_1 large, the spanning-edge product has logarithm bounded below by $-\beta_{\text{tail}}\rho \log C - O_{\beta_{\text{tail}},\rho}(1)$; the nearby-edge product is bounded below by a positive constant because

$$\sum_{e\colon e \cap J_i \neq \varnothing,\ |e|>K} |e|^{-2} = O(1).$$

The probability is at least $cC^{-\beta_{\text{tail}}\rho}$. The strict slack $\rho < \theta^2$ allows C_1 to absorb $6e/c$, giving the displayed bound. Candidate centres are separated by $9K$; direct interval counting gives at least $C/6$ of them for $C \geq 30$. Linearity of expectation proves the last assertion; independence between blocks is not used. $\square$

References

[ACCN88] Michael Aizenman, J. T. Chayes, Lincoln Chayes, and C. M. Newman. “Discontinuity of the magnetization in one-dimensional inverse-square Ising and Potts models”. In: *Journal of Statistical Physics* 50.1–2 (1988), pp. 1–40. DOI: 10.1007/BF01022985.

[ADCS15] Michael Aizenman, Hugo Duminil-Copin, and Vladas Sidoravicius. “Random currents and continuity of Ising model’s spontaneous magnetization”. In: *Communications in Mathematical Physics* 334.2 (2015), pp. 719–742. DOI: 10.1007/s00220-014-2093-y. arXiv: 1311.1937 [math-ph].

[Aiz82] Michael Aizenman. “Geometric analysis of φ^4 fields and Ising models. Parts I and II”. In: *Communications in Mathematical Physics* 86.1 (1982), pp. 1–48. DOI: 10.1007/BF01205659.

[AN86] Michael Aizenman and C. M. Newman. “Discontinuity of the percolation density in one dimensional inverse-square percolation models”. In: *Communications in Mathematical Physics* 107.4 (1986), pp. 611–647. DOI: 10.1007/BF01205489.

[CDL26] Loren Coquille, Paul Dario, and Arnaud Le Ny. *Quantitative delocalisation for the Gaussian and q-SOS long-range chains*. To appear in *Annales Henri Lebesgue*. 2026. arXiv: 2412.15782v2 [math.PR].

[DCGT24] Hugo Duminil-Copin, Christophe Garban, and Vincent Tassion. “Long-range models in 1D revisited”. In: *Annales de l’Institut Henri Poincaré B, Probabilités et Statistiques* 60.1 (2024), pp. 232–241. DOI: 10.1214/22-AIHP1355. arXiv: 2011.04642 [math.PR].

[Dum18] Hugo Duminil-Copin. “Random currents expansion of the Ising model”. In: *European Congress of Mathematics*. Ed. by Volker Mehrmann and Martin Skutella. Zürich: European Mathematical Society, 2018, pp. 869–889. DOI: 10.4171/176-1/39. arXiv: 1607.06933 [math-ph].

[Dys69] Freeman J. Dyson. “Existence of a phase-transition in a one-dimensional Ising ferromagnet”. In: *Communications in Mathematical Physics* 12.2 (1969), pp. 91–107. DOI: 10.1007/BF01645907.

[ES88] Robert G. Edwards and Alan D. Sokal. “Generalization of the Fortuin–Kasteleyn–Swendsen–Wang representation and Monte Carlo algorithm”. In: *Physical Review D* 38.6 (1988), pp. 2009–2012. DOI: 10.1103/PhysRevD.38.2009.

[FK72] C. M. Fortuin and P. W. Kasteleyn. “On the random-cluster model. I. Introduction and relation to other models”. In: *Physica* 57.4 (1972), pp. 536–564. DOI: 10.1016/0031-8914(72)90045-6.

[FKG71] C. M. Fortuin, P. W. Kasteleyn, and Jean Ginibre. "Correlation inequalities on some partially ordered sets". In: *Communications in Mathematical Physics* 22.2 (1971), pp. 89–103. DOI: 10.1007/BF01651330.

[FS81] Jürg Fröhlich and Thomas Spencer. "The Kosterlitz-Thouless transition in two-dimensional Abelian spin systems and the Coulomb gas". In: *Communications in Mathematical Physics* 81.4 (1981), pp. 527–602. DOI: 10.1007/BF01208273.

[FS82] Jürg Fröhlich and Thomas Spencer. "The phase transition in the one-dimensional Ising model with inverse-square interaction energy". In: *Communications in Mathematical Physics* 84.1 (1982), pp. 87–101. DOI: 10.1007/BF01208373.

[FZ91] Jürg Fröhlich and Bogusław Zegarlinski. "The phase transition in the discrete Gaussian chain with $1/r^2$ interaction energy". In: *Journal of Statistical Physics* 63.3–4 (1991), pp. 455–485. DOI: 10.1007/BF01029195.

[Gar23] Christophe Garban. *Invisibility of the integers for the discrete Gaussian chain via a Caffarelli-Silvestre extension of the discrete fractional Laplacian*. Revised May 2024. 2023. arXiv: 2312.04536v2 [math.PR].

[Geo11] Hans-Otto Georgii. *Gibbs Measures and Phase Transitions*. 2nd ed. Vol. 9. De Gruyter Studies in Mathematics. Berlin and Boston: De Gruyter, 2011. ISBN: 978-3-11-025029-9.

[GHS70] Robert B. Griffiths, Charles A. Hurst, and Seymour Sherman. "Concavity of magnetization of an Ising ferromagnet in a positive external field". In: *Journal of Mathematical Physics* 11.3 (1970), pp. 790–795. DOI: 10.1063/1.1665211.

[IN88] John Z. Imbrie and C. M. Newman. "An intermediate phase with slow decay of correlations in one dimensional inverse-square percolation, Ising and Potts models". In: *Communications in Mathematical Physics* 118.2 (1988), pp. 303–336. DOI: 10.1007/BF01218582.

[KH82] K. H. Kjaer and H. J. Hilhorst. "The discrete Gaussian chain with $1/r^n$ interactions: exact results". In: *Journal of Statistical Physics* 28.4 (1982), pp. 621–632. DOI: 10.1007/BF01011871.

[LL80] L. D. Landau and E. M. Lifshitz. *Statistical Physics. Part 1*. 3rd ed. Vol. 5. Course of Theoretical Physics. Oxford: Pergamon Press, 1980.

[NS86] C. M. Newman and L. S. Schulman. "One dimensional $1/|j-i|^s$ percolation models: the existence of a transition for $s \leq 2$". In: *Communications in Mathematical Physics* 104 (1986), pp. 547–571. DOI: 10.1007/BF01211064.

[Rue68] David Ruelle. "Statistical mechanics of a one-dimensional lattice gas". In: *Communications in Mathematical Physics* 9 (1968), pp. 267–278. DOI: 10.1007/BF01654281.

[SH83] J. Slurink and H. J. Hilhorst. "Roughening behavior of a one-dimensional crystal surface with inverse square potential". In: *Physica A: Statistical Mechanics and its Applications* 120.3 (1983), pp. 627–634. DOI: 10.1016/0378-4371(83)90072-9.

[She05] Scott Sheffield. *Random Surfaces*. Astérisque 304. Société Mathématique de France, 2005. ISBN: 978-2-85629-187-0. DOI: 10.24033/ast.697. arXiv: math/0304049.

[Tho69] David J. Thouless. "Long-range order in one-dimensional Ising systems". In: *Physical Review* 187.2 (1969), pp. 732–733. DOI: 10.1103/PhysRev.187.732.

[Vel06] Yvan Velenik. "Localization and delocalization of random interfaces". In: *Probability Surveys* 3 (2006), pp. 112–169. DOI: 10.1214/154957806000000050.